SUPPORTING THE REGENERATION PROCESS OF A DIESEL PARTICULATE FILTER WITH THE ADDITION OF HYDROGEN AND HYDROGEN/CARBON MONOXIDE MIXTURES: DIESEL ENGINE AFTERTREATMENT SYSTEM

A Thesis submitted for the degree of Doctor of Philosophy

By

Stephen Hemmings

School of Engineering and Design

Brunel University

United Kingdom

July 2012

ABSTRACT

This investigation aims to enhance the regeneration performance of a diesel particulate filter. This is achieved by introducing various chemical components to the regeneration process, which are representative of what can be generated 'on board' a vehicle using an exhaust gas fuel reformer. By researching the effects of introducing such components using a periodic injection cycle the aim is to reduce the volume of 'reformates' required to assist in proficient diesel particulate filter regeneration. As a result, this study also aims to support future work in the development of exhaust gas fuel reformer design for DPF aftertreatment applications.

All experiments were performed using a Ford Puma 2.0 litre diesel engine. A test rig was constructed and installed that featured a mini diesel particulate filter housed within a tubular furnace. Exhaust gas could be sampled directly from the exhaust manifold and fed through the DPF. Exhaust gas measurements were taken both pre and post DPF using a FTIR spectrometer.

It was shown that the regeneration process could be supported substantially by the introduction of hydrogen. Similar properties were also demonstrated when introducing a hydrogen-carbon monoxide mixture. The introduction of these species allowed for the regeneration process to be implemented at filter temperatures substantially lower than the passive regeneration temperature. Furthermore, by introducing these simulated reformates using a periodic injection strategy, it was evident that similar benefits to the regeneration process could be attained with significantly less volumes of simulated reformates.

In an attempt to effectively utilise the carbon monoxide generated during hydrogen production by an exhaust gas fuel reformer, this study defined an optimised hydrogen/carbon monoxide mixture ratio of 60% (v/v) hydrogen balanced with carbon monoxide. At this optimised mixture ratio, the filter demonstrated the highest regeneration efficiency of all ratios tested. Such data could be utilised in future work in the development of fuel reformer design.

ACKNOWLEDGEMENTS

I would firstly like to thank my supervisor, Prof. Thanos Megaritis for all the direction and support provided throughout this study. Secondly I would like to acknowledge the role of Prof. Hua Zhao as second supervisor. I would also like to thank all the technicians at Brunel University that were involved in the project with particular thanks going to Ken Anstiss and Clive Barrett.

I would also like to acknowledge MKS for supply and fitment of the FTIR analyser, with specific gratitude going to Paul Hughes.

In addition I would like to gratefully acknowledge the financial support for this work provided by the Engineering and Physical Science Research Council (Grants EP/F025416/1 and EP/G038007/1).

NOMENCLATURE

Abbreviations

AA	Automobile Association Ltd
BDC	Bottom dead centre
BMEP	Brake mean effective pressure (Bar)
BSFC	Brake specific fuel consumption (kg/kWh)
CI	Compression ignition
CoV	Coefficient of variance
DPF	Diesel particulate filter
ECU	Electronic control unit
EGR	Exhaust gas recirculation
EU	European union
FTIR	Fourier transform infrared
HRR	Heat release rate (J/deg)
ICU	Injection control unit
MAF	Mass air flow (kg/hr)
NPCH	Nitrated polycyclic aromatic hydrocarbons
OEM	Original equipment manufacture
PAH	Polycyclic aromatic hydrocarbons
PID	Proportional integral derivative
ppmC	Parts per million of carbon
SCR	Selective catalytic reduction
SEM	Scanning electron micrograph
SNR	Signal to noise ratio
SOF	Soluble organic fractions
SOL	Solid organic fractions
TCD	Thermal conductivity detector
TDC	Top dead centre
v/v	Volume/volume of exhaust gas

Symbols

A_p	Frequency factor (s^{-1})
BP	Brake power (kW)
C_{in}	Trap inlet particulate concentration (kg/m^3)
Cp	Specific heat (J/g K)
CV	Calorific value (kJ/g)
dm_p/dt	Soot oxidation rate (mg/s)
$dQn/d\theta$	Heat release rate as function of crank angle
E_p	Activation energy (kJ/mol*K)
m	Reaction order
mf	Mass flow rate (g/s)
m_p	Net particulate mass (mg)
η	Efficiency (%)
ηf	Trap efficiency (%)
Q	Exhaust volumetric flow rate (m^3/hr)
R	Gas constant (kJ/mol*K)
RR	Reaction rate ($mol/l^{-1}/s^{-1}$)
SV	Space velocity (hr^{-1})
µm	Micron
V	Cylinder volume (m^3)
Vrec	DPF reactor volume (m^3)
γ	Gamma
θ	Crank angle degrees
Δ	Difference

Chemical symbols

Ag	Silver
AL_2O_3	Aluminium oxide
$BaCO_3$	Barium carbonate
$Ba(NO_3)_2$	Barium nitrate
C	Carbon
CH_2O	Formaldehyde
CH_3COOH	Acetic acid
CH_4	Methane
CO	Carbon monoxide
$CO(NH_2)_2$	Urea
CO_2	Carbon dioxide
FeCrAl	Iron chromium aluminium alloy
HC	Hydrocarbons
H_2	Hydrogen
H_2O	Water
H_2SO_4	Sulphuric acid
N_2	Nitrogen
NH_3	Ammonia
NO	Nitrogen oxide
NOx	Oxides of nitrogen
NO_2	Nitrogen dioxide
N_2O	Nitrous oxide
O_2	Oxygen
PM	Particulate matter
Rh	Rhodium
SiC	Silicon carbide
SO_2	Sulphur dioxide
SO_3	Sulphur trioxide
SO_4	Sulphate particulates
THC	Total hydrocarbons

CONTENTS

TABLE OF FIGURES

TABLE OF TABLES

TABLE OF EQUATIONS

CHAPTER 1

INTRODUCTION

CHAPTER 1 – INTRODUCTION

1.1 Introduction

Recent decades have seen a considerable increase in the sales of diesel powered vehicles. This is largely due to the benefits obtained in fuel consumption and lower carbon monoxide emission. However, these benefits come with a corresponding penalty increase in both oxides of nitrogen (NOx) and particulate matter (PM). PM is of significant concern due to its carcinogenic classification as well as its connection to a number of cardiovascular and respiratory problems [Mayer et al (2004)]. As a result, increasingly stricter emission regulations in both the U.S and Europe have been introduced, enforcing the need for more proficient emission controls including technical advancements in the control of DPFs [Schaefer et al (2009), Pyzik et al (2011) and Liu et al (2011)].

A DPF filter is the most commonly adopted technology for PM reduction and can typically demonstrate a filtration efficiency of as high as 90% [Schaefer Sindlinger et al (2007) and Li et al (2004)]. The structure of the filter consists of a series of rectangular tubes. Each tube is blocked at alternate ends resulting in the exhaust gas flow being forced to travel through the tube walls which feature a number of pores. In turn, the flow is filtered resulting in particulates being deposited on the filter walls. The filtration process increases the exhaust back pressure and hence the exhaust temperature. Once the exhaust temperature exceeds the temperature required for PM oxidation, the DPF regenerates for a period of a few minutes [Hanamura et al (2009) and Eastwood (2010)].

The increase in exhaust back pressure generated by the implementation of DPF technology can cause adverse effects on available engine torque and fuel consumption. Therefore, a DPF requires frequent and efficient regeneration. During typical urban use, when the exhaust temperature is relatively low, passive regeneration is not always possible as the process requires significant heat (in excess of approximately 500°C) in order to oxidise PM [Park et al (2010), Kandylas and Koltsakis (2002) and Yamamoto et al (2009)]. If the DPF is continually blocked without regeneration, it is possible for the filter to become excessively blocked. In this state the filter can no longer be regenerated in vehicle resulting in the DPF having to be removed and

actively regenerated, a process that can incur a significant cost to the customer. In 2011, a variety of cases were reported where small engined diesel vehicles, designed for urban use, demonstrated problems with excessively blocked DPFs [Rizi (2011)]. These factors resulted in The Automobile Association Ltd (The AA) stating later in 2011, that it would prove wise to avoid purchasing a diesel engine vehicle fitted with a DPF if it is to be used for urban, stop/start driving due to problems with incomplete regeneration when used for such an application [The Automobile Association (2011)]. Due to the issues faced with passive regeneration, alongside DPFs being a necessity to meet modern emission standards, focus has recently been directed towards methods of active regeneration.

One of the most common methods of active regeneration is to inject diesel fuel into the exhaust flow, pre DPF. This is in an attempt to increase the exhaust temperature to within the soot oxidation temperature range and hence support the DPF regeneration process [York et al (2007) and Bensaid et al (2010)]. However, recent studies into the addition of H_2 to the DPF regeneration process have proved successful [Bromberg *et al* (2001)]. Additional research has also demonstrated that the benefits of introducing H_2 to the regeneration process can be further enhanced with the addition of CO [Macleod and Lambert (2002) and Tadrous *et al* (2010)]. The addition of such components allows for regeneration to occur at lower exhaust temperatures, a factor that increases the durability of the system. In addition to this, such components also increase the speed in which full regeneration is achieved. A characteristic which results in improved fuel economy for the system [Theinnoi *et al* (2010)].

In addition to DPFs, research has proven that other exhaust aftertreatment devices also benefit from the addition of H_2 including catalytic converters and NOx traps [Abu-Jrai *et al* (2008), Bromberg *et al* (2004) and Wen (2002)]. This has resulted in the development of the Exhaust Gas Fuel Reforming process, a technique that allows for production of hydrogen rich reformate 'on board' the vehicle.

Improving the DPF regeneration process using components that could be generated on board using an exhaust gas assisted fuel reformer is the starting point for this thesis.

1.2 Objectives of the Project

The objectives of this study are as follows:

1. Establish the temperature at which the passive regeneration process of a DPF filter is initiated and attempt to support that process with the addition of H_2. The volumes of hydrogen introduced are to be representative of what can be generated 'on board' using an exhaust gas fuel reformer.

2. Introduce hydrogen to the DPF regeneration process using a variety of periodic strategies in an attempt to reduce the volume of H_2 required for proficient regeneration quality. Identify an optimised periodic injection strategy.

3. Introduce a H_2/CO mixture to the DPF regeneration process using both constant and periodic injection strategies in order to investigate the effects of the mixture and the delivery method on both the regeneration process and the chemical composition of the exhaust gas post DPF.

4. Identify the effect of varying both engine load and space velocity on the regeneration process.

5. Introduce H_2/CO at a variety of mixture ratios, using a constant injection strategy, to the DPF in order to establish an optimised mixture ratio that can be utilised to assist in the design of an on board exhaust gas fuel reformer.

6. Establish whether during the application of hydrogen/diesel dual fuelling, sufficient residual hydrogen is present in the exhaust stream to successfully support the DPF regeneration process.

1.3 Outline of Thesis

Following this introductory chapter is the literature review chapter. The literature review begins by outlining the effect of diesel engine emissions on both human health and the environment.

This is followed by examples of the various emissions legislation that has been implemented worldwide. The next section of this chapter outlines the various aftertreatment technologies currently in use, including; DPFs, EGR and catalytic converters. The final two sections of this chapter outline the fundamental operating principles behind both gas chromatography and fourier transform infrared spectrometry.

The methodology chapter describes the experimental set up and test procedures adopted throughout this study. The first section outlines details about the prototype research engine and its design differences when compared to the mass produced equivalent. This is followed by descriptions of the various devices and techniques adopted for engine control and measurement of various engine outputs. The subsequent section outlines the layout of the aftertreatment test rig and the relevant operating procedures adopted throughout testing. The final sections of this chapter outline the set up and procedures adopted when using the gas chromatograph and fourier transform infrared spectrometry analyser for measurement of specific diesel exhaust species.

The following chapter, the fourth, identifies whether hydrogen can be adopted to support the passive regeneration process. Following introduction and methodology sections, this chapter begins by establishing the temperature at which passive regeneration occurs. Once identified, the following sections outline the effects of introducing hydrogen, at increasing concentrations, to the passive regeneration process. Both constant and periodic injection strategies are investigated. Following this, the chapter is then concluded with a summary section.

The next chapter outlines the effect of introducing a H_2/CO mixture to the DPF regeneration process. This chapter begins with introductory and methodology sections. The subsequent sections investigate the impact of implementing the following variables:

(1) 2.7% mixture concentration at exhaust temperature 520°C.
(2) 2.7% mixture concentration at exhaust temperature 440°C.
(3) 4.5% mixture concentration at exhaust temperature 440°C.
(4) The impact of DPF space velocity on the regeneration process
(5) The impact of engine load on the regeneration process

The final section of this chapter summarises the work completed during this investigation

The following chapter, the sixth, looks at the effects of introducing a H_2/CO mixture gas to the regeneration process at varying ratios. Following a methodology section that outlines modifications made to the aftertreatment test rig, the remaining results and discussion sections demonstrate the effects of varying the mixture ratio on filter temperature, regeneration profile and exhaust emissions post filter. The final section then concludes the chapter with a brief summary.

The penultimate chapter of this study attempts to establish whether the application of hydrogen and diesel dual fuelling results in sufficient hydrogen being present in the exhaust stream to aid in supporting the regeneration process. This chapter begins with an introductory section that is followed by a methodology section, which features the various test points that were adopted throughout the investigation, including a variety of engine speed and load conditions as well as a number of different hydrogen concentrations. The remainder of this section outlines the effect of hydrogen and diesel dual fuelling on a number of engine characteristics including fuel consumption and ignition delay. In addition, the effect of dual fuelling on various emissions (CO, CO_2, NOx and THC) is also demonstrated. The final section of this chapter summarises the investigation.

The final chapter of this study summarises the conclusions drawn from the investigations outlined in chapters 4 to 7. This is followed by recommendations for future work.

CHAPTER 2

LITERATURE REVIEW

CHAPTER 2 - LITERATURE REVIEW

2.1 The impact of diesel engine exhaust emissions

As concerns regarding the effect of engine emissions on both human health and the earth's atmosphere continue to grow, national governments are implementing increasingly more stringent emissions legislation. In an effort to adhere to these ever tightening regulations the automotive industry is constantly required to design and implement new and novel emission reduction techniques [Challen and Baranescu (1999)].

Complete combustion of a hydrocarbon (HC) diesel fuel would result in the formation of water and carbon dioxide (CO_2). However, due to a variety of reasons, combustion of hydrocarbon fuels is never complete resulting in the formation of a number of species including; unburned hydrocarbons, aldehydes, carbon monoxide (CO) and oxides of nitrogen (NO_x). When released into the earth's atmosphere, species such as carbon monoxide and oxides of nitrogen can subject significant damage to the earth's ozone layer. As a result further enhancement of the 'global warming' effect is incurred. Another environmental impact of exhaust emissions is the generation of 'smog.' This occurs when the nitrogen oxides and hydrocarbons in exhaust emissions react with sunlight. This forms a thick, black fog that settles very low to ground level. Besides the apparent risk of increased accidents due to poor visibility, the presence of smog has a devastating impact on human health. This includes irritation to eyes, as well as coughing and breathing difficulties [Husselbee (1984)].

It has been identified in recent studies by Wyman (2012) that 80% of central London's most harmful air pollutants are the result of vehicle tailpipe emissions with the predominant source being from diesel powered vehicles. The European Commission state that deaths caused as a result of air pollution exceed the number of deaths as a result of road accidents within the European Union (EU), with approximately 310,000 pollution related deaths each year [Wyman (2012)]. Such deaths can be the result of carbon monoxide replacing the red blood cells within the human body causing a reduction in oxygen supply. In more minor cases this can result in headaches and drowsiness. Other substances such as sulphur and particulates can also have a devastating impact on human health in the form of a variety of respiratory problems and even

cancer [Husselbee (1984), Challen and Baranescu (1999)]. It has been estimated by the European Commission that the healthcare costs incurred as a result of being subjected to air pollution within the EU are approximately €427-790 billion per year [Wyman (2012)].

2.2 Worldwide legislation

As a result of the growing awareness of the detrimental impact of exhaust emissions on both human health and the earth's atmosphere, the first stage of European emissions legislation was outlined and implemented in 1992. Ever since, these regulations have been frequently updated and tightened as a result of the increasing concern of national governments as well as the introduction of various emission reduction technologies. Currently, all European vehicles must adhere to Euro 5 regulations introduced in 2009, however the regulations for Euro 6 are currently outlined and expect to be implemented for 2014 [Challen and Baranescu (1999)].

In the past decade a significant increase in the sales of diesel powered vehicles has been evident, this is primarily due to the substantial benefits regarding fuel economy and lower CO_2 emissions. However, these advantages come with an increase in NO_x emissions. Due to these different characteristics it is apparent that the diesel engine requires a specific set of regulations, differing to those outlined for the gasoline equivalent. The European regulations for a diesel passenger car are outlined in Table 2-1 below. When analysing this table the constant tightening of emissions regulations since 1992 is clearly evident [Official journal of the European Union (2007)].

*Denotes diesel engines with indirect fuel injection

† Denotes diesel engines with direct fuel injection

Standard	Year	Mass of carbon monoxide	Mass of oxides of nitrogen (g/km)	Combined mass of total hydrocarbons and oxides of nitrogen	Mass of particulate matter (g/km)
EU Stage 1	1992	2.72* / 3.16†	-	0.97* / 1.13†	0.14* / 0.18†
EU Stage 2	1996	1	-	0.7* / 0.9†	0.08* / 0.1†
EU Stage 3	2000	0.64	0.5	0.56	0.05
EU Stage 4	2005	0.5	0.25	0.3	0.025
EU Stage 5	2009	0.5	0.18	0.23	0.005
EU Stage 6	2014	0.5	0.08	0.17	0.005

Table 2-1. Diesel emission regulations for Europe [Official journal of the European union (2007), Hillier and Coombes (2004)]

Table 2-2 demonstrates the Tier two emissions legislation for the USA which has been steadily incorporated since 2004. Unlike European regulations, this standard has 8 bins which all feature different emission limits. Bin 1 features vehicles with zero emissions while bin 8 is for vehicles that feature the maximum allowable emission levels for a passenger car. Car manufacturers are to state what emission limits they can adhere to and hence which bin their product falls into. Tier 2 regulations feature an allowance for an increase in vehicle emissions after a period of 5 years or 50,000 miles this is to cater for engine wear reducing engine efficiency [US environmental protection agency (2000)].

Similar to European legislation, American emissions regulations have seen significant tightening over the past decade as allowable emissions limits were drastically reduced with the replacement of Tier 1 for Tier 2. Both Europe and the USA have introduced tax penalties if the stated emission targets are not met [US environmental protection agency (2000)].

BIN	Intermediate life (50,000 miles)					Full service life (120,00 miles)				
	NMOG	CO (g/mil	NOx (g/mil	PM (g/mil	HCHO (g/mil	NMOG (g/mil	CO (g/mil	NOx (g/mil	PM (g/mil	HCHO (g/mil
8	0.1	3.4	0.14	-	0.015	0.125	4.2	0.2	0.02	0.018
7	0.07	3.4	0.11	-	0.015	0.09	4.2	0.15	0.02	0.018
6	0.07	3.4	0.08	-	0.015	0.09	4.2	0.1	0.01	0.018
5	0.07	3.4	0.05	-	0.015	0.09	4.2	0.07	0.01	0.018
4	0.07	-	-	-	-	0.07	2.1	0.04	0.01	0.011
3	-	-	-	-	-	0.055	2.1	0.03	0.01	0.011
2	-	-	-	-	-	0.01	2.1	0.02	0.01	0.004
1	-	-	-	-	-	0	0	0	0	0

Table 2-2. Emission regulations for the USA (Tier 2) [US environmental protection agency (2000)]

Japan was one of the first countries to implement emission regulations with the first standards being implemented in 1986. However, the following decade did not see a significant tightening of these regulations resulting in Japanese emission standards being relatively relaxed when compared with other international standards of that period. Since 2002, Japan has implemented emissions regulations comparable to that of the EU. The most recent addition was in 2009 with restrictions on the following emissions for diesel powered passenger vehicles; CO (0.63 g/km), HC (0.024 g/km), NOx (0.08 g/km) and PM (0.005 g/km) [Japanese Emission Standards for Diesel Passenger Cars (2009)]

It is evident from the previous sections that exhaust emissions incur a significant detrimental impact on both the environment and human health. As a result governments worldwide have implemented continuously tighter emissions legislation putting further pressure on the automotive industry to develop newer and more efficient emission reduction techniques. When considering these factors further research into advanced exhaust after treatment techniques is clearly justified.

2.3 Formation of diesel engine emissions

As previously mentioned, a diesel engine running at ideal conditions would only emit water and CO_2. However, in practice, ideal conditions are never achieved and hence incomplete combustion of the hydrocarbon diesel fuel is apparent. This results in a variety of chemical

species being formulated. It is necessary to understand the mechanism behind the formation of these various chemical species in order to design and optimise sufficient after treatment technologies.

2.3.1 Unburned hydrocarbons

Unburned hydrocarbon emission is the result of unburned or partially burned fuel. The injection event on a CI engine occurs just before top dead centre (TDC) on the compression stroke. During this event, the fuel must mix with the compressed air to form a mixture that is within combustible limits. If the mixture surrounding the reaction zone is too lean to auto ignite or support a propagating flame then the fuel found in these areas can remain unburned and become the source of unburned hydrocarbon emission. The longer the period between injection and combustion (delay period) then the more unburned hydrocarbons produced. It must also be noted that an overly rich mixture can also be the source of unburned hydrocarbons as the mixture contains insufficient air to auto ignite. In this case, the excess fuel can only be burned during the expansion process once the mixture has been subjected to more air [Heywood (1988), Stone (1999), Challen and Baranescu (1999)].

A second primary source of unburned hydrocarbon emission is the result of trapped fuel in the injector nozzle sac (small volume located at the tip of the nozzle) entering the combustion chamber late in the cycle where the temperature and pressure is no longer sufficient for the fuel to auto ignite, resulting in unburned fuel being expelled from the cylinder during the exhaust stroke [Stone (1999)].

2.3.2 Nitrogen Oxides

The combination of nitrogen oxide (NO) and nitrogen dioxide (NO_2) is referred to as nitrogen oxides (NOx). NO is one of the primary sources of acid rain while both NO and NO_2 have a detrimental effect on the Ozone layer as well as being one of the primary sources of photochemical smog [Plint and Martyr (1999)].

Typically 70-90% of NOx consists of NO while the remainder is NO_2. Unlike other CI engine emissions which are generated as a result of incomplete combustion, NOx is formed when nitrogen from the atmosphere becomes oxidised within the combustion chamber. For this reaction to occur a plentiful supply of oxygen and a significant level of heat is required. This is supported in figure 2-1 below, where excessive NOx concentration levels (5000 ppm) are reached as a result of an ample supply of oxygen ($\phi \leq 1$) and a substantial flame temperature (in excess of 2400K.) [Johnson (2008) and Won (2010)].

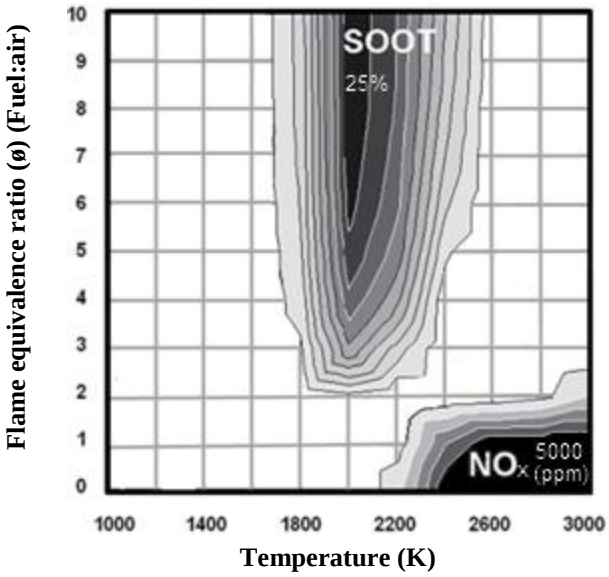

Figure 2-1. Diesel NOx and soot formation as a function of equivalence ratio and flame temperature [Won (2010)].

The formation of NO is demonstrated below by the Zeldovich mechanism [Challen and Baranescu (1999)]:

$$O + N_2 = NO + N$$

$$N + O_2 = NO + O$$

$$N + OH = NO + H$$

NO is primarily formed in the high temperature burned gas regions of the diesel combustion chamber. These regions are formed when gas inside the chamber burns before the peak cylinder pressure has been reached. As a result, once peak cylinder pressure is attained the gas is

increased to a temperature higher than that of any other part of the fuel/air mixture. This excessive temperature is ideal for rapid NO formation [Challen and Baranescu (1999)].

Due to diesel engines injecting fuel just before the commencement of combustion, the distribution of fuel within the cylinder is typically non uniform throughout the early stages of the combustion process. NO formation is at its highest where fuel/air ratios within the burned gas regions are closest to stoichiometric [Heywood (1988)].

As a result of these two features, nearly all NOx emission is formed between the start of combustion and the first 20° of crank angle. Therefore most NOx reducing techniques are focused on this critical period [Challen and Baranescu (1999)].

Nitrogen dioxide is formed from nitrogen oxide. It is commonly believed that the conversion from NO to NO_2 is the result of reactions such as the one shown below [Stone (1999)]:

$$NO + HO_2 = NO_2 + OH$$

As previously mentioned, NO_2 typically accounts for only a small portion of overall NOx emission due to a majority of it being rapidly cooled by the excess oxygen present in the cylinder and hence freezing its formation [Challen and Baranescu (1999)].

It must be noted that although many techniques exist to reduce NOx emissions, these are mainly based on the principle of reducing combustion temperatures. This results in an increase in particulates and hydrocarbon formation as well as being detrimental to fuel consumption [Challen and Baranescu (1999)].

2.3.3 Particulates and Smoke

Particulate matter (PM) is generated as a result of incomplete combustion. Majewski and Khair (2006) define PM as any solid or liquid matter present in a cooled and diluted exhaust sample. Alongside NOx emission, PM is one of the major concerns regarding diesel emissions. This is not only due to the major contribution to global warming and the formation of smog but also due to

the adverse effect that PM has on human health. These effects include both cardiovascular and respiratory issues. [Challen and Baranescu (1999)].

Research performed by Zabetta and Hupa (2005) and Yao (2009) identify that PM formation is a four stage process. During the first stage, intact segments of fuel or lubricant that survived combustion decompose to form precursors for carbon processes. As a result, carbon compounds such as graphene can be formed. The second stage involves the enlargement of these carbon compounds hence forming carbon particles. In the third stage these particles begin to agglomerate resulting in larger clusters or chains of particles forming soot. The final stage sees further agglomeration between the soot particles, ash and incompletely combusted oil and fuel to form particulate matter. Figure 2-2 is a schematic of diesel particulate matter on completion of the four stages.

Particulate matter is often categorised into three main groups; solid fractions (SOL), soluble organic fractions (SOF) and sulphate particulates (SO_4) [Majewski and Khair (2006)].

The solid fraction includes ash and carbon. Carbon, when finely dispersed, appears as smoke from the exhaust tailpipe. Early diesel engines were renowned for emitting excessive smoke before recent developments in PM filters and advancements in engine design [Haddad and Watson (1984)]. As previously mentioned, carbon is also the source of soot which forms in localised fuel rich regions. These regions occur as a result of non uniform fuel distribution within the cylinder. Figure 2-1 (section 2.3.2) demonstrates that beyond an equivalent ratio of 2, an increase in the richness of the equivalent ratio results in a linear increase in the concentration of soot. However, this relationship is only apparent within a specific flame temperature range. Below this range, the low temperature limits the level of soot that can be produced while exceeding the range results in the soot being oxidised [Won (2010)]. The other solid fraction of particulate matter is ash. Ash consists of an array of components including various iron oxides (rust sourced from the exhaust manifold), metal oxides (as a result of engine wear) as well as impurities and components formed as a result of burning additives contained within the lubrication oil [de Blas (1998) and Majewski and Khair (2006)].

The soluble organic fraction refers to the hydrocarbons present in the particulate matter. These hydrocarbons are the result of evaporated and atomised oil as well as a very small volume of fuel evading oxidation in the cylinder. These hydrocarbons begin to be adsorbed by the primary carbon particles to form the typical particulate matter structure shown in Figure 2-2 [Kittelson *et al* (1999)]. A scanning electron micrograph (SEM) of typical particulate matter is also demonstrated in figure 2-3 where the grains of carbon/ash are clearly visible alongside various hydrocarbons and sulphuric acid particles [Wyman (2012)].

Sulphate particulates refer to the sulphate and bound water within the particulate matter. Typically these components form 14% of the overall composition. As with hydrocarbons, sulphate particles can be adsorbed forming a sulphate layer around the primary carbon particles. It can be noted in figure 2-2 that sulphuric acid is also present. This is a result of a small quantity of sulphur (2-5%) leaving the combustion chamber as sulphur trioxide this can react with water and form sulphuric acid as demonstrated below:

$$SO_3 + H_2O = H_2SO_4$$

The remaining sulphur content exits the combustion chamber as sulphur dioxide. [Majewski and Khair (2006) and Kittelson *et al* (1999)]:

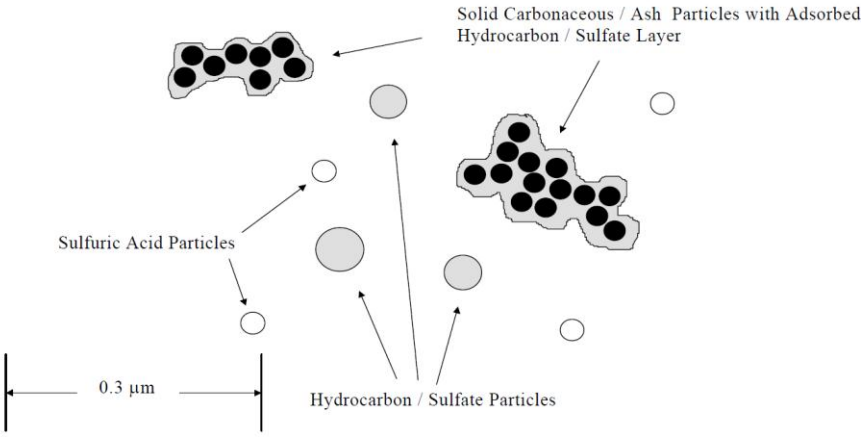

Figure 2-2. Schematic of diesel particulate matter [Kittelson *et al* (1999)].

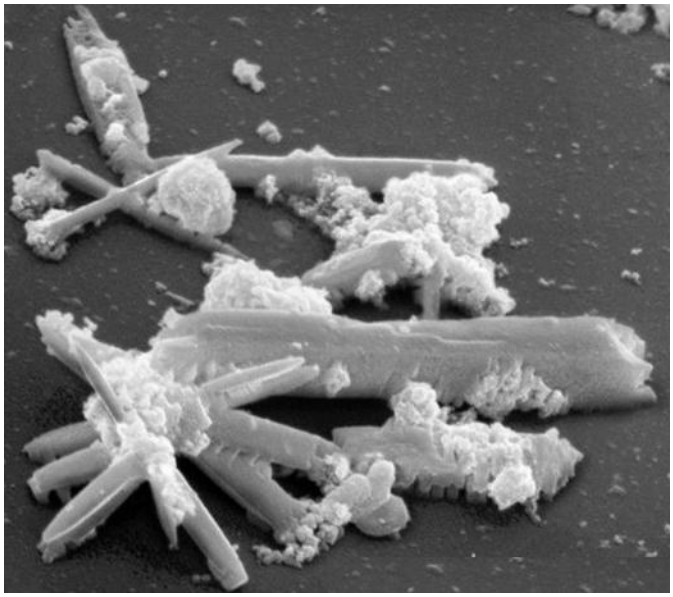

Figure 2-3. SEM of typical particulate matter [Wyman (2012)].

2.3.4 Carbon Monoxide

Carbon monoxide (CO) is a toxic gas that causes death by suffocation. This is due to the ease in which CO combines with the haemoglobin of the blood, preventing the transportation of oxygen round the body. Inhaling as little as 0.3% by volume can result in death within a 30 minute period. CO is a result of incomplete combustion of hydrocarbon fuel, it is very dependent on the air/fuel ratio and increasing the richness of the mixture above stoichiometric, directly increases the volume of CO emitted. However, due to CI engines running significantly lean of stoichiometric the CO levels are typically well below what European legislation requires. Incomplete mixing or combustion occurring in rich areas are typically the causes of any CO being emitted from a CI engine [Wellington and Asmus (1995), Brady (1996), Challen and Baranescu (1999)].

2.3.5 Unlegislated emissions

Modern emission legislation does not cover all components of diesel exhaust emission. A variety of unlegislated emissions still remain which have been subjected to scrutiny in recent years. This is primarily due to the increasing awareness of the impact that such components have on

human health. As a result there is a strong possibility that such emissions will be included in future legislation rendering it important to understand the mechanisms behind their formation.

Aldehydes are primarily formed in oxygen rich conditions and are therefore predominant in diesel exhaust gas. They are formed as a result of incomplete combustion. Along with aromatic hydrocarbons, aldehydes are the source of diesel exhaust odour, a characteristic that has long been associated with diesel engines. Some aldehydes demonstrate toxic properties and even in small quantities can cause significant irritation to the eyes and nose. Aldehydes such as formaldehyde, acetaldehyde and acrolein are recognised as being carcinogenic as well as a source of photochemical smog. As a result, aldehydes have come under much scrutiny in recent years. It must be noted that with the implementation of an oxidation catalyst the conversion of aldehydes can be as high as 70% [Challen and Baranescu (1999) and McWilliam (2008)].

Polycyclic aromatic hydrocarbons (PAH) exist both in the vapour phase and particulate phase and are a concerning component of diesel exhaust emission due to their carcinogenic properties. The works of Borras *et al* (2009) identify high temperature combustion, engine oil and unburned fuel as being the main sources of PAH emission. This study also indicates that the formation of PAH emission is strongly dependent on driving conditions with significantly high PAH presence during cold start and accelerating cycles. As with aldehydes, PAHs can be reduced with an oxidation catalyst. However, the efficiency of this process is dependent on the mass of the component. Lighter polycyclic aromatic hydrocarbons can demonstrate high conversion rates of 80% while heavier components can demonstrate as little as 30% conversion efficiency. It must also be noted that due to nitrating components in the exhaust there is also the risk of nitrated polycyclic aromatic hydrocarbon formation (NPCH), some of which feature carcinogenic and mutagenic properties [Challen and Baranescu (1999)].

2.4 After Treatment of CI engine emissions

The increase in popularity of diesel powered vehicles has resulted in substantial research into diesel after treatment technologies. As well as CO, HC and NOx emissions, the studies of Guanglong (1994) describe how diesel emissions also contain 50-80 times more particulate emissions than the gasoline equivalent making the target for zero emission diesel engines a

substantial task. The following section identifies a variety of after treatment methods typically adopted for modern diesel after treatment.

2.4.1 Catalytic Converters

The catalytic converter was one of the earliest emission reduction technologies to be introduced. As emission legislation has become increasingly stringent, development of the catalytic converter has been ongoing.

A typical oxidation catalytic converter is constructed of a monolith honeycomb substrate which is coated with a catalyst, typically platinum. The substrate is housed within a steel container and located between the exhaust manifold and tailpipe. Due to the presence of the catalyst coating, regulated emissions such as unburned hydrocarbons and any CO (if present) become oxidised by the surrounding oxygen rich exhaust gas flow, resulting in a conversion to water and/or CO_2 [Heywood (1988) and Ozturk (1994)]. This is demonstrated by the following reactions:

$$CO + ½\ O_2 \rightarrow CO_2$$

$$\text{Hydrocarbons} + O_2 \rightarrow CO_2 \text{ and } H_2O$$

The works of Chen and Jha (2004) describe how the catalytic converter substrate is typically constructed with high chromium, high aluminium FeCrAl alloy in a foil form. This gives various advantages over the traditional ceramic based substrate including increased robustness, ease of manufacture and the ability to adopt honeycomb cells with thinner walls allowing for lower back pressure and higher cell density.

The FeCrAl alloy substrate typically contains traces of yttrium and hafnium. Other elements can also be present including; Cerium, Lanthanum and Samarium. These components allow for the substrate to withstand temperatures of up to 1100°c, a feature which is necessary for gasoline engines due to the substantial temperatures obtained within the catalytic converter assembly. However, it must be noted that the addition of these elements can result in the alloy being difficult and expensive to manufacture to foil thickness [Chen and Jha (2004)].

Although this temperature resistance is required for gasoline engine applications, it must be noted that diesel engines operate much leaner than the gasoline equivalent and as a result feature considerably cooler exhaust gas flows (max. 800°c). Chen and Jha (2004) describe how this feature demonstrates an opportunity for the design of FeCrAl substrates to be modified improving the cost effectiveness and ease of manufacture while still resisting temperatures of up to 800°c.

The primary issue faced with catalytic converter design is the reduction of the 'light off' temperature. This is described in the work of Ozturk *et al* (1994) who described the light off temperature as being the required catalytic converter temperature necessary to convert a minimum of 50% of CO and HC. When analysing figure 2-4 below it is evident that this is achieved, for a typical diesel application, at approximately 225°c. This indicates therefore, that during the initial stages of the cold start cycle, the effectiveness of the catalytic converter is relatively low. Another issue faced with the implementation of a catalytic converter is the restrictions placed on the sulphur content of the diesel fuel (cannot exceed <0.05% by mass). This is due to the risk of the sulphur content becoming oxidised by the catalyst and forming sulphur trioxide followed by sulphuric acid. The presence of sulphate deposits could then begin to block the catalyst assembly [Stone (1999)].

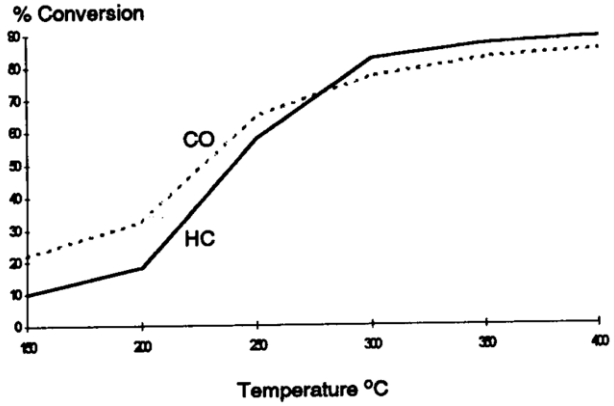

Figure 2-4. Diesel catalytic converter conversion efficiencies [Ozturk *et al* (1994)].

While HC and CO are created as a product of incomplete combustion, NOx is a by product of combustion. As a result, the reduction of NOx cannot be achieved with the application of an oxidation catalyst. Heywood (1988) describes the operating principles of an NO reduction

catalysis which adopts the CO, hydrocarbons and H_2 present in the exhaust to reduce the NO levels via a variety of reactions. In order to obtain the necessary level of these reacting species, a rich mixture is required to ensure the number of reducing species exceeds that of the oxidising species. However, for a diesel engine application this is not possible due to the diesel engine running at substantially lean conditions. As a result, a variety of research has been performed (and is still ongoing) into many novel NOx reduction methods for diesel engine aftertreatment. These various methods are generally referred to as 'DENOX' techniques.

One of the primary methods of NOx reduction in diesel exhaust gas is the implementation of Selective Catalytic Reduction (SCR). The work of Stone (1999), describes how this method is based on the addition of urea or ammonia into the exhaust flow, which can then perform high NOx conversion when contacted with a catalyst surface. Studies performed by Hirata *et al* (2009) identify that the amount of aqueous urea solution (forming NH_3) injected into a SCR system must be precisely controlled to equal the level of NOx emission to ensure there is no redundant solution emitted from the exhaust. Hirata *et al* (2009) also describe how the adoption of urea to generate ammonia results in significant lag times between the urea injection event and NOx reduction, resulting in untreated NOx emission travelling through the SCR. The cause of this lag time is based on the time taken for the solution to reach the catalyst as well as the time required to convert the urea to NH_3. This feature is particularly prominent during transient conditions when the levels of NOx emission are constantly changing making it difficult to achieve an instantly matched urea injection response and therefore avoid untreated NOx or excessive ammonia. If achieved proficiently, the SCR technique can achieve up to 80% reduction in NOx emission.

Another popular method of DENOx after treatment is the implementation of a passive or active 'DENOx catalyst'. A passive DENOx system attempts to adopt the use of hydrocarbons already present in the exhaust gas flow to chemically reduce NOx emission. Stone (1999) describes that within the minimal temperature window of 160-220°C, oxygen and NOx both compete for HC resulting in a reduction in NOx emission. When considering the relatively cold exhaust temperatures exhibited by the diesel engine, it is evident that this temperature range can be achieved during normal engine operation. Studies by Klein *et al* (1999) indicate the primary limitation of passive DENOx systems being poor NOx conversion as a result of diesel exhaust gas

exhibiting insufficient quantities of HC. As a result an active DENOX system is typically preferred, where hydrocarbons are added to the exhaust flow by either injecting additional fuel into the exhaust stream or introducing fuel into the cylinder as a post injection event. Both Stone (1999) and Klein *et al* (1999) describe the NOx conversion potential of an active DENOx system to be approximately 20% with a typical 1.5% fuel consumption increase penalty. This surprisingly low conversion rate is the result of all the necessary conditions for sufficient conversion not occurring at the same time. This includes the amount and type of HC species as well as exhaust flow rate and temperature. Although this technology features low NOx conversion, studies by Lepperhoff *et al* (2000) discovered that further reduction of the sulphur content in diesel fuel can further enhance the NOx conversion rate of active DENOx technologies. This was demonstrated by a NOx conversion increase of 12% over the latest European drive cycle when the sulphur content was reduced from 49 to 6 wt. ppm [Klein *et al* (1999)].

2.4.2 Particulate matter traps

Due to the minimal effect that catalytic converters have on reducing soot numbers, particulate matter traps, otherwise known as diesel particulate filters, are often implemented in conjunction with a catalytic converter in an effort to reduce the exhaust soot number. Particulate matter traps are a physical filter situated in the exhaust gas flow. As the trap filters the exhaust, the base of the filter becomes increasingly contaminated with carbon particulates. As a result, the exhaust back pressure is continually increased resulting in increased exhaust temperature. Once the temperature exceeds that required for particulate matter oxidation, the accumulated particulate matter is then ideally oxidised with existing oxygen thus producing carbon dioxide, hence 'regenerating' the filter to its clean state [Heywood (1988) and Bromberg et al (2005)]. The rate of this oxidation process can be calculated by first determining the reaction rate (RR) of the particulate layer (equation 2-1). Following this, equation 2-2 can be adopted to identify the variance in particulate mass per unit of time.

$$RR = A_p \times [O_2]^m \times \exp\left[\frac{-E_p}{R \times T}\right]$$

Equation 2-1. Reaction rate of particulate layer [Janiszewski et al (2001)]

$$\left[\frac{\mathrm{dm_p}}{\mathrm{dt}}\right]_{trap} = Q \times C_{in} \times \eta_f - m_p \times RR$$

Equation 2-2. Rate of change of particulate mass in the trap [Janiszewski et al (2001)]

RR	*- Reaction rate of particulate layer*	*T*	*- Temperature*
A_p	*- Frequency factor of reaction*	m_p	*- Net particulate mass collected in trap at time (t)*
O_2	*- Oxygen concentration*	*t*	*- Time*
m	*- Reaction order*	*Q*	*- Exhaust volumetric flow rate*
E_p	*- Activation energy*	C_{in}	*- Trap inlet particulate concentration*
R	*- Gas constant*	*f*	*- Trap efficiency*

By obtaining the particulate rate of change from equation 2-2, it is possible to identify the operation mode that the filter is in. If dm_p/dt is greater than zero, then the trap is accumulating soot. If less than zero then regeneration is occurring. Equalling zero indicates that the process is in equilibrium i.e. mass of particulates trapped per unit of time is equal to the mass of soot oxidised per unit of time. This occurs when the 'balance temperature' is reached, see equation 2-3 [Majewski and Khair (2006)].

$$m_p \times RR = \eta_f \times Q \times C_{in}$$

Equation 2-3. Equilibrium, indicating balance temperature has been achieved

The three operational modes of a DPF filter are summarised by Majewski and Khair (2006) in figure 2-5 below. In the accumulation mode (A), the temperature is relatively low, resulting in a low oxidation rate. As a result soot begins to accumulate of the filter and hence increase the pressure difference across the DPF. Equilibrium mode (B) demonstrates the balance temperature has been reached (see equation 2-3). In this mode the soot oxidised is equal to the soot accumulating and hence the pressure difference remains unchanged. Between modes (B) and (C), an initial increase in temperature results in a sudden increase in the pressure difference. This is due to the increased temperature leading to an increase in volumetric flow rate (Q) and hence increased rate of particulate accumulation. However, this increased accumulation rate is overcome by the significantly increased oxidation rate as a result of the increased temperature

and hence increased reaction rate (RR). As a result the filter enters the regeneration mode (C) where the accumulated soot begins to burn off.

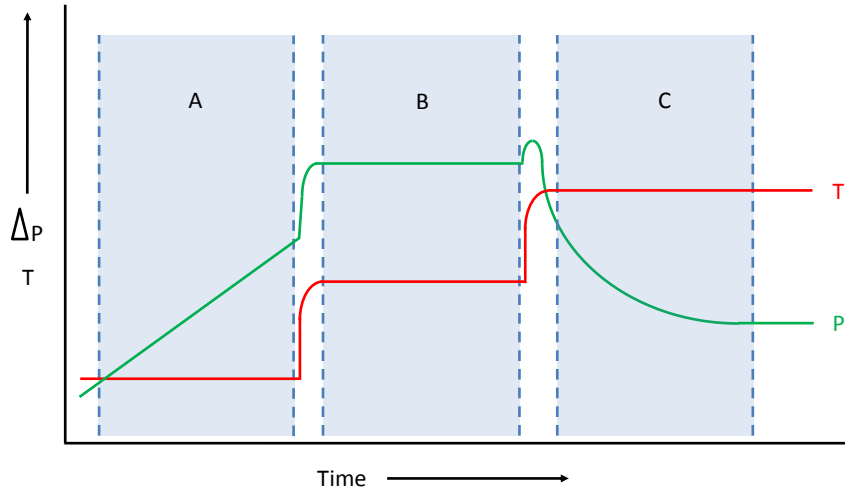

Figure 2-5. DPF operation modes [Majewski and Khair (2006)].

Figure 2-6 below demonstrates the impact of exhaust temperature on the oxidation rate of soot. The equations used to formulate this graph were derived from equations 2-1 and 2-2 (demonstrated previously on pages 38 and 39 respectively). The constant values used to generate this example are derived in the works of Lee (2010) and can be identified below in table 2-3. As previously stated an increase in exhaust temperature increases the reaction rate and hence the oxidation rate of soot for a constant engine condition. This trend is clearly defined in figure 2-6. In addition, this data also demonstrates the relationship between reaction rate and the mass of particulate matter located on the filter. It is evident that this relationship can be divided into two zones. Zone 1 demonstrates that the reaction rate of soot at a given engine condition stays constant above a defined volume of particulate mass on the filter. However, below this threshold (zone 2) the reaction rate begins to decline as the mass on the filter is reduced [Lee (2010)]. The effect of this two zone characteristic is demonstrated in figure 2-5 where it is somewhat imitated during the regeneration process (C). The initial stage of regeneration demonstrates a relatively constant rate of reduction of pressure loss across the filter as a result of the reaction rate being in zone 1. However, as the mass on the filter reduces the reaction rate begins to reduce (zone 2) which in turn results in the gradient of pressure

difference flattening out as the limits of regeneration for the given engine conditions are reached.

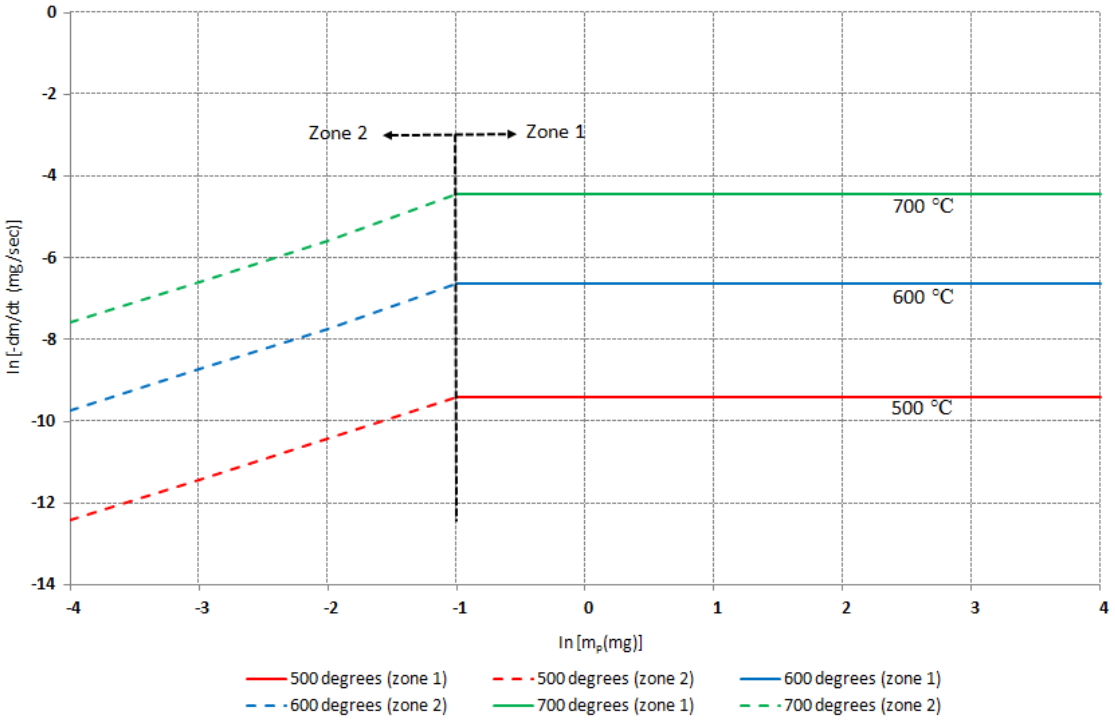

Figure 2-6. The effect of particulate mass and exhaust temperature on reaction rate

Constant	Zone 1	Zone 2	Units
A_p	1.26×10^7	1.28×10^7	1/s
E_p	155.5	151.3	KJ/mol*K
R	0.008314	0.008314	KJ/mol*K
O_2	0.21	0.21	%
m	1	0.8	-

Table 2-3. Constant values (Lee 2010)

Particulate matter traps are typically constructed of ceramic materials such as silicon carbide or cordierite. The structure of the trap consists of a series of rectangular tubes. Each alternative tube is blocked at one end resulting in the exhaust gas flow being forced to travel through the tube walls which feature a number of pores. In turn, the flow is filtered resulting in particulates

being deposited on the filter walls [Hanamura *et al* (2009)]. This process is demonstrated below in figure 2-7.

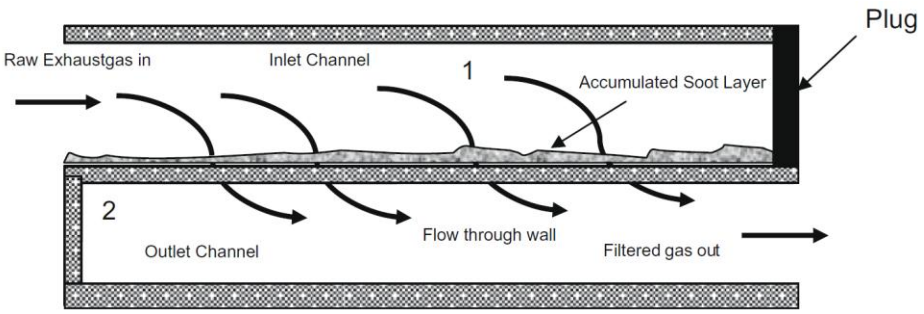

Figure 2-7. Operating principles of a particulate matter trap [Zheng and Banerjee (2009)].

The initial stage of the DPF filtering process is recognised as the 'depth filtration' stage. This is where the smaller range of soot particles (<μm) become trapped in the filter pores and gradually reduce both the permeability and porosity of the DPF. As the depth filtration stage continues, eventually areas of the DPF begin to reach their maximum packing density, rendering the pores impermeable. As a result, soot begins to accumulate in these areas (see figure 2-7) recognised as the second stage of filtration; the 'cake formation' stage [Bensaid *et al* (2009)].

Although particulate traps can typically demonstrate a 90% filtering efficiency they are not without a number of application issues. Firstly, during the loading process, the particulate matter accumulated on the trap results in an increase in exhaust back pressure. The effect of this is a corresponding increase in brake specific fuel consumption. This trend continues until the filter is fully loaded and the trap begins to regenerate. As a result, it is beneficial to the system that the trap regenerates as close to the fully 'clean' condition as possible. The loading and regenerating cycle and its influence on exhaust back pressure and BSFC can be identified below in figure 2-8.

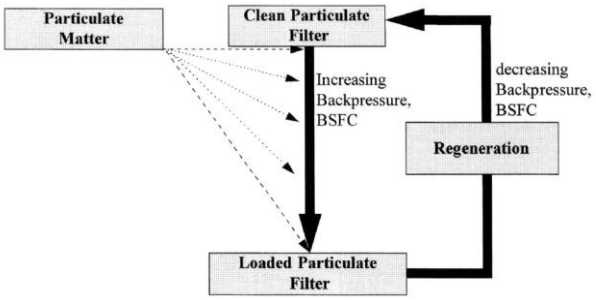

Figure 2-8. The effect of trap loading and regeneration on back pressure and BSFC [Summers *et al* (1996)].

Another application issue is highlighted during the ignition of the accumulated particles. It is critical that this process is sufficiently controlled as the resultant high temperatures and thermal stress can induce damage to the filter. This is supported by Park *et al* (2010) who state that although ceramic materials demonstrates a high melting point and low production costs, they do feature a low thermal shock resistance which can result in cracks when subjected to large thermal change.

Finally, under normal operating conditions, and with no additional controls, diesel exhaust gas temperature is typically too low to oxidise accumulated particulate matter which features a self ignition temperature of 500-550°c. As a result oxidisation is typically achieved by reducing the self ignition temperature of the diesel particulates via the introduction of catalyst coatings. However, during the cold start cycle or periods of low engine speed, even this reduced ignition temperature cannot be achieved due to insufficient exhaust gas temperature. Therefore, additional techniques are required to increase exhaust temperatures and hence ensure consistent regeneration events. Such methods can include modifications to injection timing, the introduction of intake air throttling, adjustments made to the engine operating map, electrically heating the trap or injecting additional fuel upstream of the filter [Tadrous *et al* (2010), Eastwood (2010) and Heywood (1988)].

Particulate traps are typically implemented in conjunction with a catalyst in order to meet present emission legislation. As previously discussed, this is due to the minimal effect that catalysts have on reducing soot numbers. When used in conjunction, Schaefer *et al* (2009)

indicate the importance of understanding the interaction between the two sub systems in order to identify the most beneficial exhaust system arrangement. In this study Schaefer *et al* (2009) describe how situating a catalyst before the particulate trap aids in improving cold start NOx emissions due to the catalyst warm up time being reduced, while placing the particulate trap in front of the catalyst will result in ideal regeneration management. The impact of this arrangement is further supported by the works of Hirata *et al* (2009) who identified that placing a particulate trap upstream of an SCR catalyst although beneficial to the regeneration process, resulted in an increased volume before the catalyst, reducing the exhaust temperatures at the catalyst and hence reducing the NOx conversion efficiency. However, regardless of arrangement, implementing both a catalyst and particulate trap can still prove costly and complex. As a result, one of the main objectives of modern aftertreatment research is to attempt to amalgamate the two sub systems. An example of this is found in the works of Ballinger *et al* (2009) who describe the union of an SCR system with a particulate trap by coating the walls of the trap with the SCR coating, significantly reducing the cost and packaging issues.

2.4.2.1 Space velocity

Another factor that influences both catalytic converter and particulate matter trap performance is space velocity. Space velocity indicates the volume of exhaust gas treated per unit of time. Equation 2-4 below demonstrates how the exhaust gas volumetric flow rate (Q(m^3/h)) and the reactor volume (Vrec(m^3)) can be adopted to calculate the number of times the reactor volume is filled per hour.

$$SV_{(hr^{-1})} = \frac{Q_{(m^3/h)}}{Vrec_{(m^3)}}$$

Equation 2-4. Space velocity

Therefore, for a particulate matter trap featuring a 10cm length and a 2.54cm diameter placed in an exhaust stream with a volumetric flow rate of 35 l/m, the space velocity can be calculated to be 41444.64 hr^{-1}.

In studies performed by Kim *et al* (1997), it was concluded that for a burner type particulate trap, an increase in space velocity resulted in a reduction in peak regeneration temperatures. It is speculated by Kim *et al* (1997) that this was due to the increased exhaust flow rate encouraging convective heat transfer. As a result, more of the heat generated by the exothermic reaction was removed by the exhaust stream from the filter walls and out of the system, thus reducing the peak regeneration temperature. This characteristic is greatly beneficial to the operating life of the trap.

However, there is a limit to the benefits obtained through increasing the space velocity. Besides the practical limit of the exhaust gas flow rate being dependent on the engine operating conditions, an excessive increase in space velocity can result in trap penetration by smaller particles. For some trap designs (even ones with very high filtration efficiency), a high space velocity can result in the filtration of larger particles but have a detrimental impact on the interception of smaller particles [Mayer *et al* (2004)].

2.4.3 Hydrogen addition

A variety of research has been performed in order to assess the potential emission benefits of hydrogen as a fuel. Hydrogen demonstrates a higher specific energy than diesel as well as producing only water as a combustion by-product. In addition, introducing hydrogen to the diesel combustion process can result in faster and more thorough combustion as a result of hydrogen burning considerably faster than diesel. McWilliam (2008), Megaritis and Tsolakis (2004), Megaritis and Tsolakis (2005) and Tsolakis *et al* (2004) have identified that the application of H_2 to the diesel combustion process can result in significant decreases in PM, CO, HC and fuel consumption. However, this is at the cost of an increase in both NOx and soot emissions. Bari and Esmaeil (2010) identified that hydrogen addition improved combustion as a result of hydrogen demonstrating a flame speed nine times faster than diesel. This characteristic results in higher peak pressures closer to TDC and hence increased work.

Hydrogen can also be adopted in conjunction with exhaust aftertreatment devices to aid in improving conversion efficiencies. This is apparent in the works of Satokawa *et al* (2003) who investigated the effects of hydrogen addition over an Ag/Al_2O_3 catalyst. This study identified a

significantly increased conversion efficiency of NO to NO_2 by O_2, especially apparent at low temperatures. It was concluded in this investigation that this was primarily due to the hydrogen activating hydrocarbons which in turn increase the conversion efficiency of the SCR catalyst (see section 2.4.1). The emission reducing advantages of hydrogen are further supported in the works of Wichterlova *et al* (2005) who also identified significantly high NOx conversion by an SCR catalyst with hydrogen addition. In this study it is assumed that the hydrogen itself partakes directly in the NOx reducing reaction.

Hydrogen can also be adopted to aid in particulate filter regeneration. As discussed in the previous section of this study, under normal operating conditions, the exhaust temperature of a diesel engine is not high enough to oxidise accumulated soot. In studies performed by Bromberg *et al* (2005) and Bromberg *et al* (2001) hydrogen was introduced to the exhaust stream in an attempt to initiate an exothermic reaction and hence support the regeneration process. These studies identified that the addition of hydrogen not only supports the regeneration process but can also increase the reliability and operating life of the filter due to reduced thermal stress.

2.4.4 Plasma aftertreatment

Plasma aftertreatment is another denox method, which is still currently in the early development stages. The system functions using two stages. In the first, a pulsed electrical field is introduced into the exhaust flow. This electrical field causes the gas molecules that form NOx to be broken down. Energetic electrons and O and N free radicals are what remain. Due to the oxygen rich exhaust flow and the collision of molecules in the exhaust, NO is then oxidised, forming NO_2. During the second phase, a catalyst is adopted to convert the NO_2 into nitrogen (N_2) [PSA (2001)].

Studies performed by Chae (2003) and Tonkyn (2003) identify the primary benefit of this technology as being the wide temperature window that high NOx conversion rate can be achieved. This includes high conversion at temperatures as low as 100°c. This is a significant advantage over traditional NOx reduction methods which demonstrate very poor conversion efficiency at low temperatures, especially apparent during the cold start cycle. Another

advantage of this technology is the immunity to sulphur, which as previously discussed, can be detrimental to other after treatment systems such as catalytic converters.

2.4.5 Exhaust gas recirculation

Exhaust gas recirculation (EGR) is another method of reducing NOx emission in diesel engines. This technology consists of an electronically controlled valve that allows a quantity of exhaust gas to be circulated back into the inlet manifold. The effect of this is the displacement of oxygen in the combustion chamber by the exhaust gas [Heisler (1999)]. This is demonstrated in figure 2-9 below where the introduction of 0.2g of EGR displaces the total charge mass reducing it from 1.5g (without EGR) to 1.3g [Ladommatos *et al* (1999)].

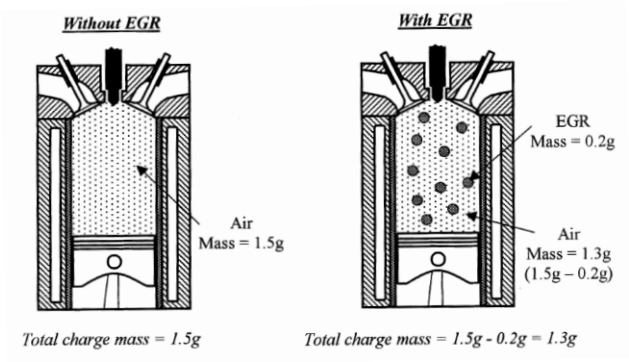

Figure 2-9. Displacement of charge mass by EGR [Ladommatos *et al* (1999)].

As demonstrated in section 2.3.2, NOx emission is formed when there is a plentiful supply of oxygen and significantly high temperature. With the introduction of EGR, the air inside the cylinder is displaced with a sample of exhaust gas, resulting in less oxygen available to form NOx. EGR also reduces the peak combustion temperatures within the cylinder due to exhaust gas having a higher specific heat (Cp) than air. This reduction in temperature again aids in the reduction of NOx formation. The increase in Cp with the addition of EGR is demonstrated in figure 2-10 below for a diesel engine at 32:1 air/fuel ratio.

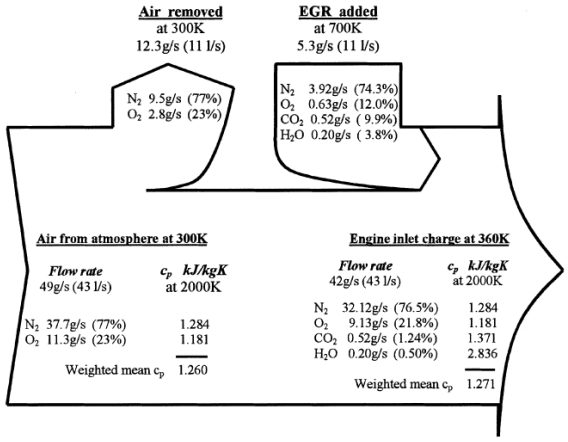

Figure 2-10. The effects of 25% EGR on the inlet charge [Ladommatos *et al* (1999)].

EGR concentration is typically identified by noting the variance in the inducting air flow volume of the engine. Due to diesel engines being unthrottled a reduction demonstrated by a volume air flow meter placed on the induction side of the engine will be approximately equal to the volume flow rate of EGR (assuming no change in volumetric efficiency). This is demonstrated in figure 2-10 where the volume flow rate of the air displaced and the EGR is equal at 11 l/s.

Although EGR has a substantial reducing effect on NOx formation, there is however limits to the extent in which it can be adopted. Studies by Ladommatos *et al* (1999), describe how the displacement of air by EGR results in a reduction in the oxygen mass flow rate. This is demonstrated in figure 2-10 where the O_2 mass flow rate is reduced from 11.3 g/s to 9.13 g/s. Although most of this is a result of reduced volumetric efficiency, a significant part of this reduction is the result of EGR not featuring as high an oxygen content as the air it replaces. This effect is recognised as the 'dilution effect' [Ladommatos *et al* (1999)]. Stone (1999) identifies that the result of the dilution effect is the presence of insufficient oxygen present to perform thorough combustion. The result of which is a possible increase in the formation of hydrocarbons, soot and CO as well as having a detrimental impact on fuel consumption. Therefore, to achieve a compromise between NOx, HC, CO and soot, it is necessary to implement optimised EGR values which are dependent on engine load and speed. The maximum EGR levels are adopted at the lowest speed and load conditions where a large amount of excess air is present. This can include up to 50% EGR at idle. However, during increasing speed and load conditions, the level of EGR must be decreased in order to maintain an optimised level of EGR

ensuring the best compromise can be achieved between NOx, HC, CO, soot and fuel consumption.

Studies by McWilliam (2008) and Ladommatos *et al* (1999) both describe how the introduction of EGR can increase the temperature of the inlet flow supplied to the cylinders. This is shown in figure 2-10 where the air temperature is increased from 300K to 360K with the addition of 25% EGR. This temperature increase can result in a reduction in volumetric efficiency as well as an increase in the gas temperature within the cylinder during the compression stroke and combustion. Therefore, it is typical for the EGR flow to be cooled between the exhaust and inlet manifold. However, in the works of Ladommatos *et al* (1999) it is identified that this method is largely ineffective at high levels of EGR.

Another significant disadvantage of EGR implementation is described by Aldajah *et al* (2007) who identified EGR as being a cause of oil degradation. This is due to the excess soot in the inlet charge contaminating the engine oil. This characteristic is also outlined by Abd-Alla (2002) who discusses how the addition of EGR can result in reduced oil lubrication and therefore increased engine wear. However, it must be noted that a high proportion of this wear is considered to be due to the presence of sulphur oxide in the recirculated gas. As previously discussed in this present study, the sulphur content in diesel fuel is constantly being revised and reduced.

2.4.6 NOx trap

Another modern denox technology is the NOx trap. When first introduced for lean burn gasoline engines, such technology demonstrated a significant reduction in NOx emission. As a result significant research has been performed in order to gain the same reduction benefits when implemented in a diesel exhaust. As stated in a report by MECA (2000) a 90% reduction in NOx emission can be achieved with the implementation of a NOx trap.

The operating principles of a NOx trap are demonstrated in figure 2-11 below. The NOx trap is situated in the exhaust stream. During normal operating conditions, NOx emission from the diesel combustion event enters the NOx trap. As previously stated in section 2.3.2, 70-90% of NOx emission is NO. The first stage of the NOx reduction process is to oxidise the NO into NO_2 as

this is adsorbed more easily than NO. This is performed by a catalyst site featuring a precious metal, typically platinum [MECA (2000)]. The oxidation process is demonstrated below [Johannes *et al* (2007)]:

$$\text{OXIDATION: } NO + 1/2O_2 = NO_2$$

Featured between the catalyst site and an aluminium oxide base are barium carbonate deposits ($BaCO_3$). The NO_2 is adsorbed by the $BaCO_3$ converting it to barium nitrate ($Ba(NO_3)_2$) and hence trapping and holding the NO_2. As a result of this reaction, CO_2 is emitted [Stone (1999)]. The adsorption process is demonstrated below [Johannes *et al* (2007)]:

$$\text{CHEMISORPTION: } BaO + 2NO_2 + \tfrac{1}{2}O_2 = Ba(NO_3)_2$$

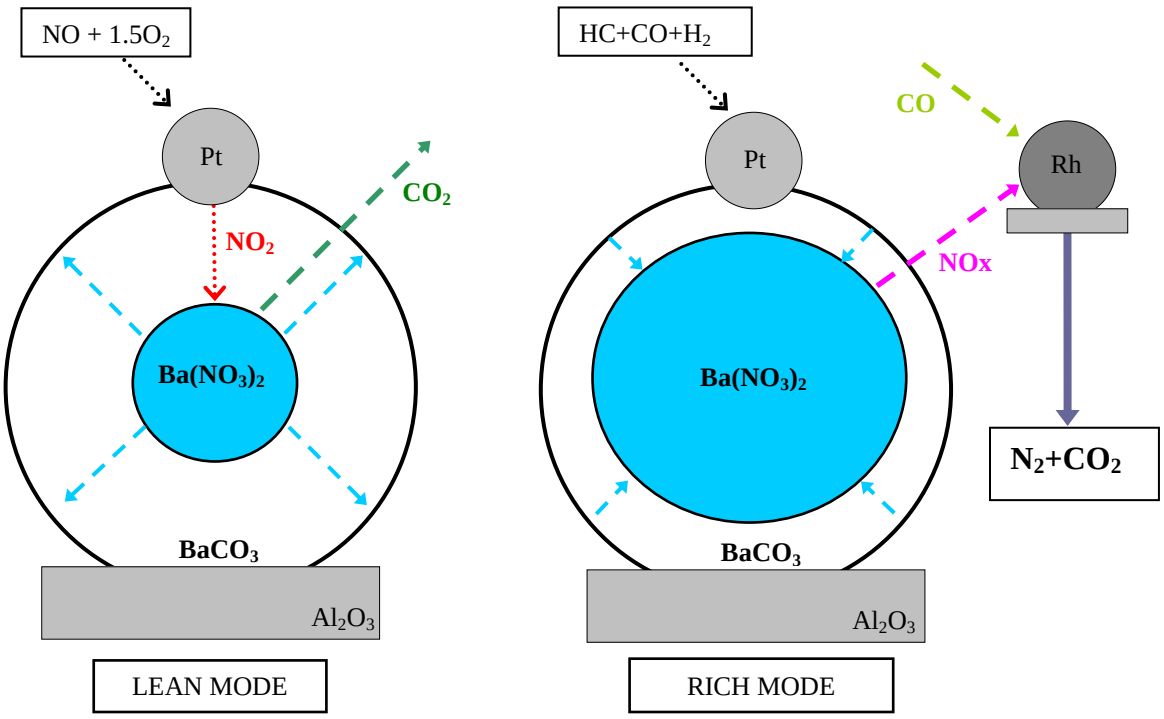

Figure 2-11. The operating principles of a NOx trap during lean and rich conditions

As demonstrated in figure 2-11, there is a practical limit to the amount of NO_2 that can be stored by a NOx trap and as a result the trap needs to be constantly regenerated. This is achieved by

briefly subjecting the trap to a rich environment. As previously stated in section 2.4.1 of this study, diesel engines run at substantially lean conditions. Therefore, a rich environment needs to be generated. This is commonly achieved either by introducing EGR, injecting a small volume of diesel fuel into the exhaust, or implementing 'in cylinder' regeneration. This technique involves the introduction of additional fuel into the cylinders while simultaneously throttling the engine intake flow resulting in the engine running under rich conditions [West *et al* (2004)].

Following exposure to a rich environment, the barium nitrate can then regenerate back to barium carbonate by adopting the hydrocarbons, carbon monoxide and hydrogen present in the rich mixture. The NOx that is easily released from this reaction is then converted to nitrogen and carbon dioxide by adopting carbon monoxide and a rhodium catalyst, similar to those adopted as a NO catalyst for gasoline engines [MECA (2000), Stone (1999)].

Although the implementation of a NOx trap can drastically reduce NOx emission from diesel engines, there are a variety of issues to consider. Firstly, as discussed in the works of Parks *et al* (2005), the implementation of a NOx trap can result in NH_3 and N_2O formation. The source of this can be from the stored NOx itself or from the exhaust gas during rich mode. Parks *et al* (2005) identified a general trend where an increase in the NOx stored resulted in an increase in NH_3 and N_20 generation.

A second limitation of NOx trap technology is the requirement for the exhaust gas to exceed a temperature of ~160°C for regeneration to take place. Therefore, the regeneration process can not occur at very low loads. This feature is identified in the works of Kong *et al* (2004), which concluded that at a speed of 15mph (exhaust temperature 145°C), a NOx trap implemented on a bus engine was unable to regenerate when diesel fuel was used as the regenerating agent. As a result of this feature, Kong *et al* (2004) investigated the effects of adopting hydrogen as a NOx trap regenerating agent. The substantial benefits compared to using diesel are demonstrated below in figure 2-12. It is evident from this graph that hydrogen does not only allow regeneration to occur at low exhaust temperatures (~120°C) but also demonstrates a much higher NOx conversion efficiency throughout the temperature range. However, as with all hydrogen based emission reduction technologies the challenge still remains of generating hydrogen on board and on demand [Kong *et al* (2004)].

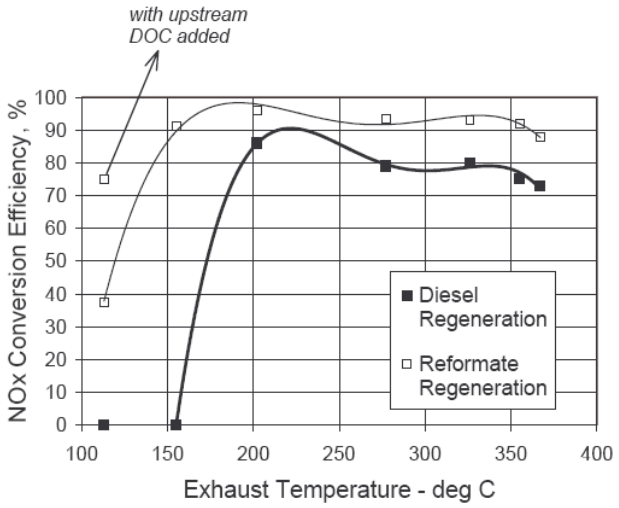

Figure 2-12. NOx conversion efficiency with diesel and hydrogen reformate [Kong *et al* (2004)].

Another limitation of NOx trap implementation is the necessity for diesel fuel that features low sulphur content. This is due to sulphur reducing the adsorption efficiency of the trap due to the formation of barium sulphate. Figure 2-13 below from the work of Guyon *et al* (2000) indicates the detrimental effect that sulphur content has on NOx trap efficiencies, even when as little as 5 parts per million (ppm). It is evident from this graph that even with a relatively low sulphur content of 50ppm, the NOx conversion efficiency is significantly reduced by approximately 40% before the engine has even reached 5000 kms.

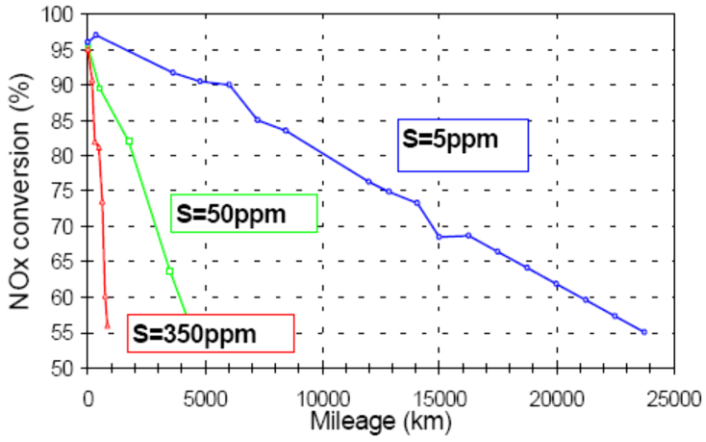

Figure 2-13. The effect of fuel sulphur content on Nox trap conversion [Guyon *et al* (2000)].

2.4.7 Diesel exhaust gas fuel reforming

The addition of hydrogen can significantly improve the performance of a number of diesel aftertreatment devices including; catalytic converters, DPFs (see section 2.4.3) and NOx traps [Abu-Jrai *et al* (2008) and Bromberg *et al* (2004)]. This has led to the development of the Exhaust Gas Fuel Reforming process, a technique that allows for production of hydrogen rich reformate 'on board' the vehicle.

During the exhaust gas fuel reforming process, diesel fuel is reformed catalytically when directly contacted with oxygen and steam already present in the exhaust gas. As a result hydrogen rich reformate is produced. The volume of hydrogen produced when using this method is dependent upon the rate of the steam, oxygen and fuel as well as the exhaust gas temperature. As a result, the operating conditions of the engine greatly influence the H_2 production [Jamal and Wyszynski (1994) and Tsolakis and Megaritis (2004)].

During the reforming process, a number of reactions occur consecutively at different stages along the catalyst. These include oxidation, partial oxidation, steam reforming, dry reforming and water gas shift. The first reaction, oxidation, occurs at the initial section of the catalyst bed. This process generates water that can then be used to form H_2 via steam reforming. Partial oxidation between diesel and oxygen can also occur on the catalyst bed. This exothermic reaction produces H_2 directly [Tsolakis and Megaritis (2004)].

Oxidation: $C_nH_{1.88n} + 1.47_nO_2 \rightarrow {}_nCO_2 + 0.94_nH_2O$

Partial oxidation: $C_nH_{1.88n} + ½\ O_2 \rightarrow {}_nCO + 0.94_nH_2$

Steam reforming: $C_nH_{1.88n} + {}_nH_2O \rightarrow {}_nCO + 1.94_nH_2$

Where *n* is the number of carbon atoms in the fuel molecule.

It is apparent from both the steam reforming and partial oxidation formulae that CO is formed as a by-product during H_2 production. However, if the CO content is sufficient it can be utilised to form both CO_2 and further additional H_2 (see chemical formula below). This is recognised as the water gas shift reaction [Abu-Jrai *et al* (2008)].

Water Gas Shift: $CO + H_2O \rightarrow CO_2 + H_2$

The previously mentioned dry reforming reaction refers to an endothermic reaction between the diesel fuel and CO_2. When exposed to temperatures in excess of 800°C, such a reaction can also produce additional H_2.

It has been identified in studies by Jarrod *et al* (2006) that the implementation of diesel fuel reformers is not without complications. Firstly, during the reforming process, carbon can build up on the catalyst bed, reducing the efficiency of the reformer. In addition to this, sulphur contained within the diesel can result in poisoning of the catalyst bed.

2.5 Gas Chromatography

Gas chromatography is a method adopted to separate out various components of a sample gas so they can be both identified and quantified. The five units that construct a typical gas chromatograph are demonstrated schematically in figure 2-14. On entering the gas chromatograph, the sample gas is carried through a column by a carrier gas. This is referred to as the 'mobile phase'. The walls of the column are coated to act as a resistance to the mobile phase, known as the 'stationary phase'. Dependent on the molecule size of the sample components the resistance to the stationary phase is varied for different components. As a result, the presence of a mobile and stationary stage causes the components to exit the column at different times. Although the most proficient separation is achieved at low temperatures, the column is heated to increase the rate of progression through the tube. This is especially necessary for components that feature large molecules and could otherwise take a considerable length of time to travel through the column. The component can be identified as a function of the time spent travelling through the column and the order in which it exits at a specific column temperature [McWilliam (2008) and Scott and Perry (1998)].

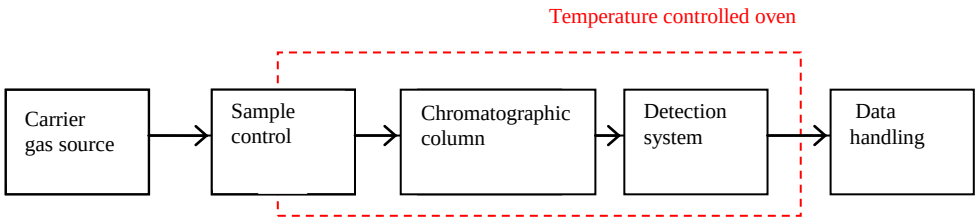

Figure 2-14. Schematic of a typical gas chromatograph [Guiochon and Guillemin (1988)].

The first unit provides the carrier gas. This is either at constant flow rate or constant pressure to ensure a steady and uniformed flow is provided to the column [Guiochon and Guillemin (1988)]. The carrier gas adopted may vary dependent on the application of the detector. An example of this is a flame ionisation detector which requires a flammable carrier gas i.e. hydrogen [McWilliam (2008)].

The second unit injects the sample gas into the constant carrier gas flow. To avoid condensation of the sample, it is critical that the injector is tightly temperature controlled. For peek accuracy it is necessary for the sample gas to vaporise in the minimal time available between the first unit and the column. This ensures that when delivered to the column, the sample gas is a plug of vapour which has been diluted by the carrier gas. If this state is not achieved, there is a risk of the sample being smeared onto the column and the results adversely effected [Guiochon and Guillemin (1988), McWilliam (2008)].

The third stage of the gas chromatograph process is the column, which is contained within an oven. It is during this stage that the various components of the sample are separated. The temperature inside the oven is steadily increased during operation in order to reduce the overall test time. However, the oven temperature is always within a typically range of ambient to 350˚c [Guiochon and Guillemin (1988), McWilliam (2008)].

The fourth stage of the process is the detection process. The operating principles of this stage are dependent on the type of detector installed. When adopted for hydrogen measurements, it is typical to adopt a Thermal Conductivity Detector (TCD). This is due to hydrogen demonstrating a significantly high thermal conductivity (0.182 W/mK) when compared to a majority of other

gases. The TCD features two channels, a reference and measuring channel. Only the carrier gas is passed through the reference channel while both the sample and reference gas is passed through the measuring channel. Situated within both channels are resistance wires which are electrically heated. Variance in thermal conductivity within the two channels is demonstrated by a differential resistance. The detector produces a voltage signal proportional to the variance in resistance. This voltage signal is proportional to the concentration of the sample component. In theory, if no sample exists and only pure carrier gas is detected, then no signal fluctuation is generated. To avoid condensation, the detector must be heated to approximately 15˚c above the oven maximum temperature (typically 365˚c) [Guiochon and Guillemin (1988), McWilliam (2008)]. The final stage, the data handling, provides a data output for the user.

2.6 Fourier Transform Infrared Spectrometry

Fourier Transform Infrared (FTIR) spectrometry is an extremely fast and sensitive measuring technique. An FTIR analyser quantifies various chemical components by passing infrared radiation through a sample and generating an infrared spectrum. The components within the sample absorb a portion of this radiation (of which is linearly proportional to the concentration) while the remainder is transmitted. The level of absorption at specific wavelengths is unique to that specie at that concentration. By comparing the area under specific absorption peaks with reference spectra taken at calibrated concentrations, the actual concentration can be interpolated from the reference data. A limitation of this method is the inability to measure non-infrared active species such as oxygen, hydrogen and nitrogen [Thermo Nicolet (2001) and MKS application note (2010)].

The operating principles of an FTIR analyser are demonstrated below in figure 2-15. A beam splitter is adopted to split an infrared beam into two optical beams. Both optical beams are reflected off separate mirrors before returning to the beam splitter. However, while one mirror is fixed in a stationary position, the other is constantly moving. This results in one beam travelling a fixed distance while the path of the other beam is constantly fluctuating. This results in the two beams ‘interfering’ with each other while vacating the process. This signal is recognised as an ‘interferogram’. This type of signal holds information in every data point for

each infrared frequency coming from the source. As a result the speed of measurement is extremely fast due to all frequencies being measured simultaneously [Thermo Nicolet (2001)].

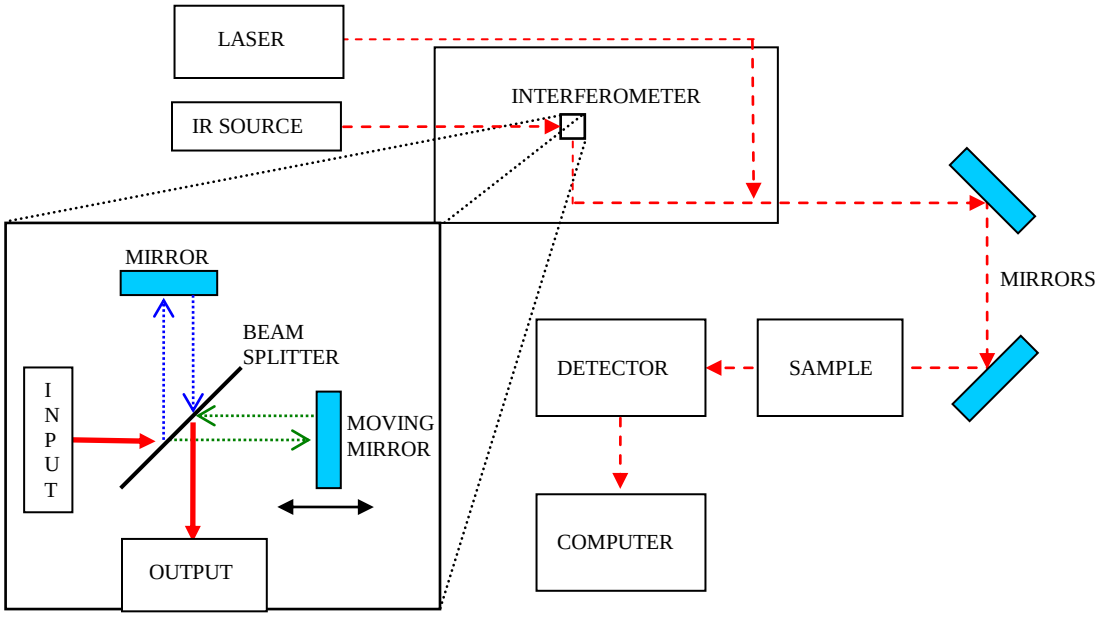

Figure 2-15. Schematic diagram of a typical FTIR analyser [Thermo Nicolet, (2001)].

From the interferometer, the beam is passed through the sample via a series of mirrors. The frequencies of energy that are absorbed by the sample are specific to that particular sample at the current concentration. The resultant interferogram signal is then read by a detector which recognises the variance in the frequencies of energy within the signal before delivering the data to a computer. The computer then adopts a Fourier Transformation technique to interpret the output from the detector and display the resultant spectrum data. This is then compared with a library of spectrum data to be able to identify the concentrations of the various components contained within the sample [Thermo Nicolet (2001) and MG2000 Software Manual (2006)].

Figure 2-16 below demonstrates spectra for ten typical components at 50ppm concentration. It is apparent from this data how the level of absorption (y axis) at a certain wavelength (x axis) is specific for each component at the given concentration.

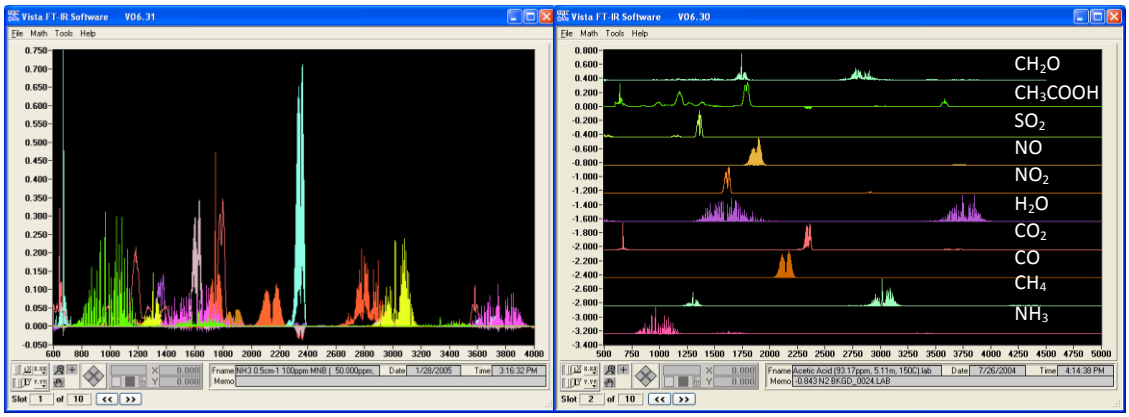

Figure 2-16. Spectra for 10 typical components at 50ppm concentration (overlay and stacked) [Marshik (2011)].

Figure 2-17 is an example of residual spectra. As previously described, to quantify components within a sample, the resultant infrared spectrum is compared to a reference spectrum contained within the software library. At times, the two spectrums demonstrate a slight discrepancy. This discrepancy in then highlighted as residual spectra. While residual spectra are typically an indication of measurement error for given species at given concentrations, it may also be evidence of the presence of a foreign specie that is not currently contained within the reference library.

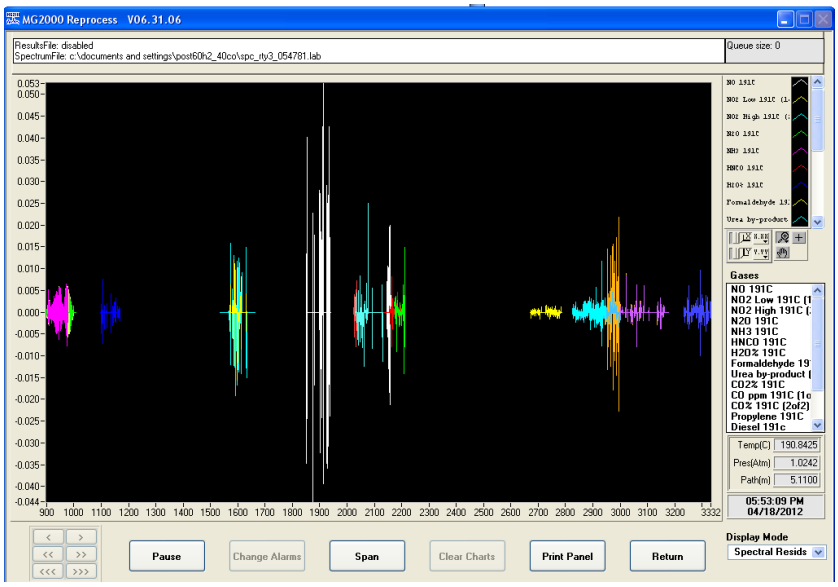

Figure 2-17. Residual spectra

CHAPTER 3

EXPERIMENTAL SET UP AND TEST PROCEDURE

CHAPTER 3 - EXPERIMENTAL SET UP AND TEST PROCEDURE

3.1 Introduction

This chapter begins by providing an overview of the engine specification and its various monitoring and control systems. This is followed by details regarding exhaust sampling and analysis as well as the layout of the DPF regeneration test rig. In addition to this, all test procedures adopted throughout this investigation will be outlined. The engine used for this investigation was a Ford 'Puma'. This direct injection, four cylinder diesel engine was manufactured by Ford Motor Company and based on the Ford Duratorq engines that featured in the Ford Mondeo and Transit. The engine features a variety of measurement and control systems that will be described in further detail in the remainder of this chapter.

3.2 Research engine

The specifications of the Ford Puma engine adopted for this study can be identified below in table 3-1:

Valves per cylinder	4
Cylinder bore	86mm
Stroke	86mm
Swept volume	1998.23cc
Compression ratio	18.2:1
Max. cylinder pressure	150 bar
Nominal bowl volume	21.7cc
Idle engine speed	750 rpm (+/-5 rpm)
Maximum no load engine speed	4800 rpm (+/-50 rpm)

Table 3-1. Engine specification for the Ford Puma

The Ford Puma engine adopted for this study is of a pre-production prototype design. As a result, the test engine features a number of design variances when compared to the mass produced equivalent. Firstly, the inlet manifold features straight cylinder feeds while the

production type features an inlet manifold designed to promote swirl of the inlet flow. Secondly, the research engine features a slightly lower compression ratio of 18.2:1 compared to the 19:1 demonstrated by the mass produced engine. This is due to the test engine being fitted with different pistons that feature a larger bowl volume. The piston bowl design featured on the prototype engine can be identified in figure 3-1.

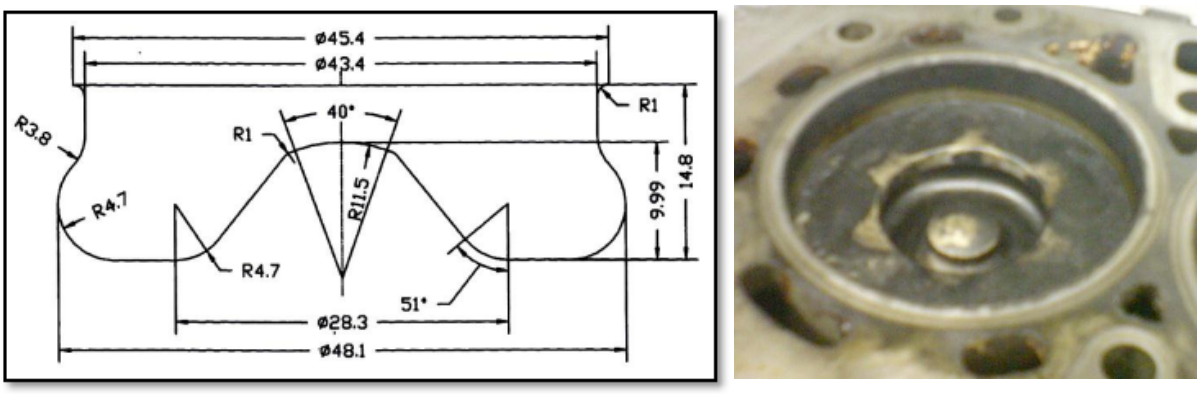

Figure 3-1. Piston bowl design [Labecki (2010)].

Finally, the Garrett turbocharger, although present, was not connected to the exhaust system during testing. This was to ensure a constant air intake pressure could be maintained.

3.3 Engine control and monitoring

3.3.1 Engine management

Access to the Electronic Control Unit (ECU) was achieved with GrEDI software running on a 486 PC. This software allowed the user to modify a variety of parameters, even during engine operation. This included injection timing, EGR and injection pressure. For all tests carried out during this investigation, a single map with fixed parameters was implemented. The GrEDI software also allowed for live monitoring of a number of outputs including; fuel flow rate, mass air flow and injection pressure. To increase the validity of this data, all measurements of interest were supported by a second measurement technique.

3.3.2 Fuel supply and fuel flow measurement

All tests were performed with red Ultra Low Sulphur Diesel. To ensure consistency in the properties of the fuel, all tests were performed from the same batch of fuel.

The research engine featured a common rail injection system supplied by Delphi Diesel Systems Ltd (DDS). The laboratory featured a main diesel pump that was used to deliver fuel to the DDS high pressure pump via an inline filter. Throughout this study the rail pressure and injection timing was set to 800 bar and 9° BTDC (single injection) respectively. This was achieved by modification of the relevant parameters within the Injection Control Unit (ICU). Fuel delivery to the cylinder was achieved via centrally mounted DDS injectors which featured a six holed nozzle. This particular common rail system featured an injector backleak which was sent directly back to the laboratory's main diesel tank.

Measurement of the engine fuel consumption could be achieved by the adoption of a measuring burette situated inline of the fuel supply. After shutting off the fuel supply to the burette, it was possible to identify the volumetric fuel flow rate by measuring the time it took to consume the burettes known volume. This data could be validated by monitoring the fuel mass flow rate demonstrated by the GrEDI software.

3.3.3 Air intake system and air flow measurement

As previously stated, throughout testing the turbocharger was bypassed and the engine ran in naturally aspirated conditions. The intake air was firstly drawn through a positive displacement rotary air flow meter and paper air filter, before entering the engine via a charge cooler (due to the charge cooler being rendered redundant, the coolant flow was switched off). For all tests performed during this study, EGR was not adopted (EGR valve fully closed).

As with the fuel consumption measurement, the mass air flow (MAF) of the engine could be monitored in real time using the GrEDI software. The type of MAF sensor adopted throughout testing featured an electrically heated platinum wire located within the inlet tract. The ECU would provide the necessary current to the wire to maintain a set point temperature. As the air

flow into the engine increased, the current required to maintain the set point temperature would increase proportionally to the increase in mass air flow. The data generated from the MAF sensor could be validated with the aforementioned rotary air flow meter which measured volumetric air flow rate. This device featured a known cyclic volume and displayed the cycles per second (Hz) on a digital readout. This data made it possible to calculate the quasi-steady volumetric flow rate of the engine. The temperature of the intake air could be monitored via a K-type thermocouple situated downstream of the air flow meter. The data from this system was fed back to a digital readout at the dyno controller.

3.3.4 Oil supply system

With the exception of the implementation of an aftermarket oil cooler, the engine lubrication system was left unmodified from the original OEM design. An oil pump driven mechanically by the timing chain was adopted to provide sufficient oil pressure. The oil pressure could be monitored at the dyno controller via an analogue gauge. To protect the engine, the system was fitted with a cut off facility, where the engine would stop running if the oil pressure dropped below the pre set minimum oil pressure reading. In addition to this the oil temperature could be monitored via a K-type thermocouple situated in the oil sump. The data from this sensor was then fed back to a digital display at the dyno controller. During testing the maximum oil temperature was set at 100°C. Any higher, and the decrease in viscosity would have resulted in unacceptable levels of engine lubrication.

3.3.5 Cooling system

A Bowman tubular heat exchanger was adopted to cool the engine coolant. The flow on the cold side of the heat exchanger was provided by a main laboratory water tank. This flow was controlled by a thermostat which maintained the engine coolant temperature to within a ˜73-80°C window. The engine coolant inlet and outlet temperatures were measured via K-type thermocouples situated in the coolant inlet and outlet pipes. The outputs from these sensors were then displayed via a digital readout situated at the dyno controller. The cooling system also featured a safety cut off facility which prevented the engine running if the coolant temperature exceeded 100°C. Before any testing on the engine commenced, the engine was always left in

idle condition until the temperature window was reached and the engine could be considered to be at full operating temperature.

3.3.6 Dynamometer

Throughout testing a Schenck W130 dynamometer was adopted for load and speed control of the research engine. A cross sectional view of this dynamometer can be identified below in figure 3-2. A toothed magnet wheel mounted on two half shafts, rotates on bearings mounted inside the dynamometer casing. DC current is utilised by the excitation coil to generate a magnetic field. This magnetic field pulses at the same frequency of the passing magnet wheel teeth, producing eddy currents. These eddy currents build up magnetic fields that produce a resistive torque to the magnet wheel. This torque can be measured via a load cell fitted to a lever arm which is connected to the dynamometer casing. In addition to this, the speed can also be measured via a speed pickup and toothed disc which generates a speed dependent voltage [Schenck, (1984)].

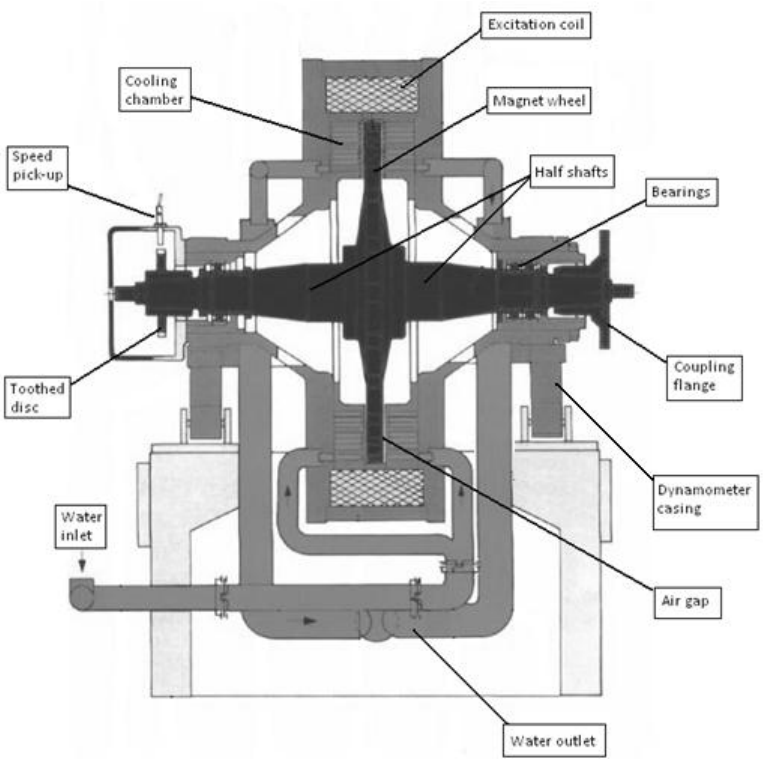

Figure 3-2. Cross sectional view of eddy current dynamometer [Schenck, (1984)].

By adjusting the strength of the resistive magnetic field as required, the dynamometer permits the user to fix either the speed or torque. This allows for the remaining parameter to be adjusted via control of the engine fuelling. The temperature of the dynamometer is controlled via a water cooling system [Schenck, (1984)].

3.3.7 In-cylinder pressure vs. crank angle measurements

In-cylinder pressure was measured from cylinder 1 using a Kistler type 6125A piezoelectric pressure transducer. This transducer was fitted into the redundant glow plug hole using a bespoke adapter sleeve. The output signal from the sensor (15.9 pC/bar) was amplified via a charge amplifier prior to data acquisition.

Crank angle was measured via a shaft encoder consisting of a 360 toothed gear wheel with separate top dead centre (TDC) flag and a GEL 244 pickup head. High resolution adjustment could be achieved via threaded adjustment rods that controlled the position of the pickup head.

In order to log the in cylinder pressure from cylinder 1 against crank angle, it was necessary to align the TDC flag with the actual TDC. This was achieved by firstly delaying the injection timing until after TDC before utilising an oscilloscope to identify the point of peak in cylinder pressure (TDC). By observing the indiscrepancy between the TDC pulse and the in cylinder peak pressure it was possible to adjust the position of the TDC flag accordingly. Once calibrated, the incylinder pressure at the correct corresponding crank angle could be logged and displayed using LabView V6 software.

3.3.7.1 Analysis of in-cylinder pressure data

If necessitated by the test requirements, it was possible to utilise the in-cylinder pressure data to calculate the net heat release rate (HRR) as a function of crank angle ($dQn/d\theta$). This was achieved using equation 3-1 below. The HRR could also be adopted to identify the ignition delay. For this study the ignition delay was defined as the time between point of injection and start of combustion. While the point of injection was taken as 9° BTDC, the point of combustion was

assumed to be where the HRR data shifted from negative (due to heat loss to the chamber walls) to positive [Stone (1999)].

$$\frac{dQn}{d\theta} = \frac{\gamma}{\gamma - 1} p \frac{dV}{d\theta} + \frac{1}{\gamma - 1} V \frac{dp}{d\theta}$$

Equation 3-1. Net heat release rate as a function of crank angle

Where γ is the ratio of specific heats: Cp/Cv. For air at pre-combustion temperatures following the completion of the compression stroke, this is expected to be approximately γ=1.35. Whilst post combustion a value of γ=1.26-1.3 is expected. The values for the most accurate heat release rate analysis are still not clearly defined. For this study a ratio of γ=1.3 was adopted and kept constant throughout the combustion cycle. This is typical for diesel engine heat release analysis [Heywood (1988)]. Crank angle is denoted by θ.

In addition, in-cylinder pressure data was also utilised to quantify combustion stability. This was achieved by identifying the maximum in-cylinder pressure over 100 cycles before calculating the coefficient of variance (CoV) between these readings. If the CoV exceeded 5% the combustion was considered to be unstable [McWilliam (2008)].

3.4 Aftertreatment device test rig: Setup and test procedure

A schematic diagram of the aftertreatment device test rig is demonstrated below in figure 3-3. The exhaust gas was sampled directly from the engine exhaust manifold. A sampling flow rate of 40 l/m was achieved by restricting the main exhaust flow via a tap situated on the main exhaust pipe. This flow rate could be increased (dependent on the test requirements) by utilising the suction side of a blower situated downstream of the DPF.

To prevent condensation of the sample as well as keeping the exhaust gas temperature constant, the sample line was heated. This was achieved by using heating tape supplied by Omegalux. A controller was adopted to adjust the temperature set point while the reference temperature was taken using a K-type thermocouple located at the cross-sectional centre of the sampling line. For all testing conditions, the sample line was set to the same temperature as that

measured at the engine manifold for that testing condition. This was to reduce any impact that the transportation of the sample from the exhaust manifold to the reactor had on the exhaust composition.

Various gases could be introduced to the sample line dependent on what bottle was connected to the system again this was dependent on the test requirements. Introduction was initiated upstream of the furnace via a solenoid valve (Burkert - type 6013) actuated by a controller. The controller allowed the user to control both the pulse rate and width of the solenoid valve, allowing for both constant and periodic injection strategies to be implemented. The volume of introduced gas could be adjusted via an inline needle valve. A pressure regulator fitted to the bottle of the introductory gas ensured the gas was delivered at a constant pressure of 2 bar for all tests.

The DPF was housed within a custom made reactor that was situated inside a Lenton CSC tubular furnace. As a result, the temperature of the reactor could be accurately controlled allowing exhaust gas temperatures to be simulated. Two reactors were manufactured for this investigation. While one design was suitable for a DPF with a 50.8mm diameter, the other was manufactured to house a DPF with a 25.4mm diameter. Drawings of these two reactor designs can be indentified in appendix A. Throughout testing the 25.4mm diameter reactor was adopted. To ensure proficient sealing, quartz paper was wrapped around the DPF before insertion into the reactor.

K-type thermocouples were adopted to measure the filter temperatures at the top, middle and bottom. In addition to this, the reactor inlet and outlet temperatures were also recorded. Pressure transducers provided by Cole Parmer Ltd (model 206) were used to measure the inlet and outlet pressures of the reactor. By subtracting the inlet pressure from the outlet pressure, it was possible to calculate the current pressure difference over the filter and hence identify the current operational status of the DPF i.e. blocking, equilibrium or regenerating (see section 2.4.2). All temperature and pressure measurements were performed in real time at a sampling rate of 0.016Hz. A PICO-ADC 20 USB-data logger and terminal board supplied by Pico Technology Ltd was utilised for data acquisition. Once acquired, this data could then be both displayed and manipulated using PicoLog data acquisition software.

On exiting the furnace, the sample flow was cooled by a water cooler. Water was then removed from the sample line via a water trap. Upstream of the blower, an inline flowmeter (calibrated for air) and tap could be utilised to control the sample line flow rate and hence the space velocity through the filter.

Exhaust gas could be sampled directly from the engine manifold via heated lines to either a Horiba 7170 DEGR or an FTIR analyser. This was in order to analyse the exhaust components pre DPF. A second sampling point was implemented directly after the furnace so post DPF exhaust gas could also be sampled. A syringe sampling point was also positioned at this location for hydrogen measurements.

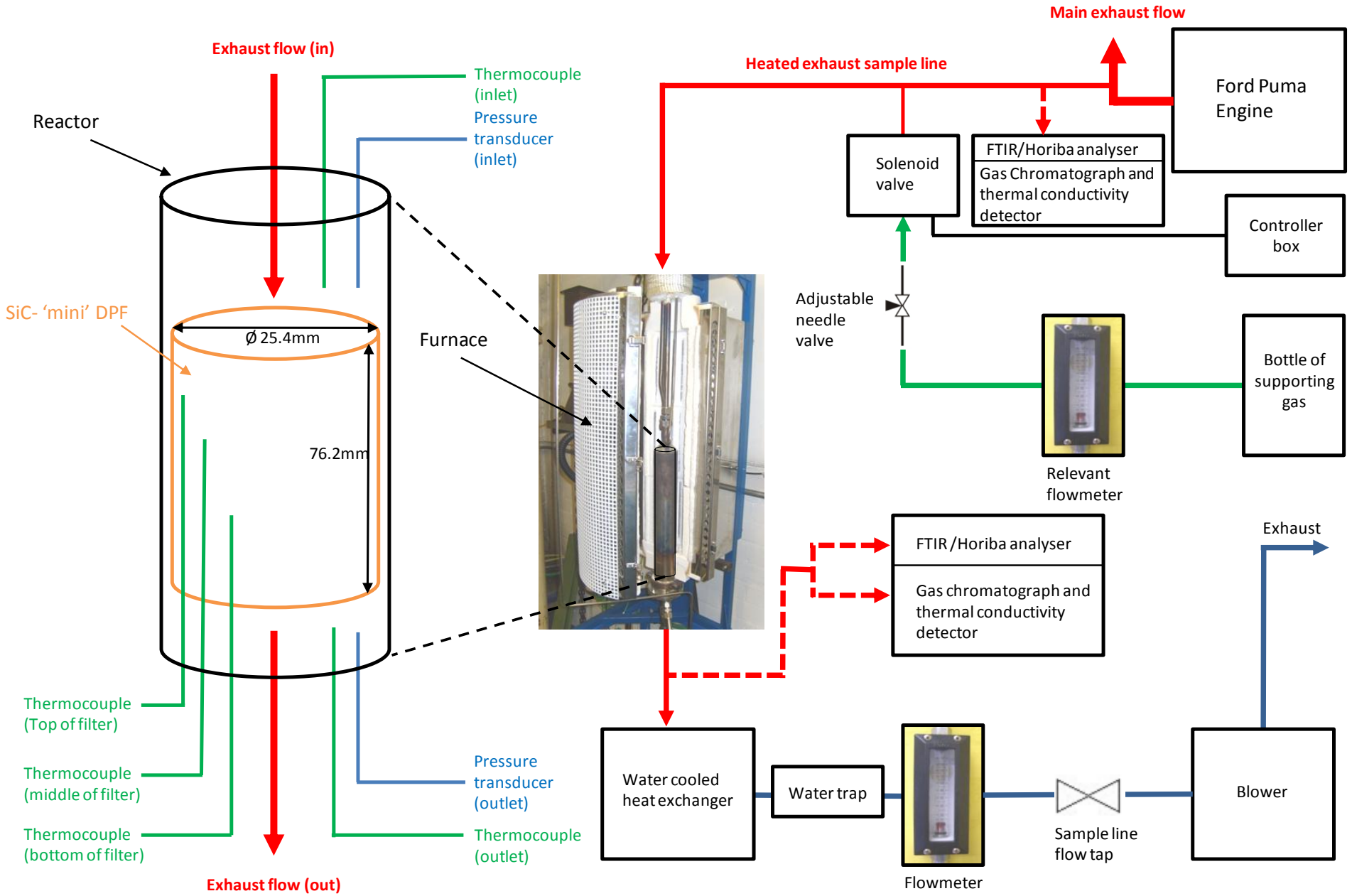

Figure 3-3. Schematic diagram of aftertreatment device test rig

3.4.1 SiC – 'mini' DPF

The SiC- 'mini' DPF adopted throughout testing was provided by Johnson Matthey. This filter was constructed of silicon carbide and did not feature a catalyst coating. As described in figure 3-3 above, the filter had a diameter of 25.4mm and a length of 76.2mm. The three thermocouples used to measure the filter temperature at the top, middle and bottom where inserted into individual square channels of the DPF, situated along the central axis of the filter.

Figure 3-4. SiC – 'mini' DPF

3.4.2 Supporting gas calibration

When H_2 or CO was used as the supporting gas, the required concentration could be calibrated by adopting a relevant flowmeter placed inline of the supporting gas delivery pipe. The volumetric flow rate of the supporting gas was adjusted (utilising a needle valve) until the desired percentage of the exhaust sampling line volumetric flow rate was achieved e.g. To achieve 8% supporting gas concentration in the exhaust sampling line demonstrating a volumetric flow rate of 70 l/m, the volumetric flow rate of the supporting gas would be set at 11 l/m.

This method was not adopted for mixture gases due to the considerable difficulties faced in attempting to obtain a relevant flow meter. Therefore, in the case of H_2/CO mixture gas, the CO concentration was measured and the flow rate adjusted until the necessary CO content was achieved that represented the required mixture concentration. CO measurements were performed using an FTIR analyser the details of which are outlined in section 3.5.1.

3.4.3 Blocking procedure

A standardised loading procedure was devised to ensure that similar levels of particulates were accumulated before each regeneration event. The loading procedure is demonstrated below in figure 3-5. During this procedure the engine load and speed was set at 4.4bar BMEP and 1500 rpm respectively. The exhaust sampling flow rate was fixed at 70lm. The filter temperature was fixed at 440°C. As the filter was loaded the flow rate was continuously

affected. As a result, the flow rate had to be frequently monitored and adjusted accordingly (this was also necessary during each regeneration cycle).

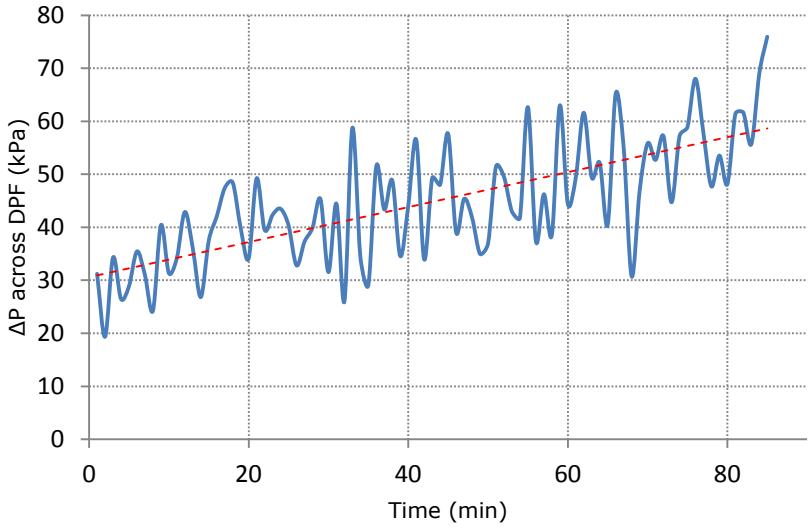

Figure 3-5. Accumulation process

In order to further standardise the accumulation process, it was ensured that the filter had been fully regenerated before each loading procedure commenced. In this state the filter demonstrated a pressure difference of approximately 20-30 kPa. The filter was considered blocked once the pressure difference between the inlet and outlet of the reactor had increased by ~50 kPa. This typically took 80-90 minutes to achieve.

3.4.4 Periodic injection strategies

As previously described in section 3.4, both periodic and constant injection strategies could be implemented by utilising the solenoid valve and controller. An example of a periodic strategy is the '10.5' strategy. This notation translates as each cycle featuring a solenoid opening event lasting 10 seconds, followed by a period of 5 seconds where the solenoid is closed. This is shown schematically in figure 3-6. This notation is standardised throughout the study for the various periodic strategies adopted.

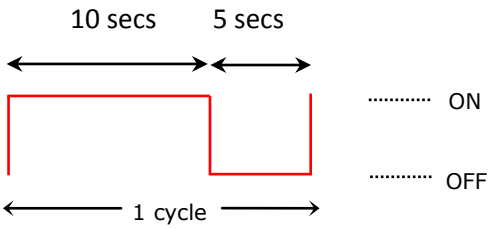

Figure 3-6. 10.5 periodic strategy

3.5 Exhaust gas sampling and measurement

With the exception of O_2 and H_2 measurements, all exhaust emission measurements carried out during this study were performed with an FTIR analyser. A 7170 DEGR Horiba gas analyser was adopted for O_2 measurements while a gas chromatograph was used for H_2 measurements.

3.5.1 FTIR set up and test procedure

As previously mentioned the aftertreatment device test rig featured two sampling points for FTIR analysis; direct from the engine manifold (pre DPF) and directly after the furnace (post DPF).

The FTIR instrument adopted for this study was a Multigas 2030 FTIR spectrometer. This unit was coupled with a FLS01 sampling device. Both units were supplied and installed by MKS Instruments UK Ltd. The FTIR instrument was cooled via liquid nitrogen supplied by BOC Speciality Gases Ltd.

The sampling unit featured a filter inline of the sample flow which reduced the build up of carbon deposits on the mirrors and/or windows housed inside the FTIR unit. This increased the time between each cell cleaning event.

To prevent condensation of the sample, heated lines were adopted to transport the sample from the sampling point to the sampling unit. The temperature of the heated lines was monitored by the sampling unit. Following recommendations from MKS for diesel exhaust applications, the temperature of both the sample lines and the gas cell within the FTIR instrument, were set at 191°C.

A predefined list of reference spectre (known as a 'recipe') was developed and provided by MKS. This comprehensive recipe had been designed for measurement of typical diesel emission components. This recipe was used throughout the study and remained unchanged. The components included in this recipe are listed below in table 3-2.

NO	CO
NO_2	Propylene
N_2O	Diesel
NH_3	Ethylene
HNCO	CH_4
H_2O	Ethane
CH_2O	Acetylene
$CO(NH_2)_2$	THC
CO_2	NOx

Table 3-2. Components included in 'diesel low speed' recipe

Before each test run the cell of the FTIR instrument and the sampling unit were purged with dry nitrogen (2 bar, 0.5 l/min) for approximately 10 minutes and a background spectrum taken. The background spectrum allows the FTIR to obtain a zero datum for each of the components being measured. In addition to this the single beam intensity was checked daily to ensure a significant drop in the beam intensity had not occurred as a result of sample deposits on the mirrors and/or windows. In the event of this occurring, the unit was dismantled and the mirrors and windows inspected and cleaned where necessary.

Data logging from the analyser was performed via MG 2000 software (version 06.31.06) which was both designed and installed by MKS.

When measuring exhaust emissions under transient conditions i.e. when a periodic injection strategy was being introduced, the sampling rate of the FTIR analyser was set to 1Hz (the maximum sampling rate of the unit) allowing for maximum data capture. However, a lower sampling rate of 0.125Hz was adopted when measuring steady state conditions i.e. when a constant injection strategy was adopted. This reduction in sampling rate incurred a significant reduction in the signal to noise ratio (SNR), demonstrated below in table 3-3. Due

to the measuring condition being steady state the effect of the lower sampling rate demonstrated a negligible to zero effect on the accuracy of the measurement data. The FTIR software featured a SNR measuring function that allowed for the effect of varying the sampling interval from 1Hz to 0.125Hz on the SNR to be identified. Table 3-3 below demonstrates the SNR at various wave numbers at both sampling intervals (results shown are mean results taken from 5 scans).

Wave number (cm^{-1}) Low- High	**SNR at 1Hz**	**SNR at 0.125Hz**
1000-1100	470	1271
2100-2200	724	1966
2900-3000	436	1169

Table 3-3. SNR as a function of sampling interval

3.5.2 Gas chromatograph set up and test procedure

Throughout this study a HP 5890 gas chromatograph fitted with a thermal conductivity detector (GC-TCD) was adopted for hydrogen measurements. Argon was used as the carrier gas. Another PICO-ADC 20 USB-data logger and terminal board was utilised for data acquisition. The fundamental principles of gas chromatography and the operating principles of a thermal conductivity detector were outlined in section 2.5.1 of this study.

For all hydrogen measurements, five samples were taken from the relevant sampling point (either pre or post filter) using five 2.5ml syringes. Each sample was taken at two second intervals. To reduce leakage, these syringes were then sealed using a rubber bung. The five samples could then be injected into the gas chromatograph at two minute intervals. Once all five samples had been measured the H_2 concentration for each sample could be calculated and the average concentration defined.

In order to set a datum for all H_2 measurements, a 5ml sample of span gas featuring a 10% H_2 (v/v) concentration was injected into the GC unit via a syringe. To enhance validity of the results, this was performed three times. All three curves were then integrated and the average measurement calculated. The results from the GC are displayed below in figure 3-7.

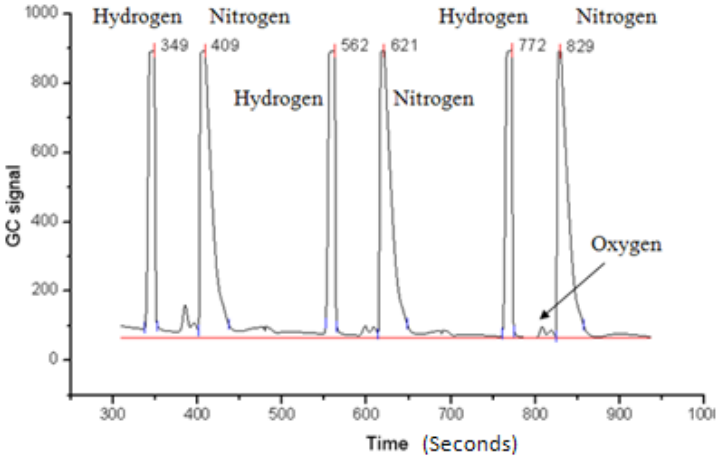

	A(X)	B(Y)	C(Y)	D(Y)	E(Y)	F(Y)	G(Y)	H(Y)
Long Name		Area	AreaIntgP(%)	Beginning X	Ending X	FWHM	Center	Height
1	Peak1	7620.311	11.14729	338	353	8.98546	349	827.764
2	Peak2	13396.793	19.59735	401	437	14.47923	409	827.693
3	Peak3	7576.0965	11.08261	552	565	9.04405	562	828.081
4	Peak4	12724.315	18.61363	614	648	13.88552	621	827.514
5	Peak5	7383.228	10.80048	761	775	8.63582	772	828.411
6	Peak6	11959.18	17.49436	824	857	13.08538	829	826.614
7								

Figure 3-7. 10% H_2 concentration

It was calculated from the data shown in figure 3-7 that 10% hydrogen concentration equated to an average integrated area of 7526.55. By utilising this calibration figure it was possible to adopt equation 3-2 below to calculate the concentration by volume for all five samples before calculating the average hydrogen concentration.

$$\frac{\text{measured integrated area}}{(7526.55/10)} = \text{H}_2 \text{ conc. by volume of sample}$$

Equation 3-2. Converting GC output signal to conc.(% v/v).

3.5.3 O_2 measurements

As previously mentioned, all O_2 measurements were carried out using a 7170 DEGR Horiba gas analyser. This analyser adopts a magneto-pneumatic type oxygen sensor. A diagram demonstrating the operating principles of this technique can be identified below in figure 3-8.

A non homogenous magnetic field is generated by applying an alternating current to an electromagnet. Due to the paramagnetic properties of O_2, when a sample containing O_2 is drawn through the magnetic field the O_2 is pulled to the stronger side of the magnetic field resulting in a pressure increase. A reference gas (N_2) is mixed with the sample at the magnetic field as well as being introduced to an area outside of the magnetic field. A detector is positioned so the differential pressure between the sample and reference gas can be measured, a value that is a function of the O_2 concentration in the sample [Mandal (2008)].

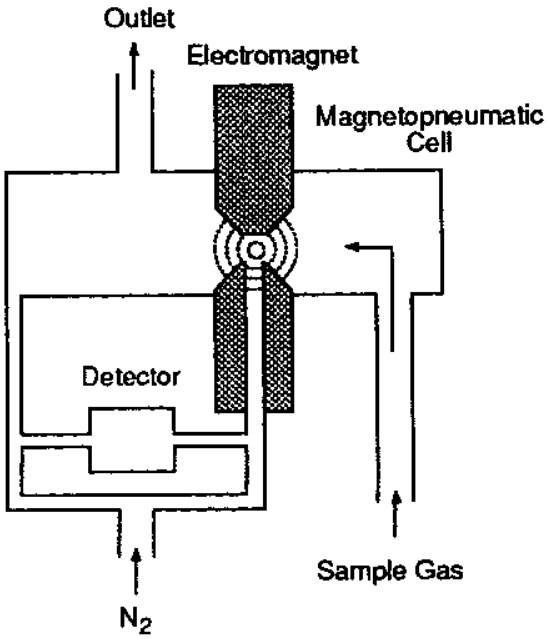

Figure 3-8. Operating principles of a magneto-pneumatic oxygen sensor [Horiba 7170 DEGR Users manual].

3.6 Reference measurements

To ensure the behaviour of the engine was consistent throughout testing, emission data was recorded before the commencement of each test run while the engine was running at set reference conditions (see table 3-4 below). This data could then be compared with previously captured data taken when the engine was running in the same conditions. Only if the engine demonstrated consistent emission output (within tolerance) would the test run commence. This not only allowed for the early detection of engine faults but more importantly enhanced the validity of the data recorded throughout this study.

REFERENCE CONDITIONS:	
Speed (rpm)	1500
Load (BMEP bar)	4.4
Injection timing (° BTDC)	9
Common rail pressure (bar)	800
RESULTANT EMISSION OUTPUT:	
Smoke (FSN)	0.49
CO (% v/v)	0.03
CO_2 (% v/v)	8.15
O_2 (% v/v)	9.58
THC (ppmC)	333

Table 3-4. Reference conditions and resultant emission output

CHAPTER 4

PERIODICALLY REGENERATING DIESEL PARTICULATE FILTER WITH HYDROGEN ADDITION

CHAPTER 4 – PERIODICALLY REGENERATING DIESEL PARTICULATE FILTER WITH HYDROGEN ADDITION

4.1 Introduction

The objective of this study is to promote DPF regeneration with the addition of hydrogen. This is to replicate the effects of supporting the regeneration process with H_2 that has been generated on board using an exhaust gas assisted fuel reformer.

This investigation begins with baseline tests to establish the minimum exhaust temperature in which passive regeneration occurs. Once defined, regeneration at this temperature is supported by the addition of H_2 at varying concentrations. It was hypothesised that by exceeding the auto ignition temperature of the injected H_2 it would be possible to generate an exothermic reaction hence increasing the temperature of the filter. This would result in an expanding regeneration temperature window towards lower exhaust gas temperatures. In addition to this such a reaction could also improve both the speed and thoroughness of the regeneration process.

This study also aims to identify the effects of introducing hydrogen to the regeneration process using a periodic injection strategy. This is in an attempt to establish if the volume of additional hydrogen required to support the regeneration process can be reduced by injecting the hydrogen periodically. This was achieved by testing and comparing two periodic injection strategies.

4.2 Experimental set up and test procedure

For this test, a set operating point of 1500 rpm and 4.4 bar BMEP (brake mean effective pressure) was adopted for all regeneration test points. Using the aftertreatment device test rig outlined in the previous chapter, the sampling flow rate through the filter was kept at a constant 70 l/m throughout the test. Using equation 2-4 from chapter 2 and the filter dimensions expressed in section 3.4.1, this resulted in a space velocity of 108,780 h^{-1}. CO_2, CO, THC and NO_x were measured using a FTIR analyser (previously described in section 3.5.1). These measurements were taken both directly from the engine manifold and

immediately after the filter. The hydrogen adopted throughout this study was of a research grade (purity: 99.9995%).

4.3 DPF regeneration by temperature

The DPF was subjected to a variety of temperatures in order to identify the lowest temperature in which the regeneration process was initiated. This was achieved by firstly blocking the filter before subjecting it to a temperature of 420°C. This process was then repeated with increasing temperature until evidence of regeneration was apparent.

It is evident from Figure 4-1 (a) and (b) that at a filter temperature window of 420°C-460°C, regeneration was not initiated. This is due to the filter being in equilibrium mode which is defined in section 2.4.2 of chapter 2 of this study. Within this balance temperature window, the actions of accumulation and regenerating are cancelling each other out. Although the trend line in Figure 4-1 (b) does demonstrate equilibrium mode, a slight decline in pressure difference is evident after 40 minutes. This could be an indication that a filter temperature of 460°C is close to the upper boundary of the balance temperature window. This is supported when analysing Figure 4-1 (c) where a further increase of 20°C results in regeneration being initiated. However at this temperature, the same cyclic process demonstrated in Figure 4-1 (a) and (b) is still apparent however the definition is enhanced, with each process lasting approximately 15 minutes. Again, this indicates that the filter temperature is beginning to exceed the balance temperature window and shift the DPF from equilibrium to regeneration mode. At a filter temperature of 520°C it is demonstrated in Figure 4-1 (d) that the DPF has clearly entered regeneration mode. This is apparent by regeneration occurring without any evidence of particulate accumulation for approximately 40 minutes. Following this initial period of regeneration the DPF then regenerated for a further 30 minutes but at a significantly slower rate.

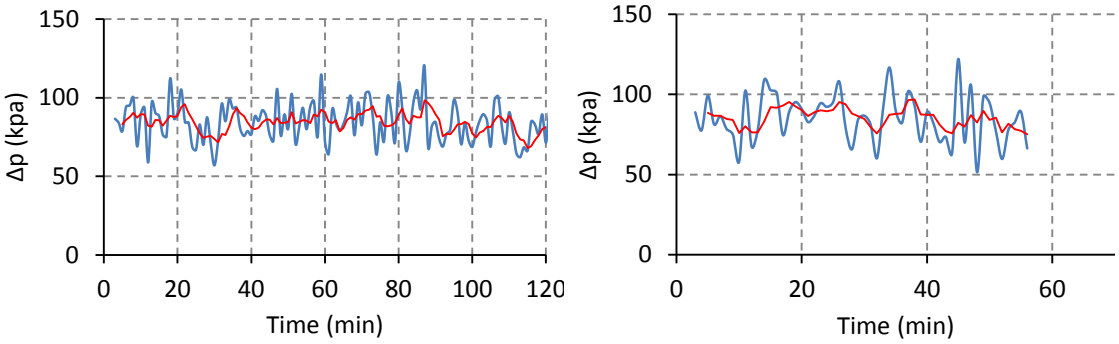

a) Filter temperature at 420°C

b) Filter temperature at 460°C

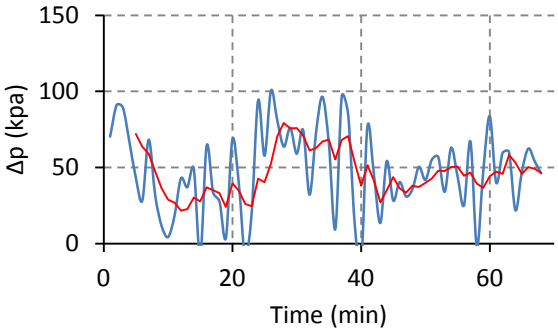

c) Filter temperature at 480°C

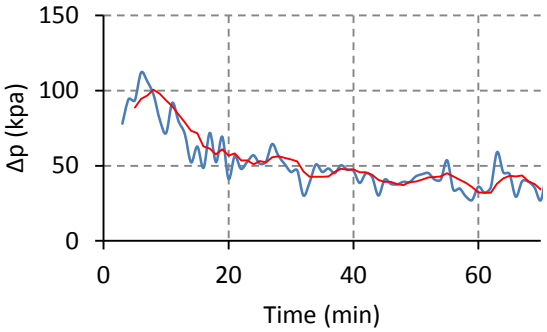

d) Filter temperature at 520°C

Figure 4-1. DPF regeneration process at various temperatures

4.4 DPF regeneration with constant H_2 addition

As identified in the previous section, passive regeneration occurs when the filter temperature is approximately 520°C. This section aims to identify if the introduction of hydrogen to the passive regeneration process enhances regeneration performance. This was achieved by introducing hydrogen at increasing concentrations of 1, 2, 3 and 4% (v/volume of sampled exhaust gas) while the filter temperature was set to 520°C. Prior to implementing each test condition, the filter was blocked following the standardised blocking procedure outlined previously in section 3.4.3. The effect of increasing hydrogen addition on both the mean filter temperature and regeneration profile are demonstrated below in figures 27 and 28.

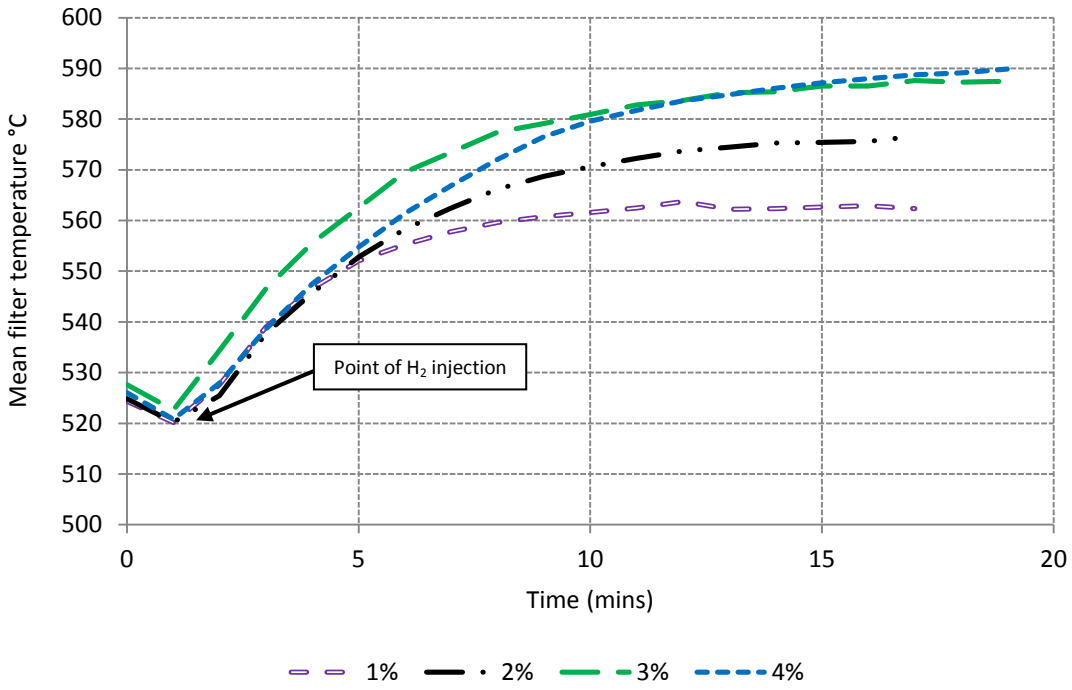

Figure 4-2. Mean filter temperature for various hydrogen concentrations

When analysing the effect of the various hydrogen concentrations on the mean filter temperature it is apparent that for all concentrations tested, the introduction of hydrogen resulted in a significant increase in the mean filter temperature. This demonstrates that the introduction of hydrogen (in excess of 1% concentration) to the regeneration process incurs an exothermic reaction. Unsurprisingly, a trend is apparent where increasing the introduced hydrogen concentration results in an increased peak filter temperature. However due to the temperature profiles generated using 3 and 4% hydrogen concentrations being relatively similar, it is assumed that further increases in the hydrogen concentration would not bring further substantial improvements in the peak filter temperature achieved.

Figure 4-3 displays the regeneration profiles for each of the concentrations tested, to improve clarity the raw pressure data has been replaced with polynomial trend lines. This method of data display is adopted throughout this study. When analysing figure 4-3, it is evident that for all hydrogen concentrations tested the resultant regeneration profile was improved over the non supported passive regeneration profile. This improvement is evident in both the regeneration thoroughness and rate for all concentrations tested. As previously described in section 2.4.2 (chapter 2), an increase in temperature results in an increase in soot oxidation. Therefore it is assumed that this improvement in the standard of regeneration is a result of the previously described exothermic reactions. It can be

concluded from this data that the introduction of hydrogen (in excess of 1% concentration) does support the passive regeneration process.

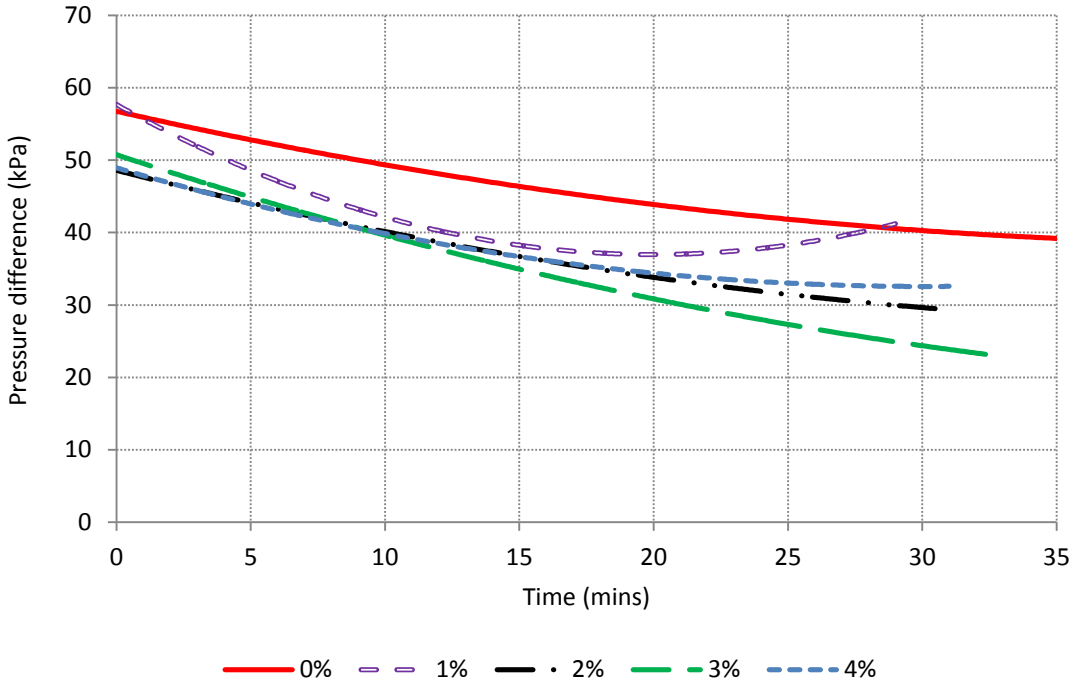

Figure 4-3. Regeneration profiles for various hydrogen concentrations

Although an improvement in regeneration quality is evident for all hydrogen concentrations tested, surprisingly, a clear trend is not apparent between increasing concentration and regeneration quality. Instead it is apparent that the standard of regeneration is remarkably similar for all concentrations tested, especially for 2, 3 and 4%. This indicates that at the high temperature that passive regeneration is initiated only minimal support is required by the additional hydrogen to fully regenerate the DPF.

Figure 4-4 demonstrates the effect of increasing the hydrogen concentration on various emission components pre to post filter. As a result of the exothermic reaction, the increased filter temperature heavily influenced the concentration of various emission components post filter. It is evident from figure 4-4 that the introduction of hydrogen to the passive regeneration process results in an increase in NOx formation post filter. This is especially apparent when the hydrogen concentration was 2% or above. This characteristic can be explained by the exothermic reaction increasing the temperature to within the NOx formation temperature window. This increased level of heat allows the nitrogen in the exhaust gas to become oxidised by the surrounding oxygen and produce NOx (as previously described in section 2.3.2).

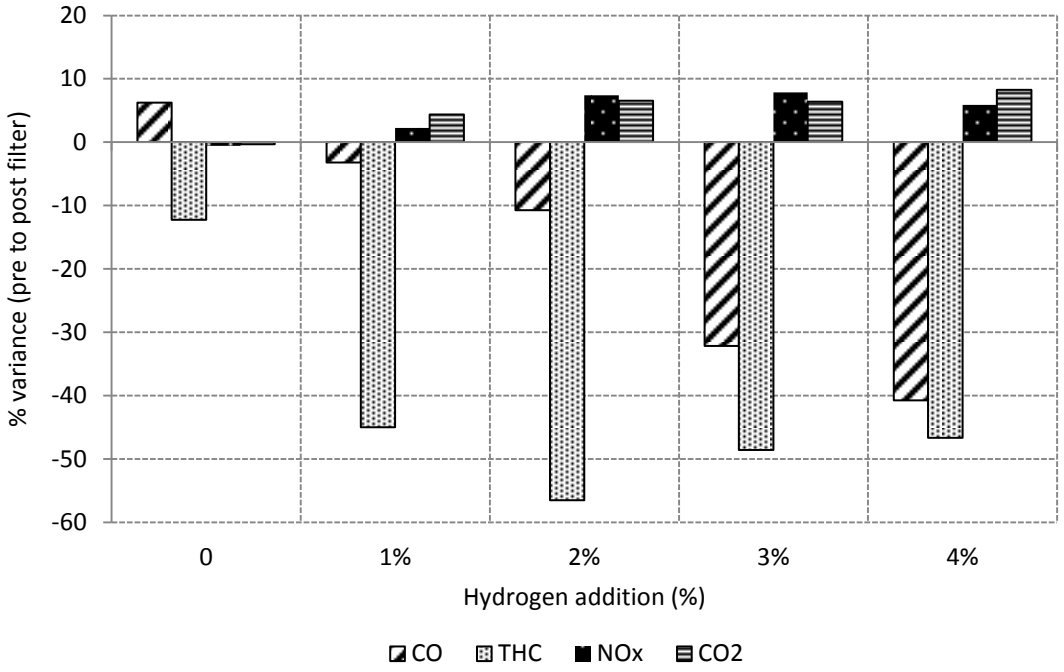

Figure 4-4. The effect of increasing H_2 concentration on various exhaust emissions

Although the addition of hydrogen induces an increase in NOx formation post filter, figure 4-4 also demonstrates a reduction in THC emissions. Again, it is assumed that this is the result of the increased filter temperature incurring increased hydrocarbon oxidation to take place. Figure 4-4 also demonstrates an increase in CO_2 post filter as the hydrogen concentration is increased. This may be somewhat explained by the previously described hydrocarbon combustion that, if complete, yields CO_2. However, it is assumed that the majority of the excess CO_2 is formed by the high filter temperature allowing for oxidation of CO. This is supported by the significant decrease in CO when additional hydrogen is implemented.

4.5 DPF regeneration with periodic H_2 addition

As previously stated, this study aims to identify the effects of introducing H_2 to the regeneration process using periodic injection strategies. For this investigation 5.5 and 10.5 periodic strategies were adopted (see section 3.4.4 for clarification of these notations) at 4% mixture concentration. Figures 4-5 and 4-6 demonstrate the resultant effects of implementing these strategies on both mean filter temperature and regeneration profile respectively. For comparison, these figures also demonstrate the mean filter temperature and regeneration profile generated by the constant strategy at 4% H_2 concentration.

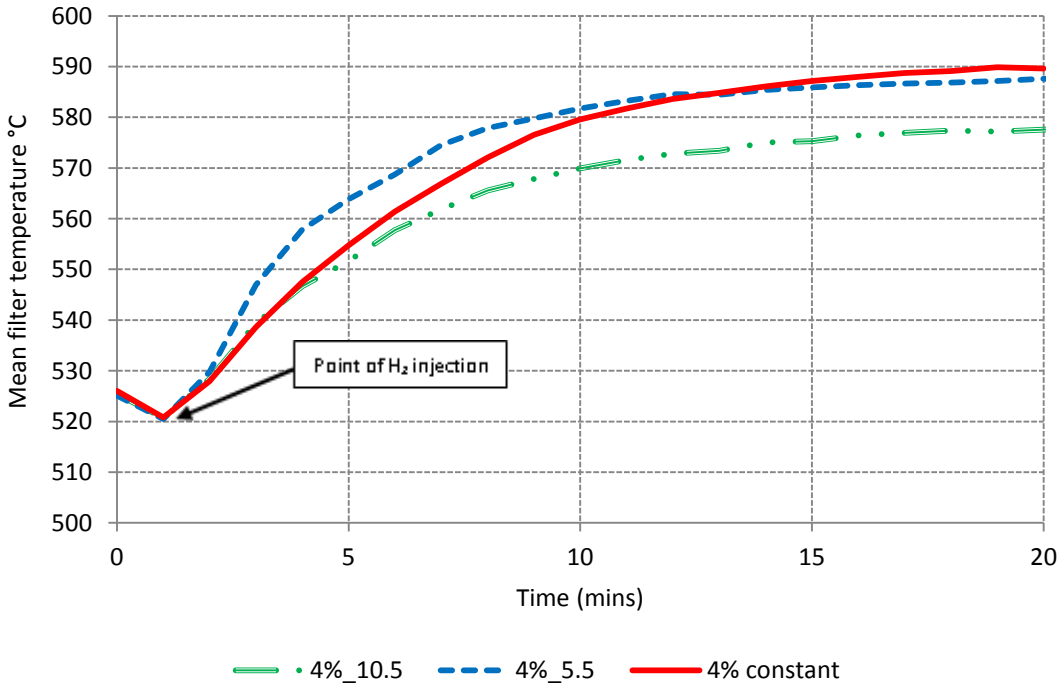

Figure 4-5. Mean filter temperature comparison for periodic and constant strategies

It is apparent from figure 4-5 that although the constant strategy induced a higher peak filter temperature when compared to that of the 5.5 injection strategy, for the first 11 minutes following the H_2 injection event, the rate of temperature increase is significantly higher when adopting the 5.5 injection strategy. It is assumed that this is the result of a so called 'triggering effect' where the frequent introduction of H_2 induces a faster rate of temperature increase when compared to the temperature profile generated using a constant strategy. The impact of the triggering effect is also evident in figure 4-6 where the 5.5 strategy initially demonstrates a faster rate of regeneration for a period of approximately 15 minutes when compared to the constant strategy. However, the quality of regeneration for both the

constant and 5.5 strategies is very similar. It is assumed that this is due to the constant strategy featuring no interruptions in the H_2 delivery, a factor that may effect the continuity of the soot oxidation reaction. However, it must be noted that the 5.5 periodic strategy achieves these comparable characteristics while utilising 50% less H_2 volume than the constant injection strategy.

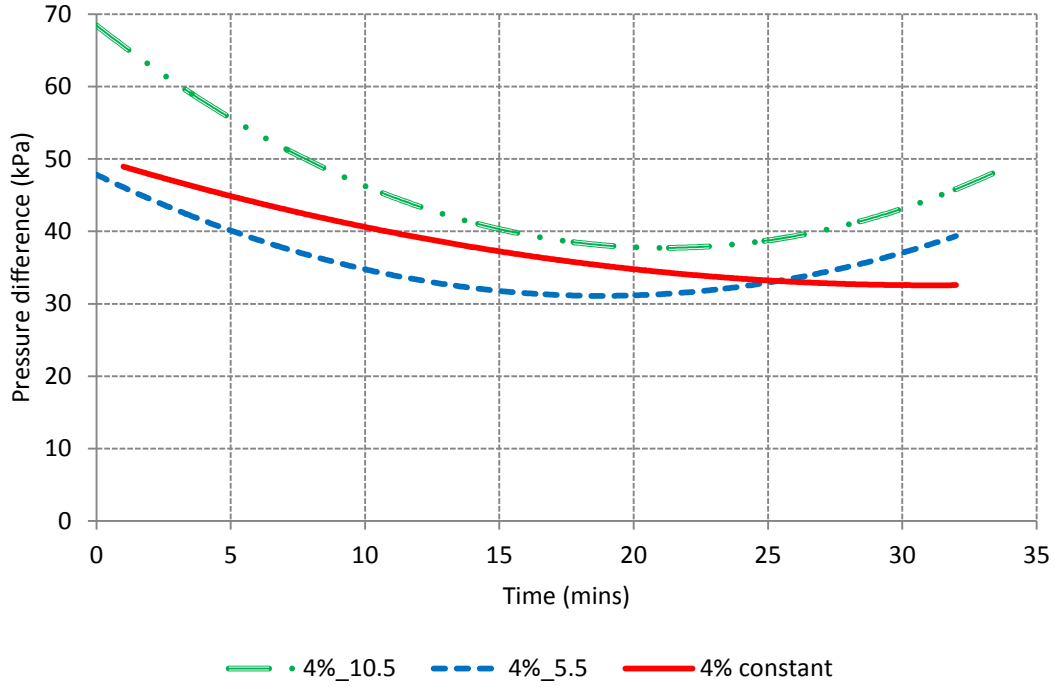

Figure 4-6. Regeneration profile comparison for periodic and constant strategies

It is evident from figures 4-5 and 4-6 that the 10.5 strategy demonstrated the lowest temperature increase as well as the poorest regeneration profile. This indicates that by decreasing the frequency of the H_2 injection events, the impact of the triggering effect is largely reduced even though the duration of each event is extended. In addition, due to the lower volume of H_2 utilised by the 10.5 strategy when compared to the constant strategy, the 10.5 strategy is also unable to generate filter temperatures as high as the constant strategy.

4.6 Effect of periodic H_2 addition on post DPF emissions

Figure 4-7 demonstrates the effects that the periodic 5.5 injection strategy had on various chemical components of the exhaust stream post DPF.

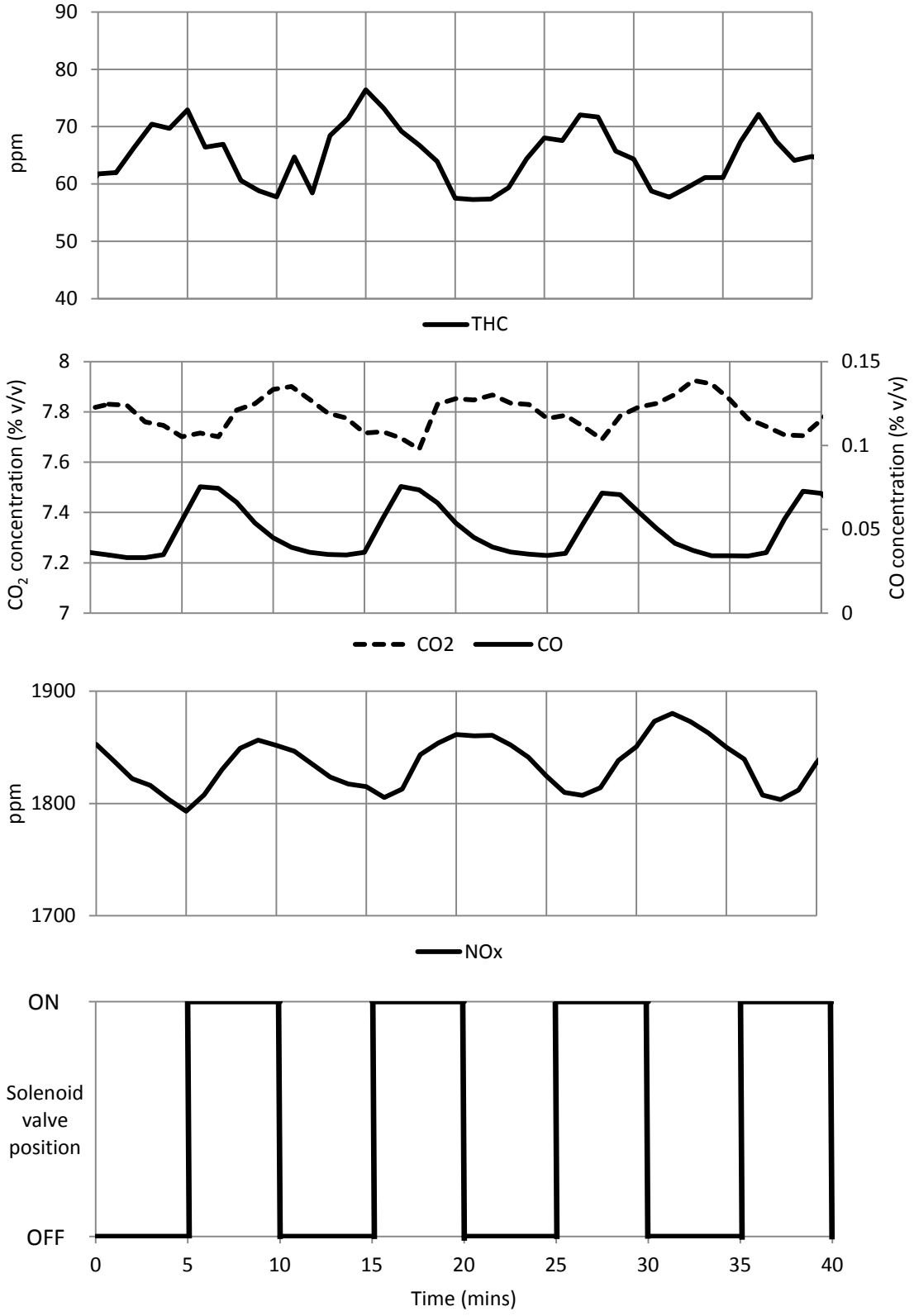

Figure 4-7. The effect of the 5.5 periodic injection strategy on various exhaust emissions post DPF

It is evident from this data that the periodic H_2 injection strategy strongly influences the concentration of CO, CO_2, NOx and THCs post filter. This is demonstrated by all four components demonstrating cyclic responses which coincide with the H_2 injection duty cycle.

It is evident from this data that following each H_2 injection event, THC is decreased while NOx is increased. The assumptions for why this occurs were previously outlined in section 4.4 of this chapter. As expected, the CO and CO_2 trends mirror each other. Shortly following each H_2 injection event, the corresponding exothermic reaction results in more CO being converted into CO_2 demonstrated by the decline in CO concentration mirrored by a rise in CO_2. This trend continues until the completion of the injection pulse.

4.7 Summary

This chapter has investigated the effects of introducing H_2 to the passive regeneration process at increasing concentrations using a constant injection strategy (no break in hydrogen delivery). This was followed by analysing and comparing the effects of implementing two periodic injection strategies at a set concentration. The effects of implementing these strategies on filter temperature, regeneration quality and exhaust gas composition were discussed. It was concluded from this study that the addition of H_2 (in excess of 1% (v/v)) to the DPF induces an exothermic reaction that increases the filter temperature and hence enhances both the speed and quality of the resultant regeneration process. These benefits were also apparent when adopting a 5.5 periodic strategy that, when compared to the effects of the equivalent constant injection strategy, resulted in comparable temperature and regeneration characteristics whilst using 50% less volume of simulated H_2 reformate than the constant injection strategy.

CHAPTER 5

CHAPTER 5 – PERIODICALLY REGENERATING DIESEL PARTICULATE FILTER WITH HYDROGEN/CARBON MONOXIDE ADDITION

CHAPTER 5 – PERIODICALLY REGENERATING DIESEL PARTICULATE FILTER WITH HYDROGEN/CARBON MONOXIDE ADDITION

5.1 Introduction

For a number of aftertreatment systems, both H_2 and CO can be adopted to enhance system performance. Past research into the development of selective catalyst reduction (SCR) systems has identified that, with the addition of H_2 to the feed gas, NOx reduction can occur at lower exhaust gas temperatures. However, to obtain these benefits a small concentration of CO must also be introduced to the gas feed [Macleod and Lambert (2002)].

The primary objective of this study is to support the regeneration process by introducing a H_2 and CO mixture. A gaseous mixture containing 60% H_2 v/v, balanced with CO is adopted throughout testing using both constant and periodic injection strategies. Ongoing research by the authors and their research partners, aims to develop a diesel emissions reduction system with enhanced performance by utilisation of H_2 and CO produced 'on board' in an exhaust gas assisted diesel fuel reformer. As previously described in section 2.4.7, exhaust gas fuel reforming involves fresh diesel fuel being reformed catalytically when directly contacted with oxygen and steam already present in the exhaust gas. As a result H_2 and CO reformates are produced, negating the need for on board storage [Tsolakis and Megaritis (2004), Tsolakis and Megaritis (2005), Abu-Jrai *et al* (2007) and Yap *et al* (2006)]. Investigating the effects of implementing these reformates to the DPF regeneration process, is the motivation for this study.

The secondary objective of this study is to identify the effects of varying space velocity and engine load on the regeneration process. This is in an attempt to identify trends that can be utilized in future work to determine engine conditions for when the mixture injection strategy should be implemented and therefore maximise the proficiency of the regeneration process.

5.2 Experimental apparatus and test procedure

For the majority of this test, a set operating point of 1500 rpm and 4.4 bar BMEP was adopted. This was only changed during the engine load investigation where the engine load

was reduced from 4.4 bar to 2.5 bar BMEP (see section 5.3.5). The engine speed remained at 1500rpm. Excluding the space velocity investigation (see section 5.3.4), the sampling flow rate through the filter was kept at a constant 70 l/m throughout testing. During the space velocity investigation this was reduced to 40 l/m. This test again adopted the aftertreatment device test rig outlined in chapter 3. Emission measurements were taken both pre and post DPF. The FTIR analyser was adopted for CO and CO_2 measurements while the H_2 measurements were achieved using the gas chromatograph. The Horiba gas analyser (7170 DEGR) was adopted for O_2 measurements. The supporting mixture used throughout testing featured a 60% (v/v) H_2 content balanced with CO (referred to throughout this study as 'the mixture'.)

5.3 Results and discussion

5.3.1 DPF regeneration with 2.7% mixture concentration at 520°C

Figure 5-1(a) and 5-1(b) demonstrate the effect of introducing 2.7% (v/v) mixture concentration, using various injection strategies, to the DPF regeneration process. As demonstrated in the previous chapter, passive regeneration occurs at a mean DPF temperature of ~520°C. In order to identify whether the various injection strategies with 2.7% mixture concentration supported the passive regeneration process, the mean filter temperature (average taken of top, middle and bottom filter temperatures) was first set to this passive regeneration temperature before implementing each of the injection strategies.

Following the implementation of a constant strategy (no break in the mixture flow) three periodic strategies were adopted; 5.5, 10.5 and 5.10. The resultant pressure data is shown in figure 5-1(b). It is apparent from figure 5-1(a) that the introduction of the mixture at 2.7% concentration (regardless of which strategy) increases the mean filter temperature from within the passive regeneration temperature window to within an increased temperature range of 535-540°C, a rise of ~25-30°C. This indicates that the introduction of the mixture using any of the four strategies induces an exothermic reaction from combustion of either the H_2, CO or both.

As a result of the mixture addition inducing exothermic reactions, it is evident that all four strategies see an initial increase in mean filter temperature. Interestingly, although the

mean filter temperature when adopting the constant strategy is not sustained as well as with the periodic strategies, the constant strategy results in the most thorough regeneration, reducing the pressure difference to that of a clean filter. An explanation for this may be the continuity of a chemical reaction between the mixture and the accumulated soot, resulting in significant soot oxidation. Such a reaction would be frequently interrupted with a periodic strategy. However, the complex chemical kinetics of this system would need to be researched further to validate such an assumption.

Following implementation of the constant injection strategy, a 5.5 periodic strategy was adopted followed by a 10.5 strategy. Both strategies resulted in similar peak temperatures and very similar regeneration profiles. Benefits from the increased mixture volume from the 10.5 strategy compared to the 5.5 strategy are only marginally apparent at ~35-40 minutes into the regeneration event when a slightly lower pressure difference is demonstrated. However, the significant increase in mixture volume is not justified by the minimal improvement in the thoroughness of regeneration. In comparison with the constant strategy, the 5.5 and 10.5 periodic strategies provide a slower rate of regeneration with the minimum filter pressure difference not being reached until 35-40 minutes after the supporting mixture has been added. In addition to this the constant strategy features a minimum filter pressure difference 45% lower than that achieved by the 10.5 and 5.5 strategies. However, this is at the cost of substantially higher volumes of mixture.

In order to identify the minimum mixture volume required to still ensure the presence of an exothermic reaction and hence proficient regeneration, a 5.10 strategy was implemented. It is apparent from figure 5-1(a) and (b) that this strategy did achieve an exothermic reaction but the peak temperature was the lowest of all the strategies attempted. In addition to this, the thoroughness of regeneration was significantly poor with only an approximate 33% reduction in the filter pressure difference compared to the fully loaded condition. As a result, for all further tests the 5.10 strategy was replaced with a 10.10 strategy.

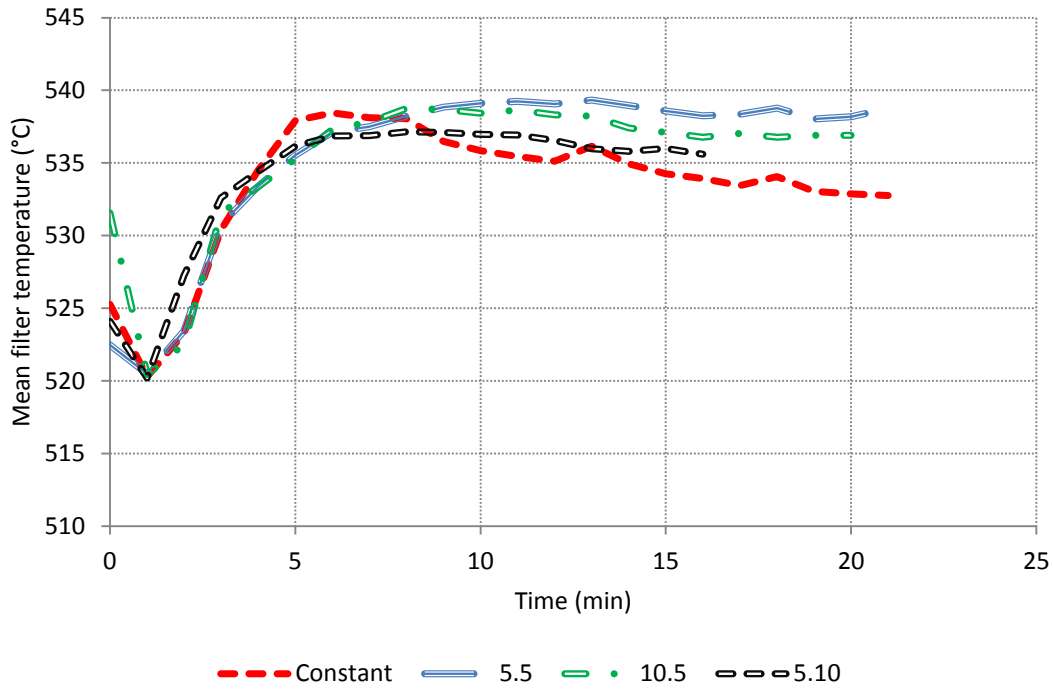

Figure 5-1 (a). Effect of 2.7% mixture addition on mean filter temperature using various injection strategies

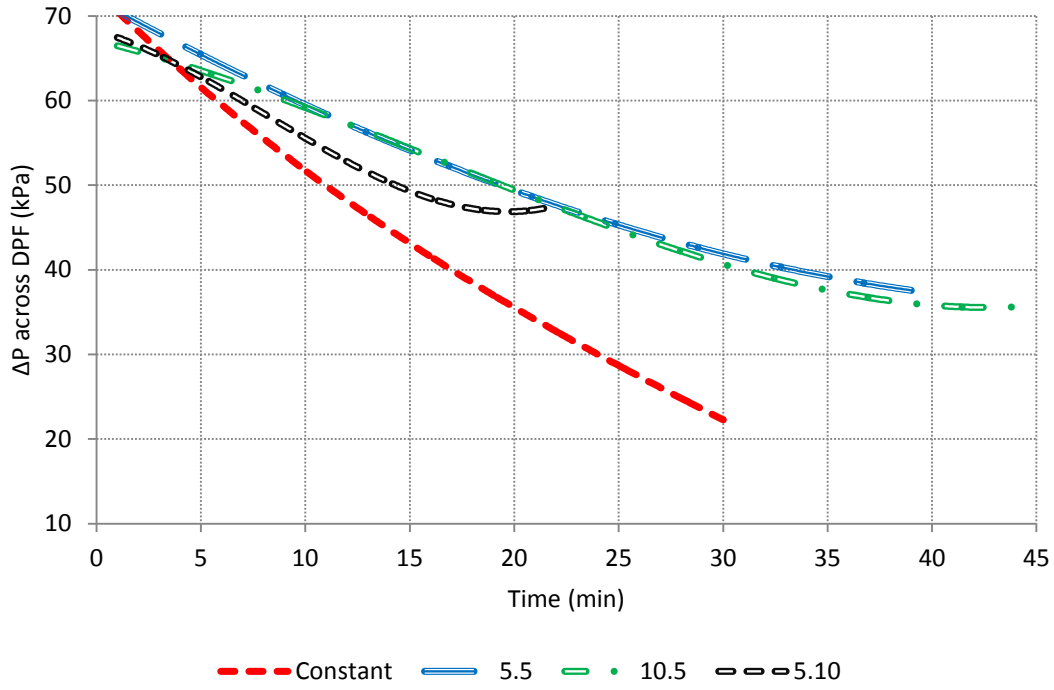

Figure 5-1 (b). Effect of 2.7% mixture addition on the regeneration process using various injection strategies

5.3.2 DPF regeneration with 2.7% mixture concentration at 440°C

The exothermic reaction featured by all the strategies attempted, indicated that with the support of the additional mixture, regeneration could be achieved at lower exhaust temperatures. As a result, regeneration was attempted at a mean filter temperature of ~440°C. Again, a 2.7% mixture concentration was adopted, using a constant injection strategy. The results are demonstrated in figure 5-2.

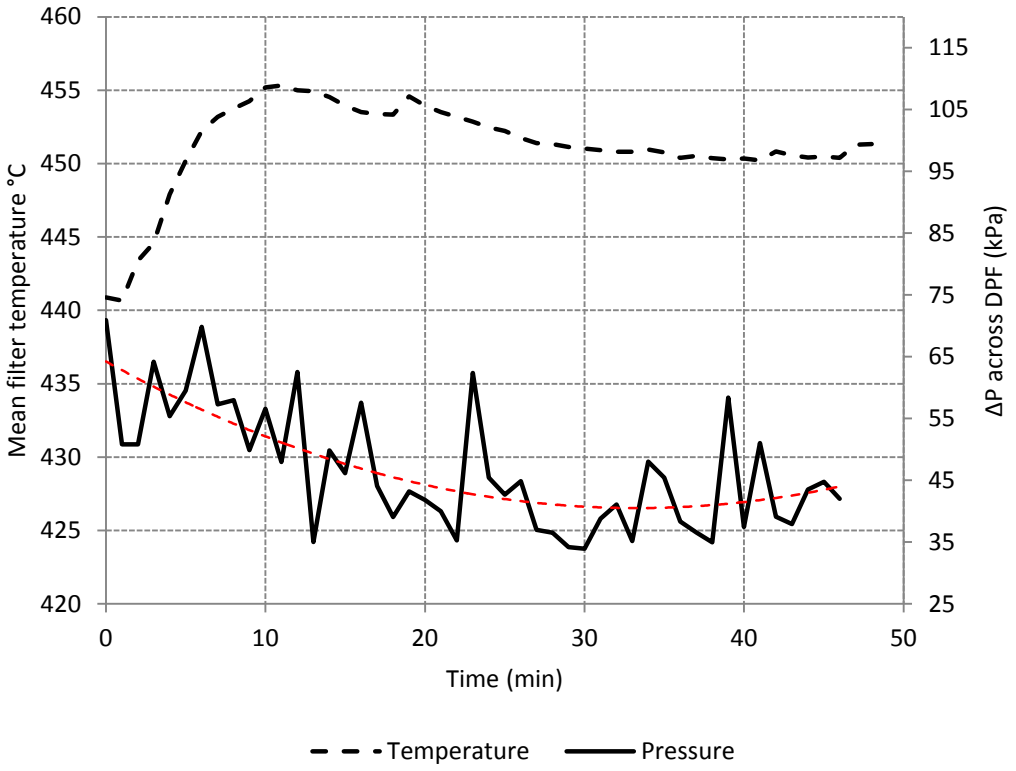

Figure 5-2. Effect of 2.7% mixture concentration, constant strategy at a mean filter temperature of 440°C.

It is evident from figure 5-2 that although at a lower furnace inlet temperature, the supporting mixture still succeeded in initiating an exothermic reaction, increasing the filter temperature by ~11°C. As a result, the regeneration process was also initiated, reducing the pressure difference by ~50%. However, this is surprising as the peak temperature is still substantially lower than the initiation temperature for passive regeneration. It is unclear without further research into the complex chemical kinetics of the DPF whether this reduction in the regeneration initiation temperature is a result of the additional supporting mixture or not. It is apparent in figure 5-2 that after 40 minutes the extremes of the regeneration temperature window are exceeded and the filter begins to re enter loading

mode. As a result it was decided to increase the concentration of the mixture at this lower furnace inlet temperature in an attempt to achieve proficient regeneration at lower exhaust gas temperatures.

5.3.3 DPF regeneration with 4.5% mixture concentration at 440°C

Figure 5-3(a) and (b) demonstrate the effect of adopting 4.5% (v/v) mixture concentration, using various strategies at a mean filter temperature of 440°C. Comparable to the previous data, all the tested strategies demonstrated evidence of the occurrence of an exothermic reaction indicated by a significant increase in mean filter temperature. It is evident from figure 5-3(b) that the constant and 10.5 strategies demonstrated the most thorough regeneration events, explained by the respective peak mean filter temperatures (demonstrated in figure 5-3(a)) being very close to the passive regeneration temperature. In comparison, the 5.5 and 10.10 periodic strategies demonstrate the lowest quality regeneration events as a result of the peak mean filter temperatures being further below the passive regeneration temperature. However, the regeneration process is still initiated and sustained at temperatures below the passive regeneration temperature for all strategies tested.

It is evident from figure 5-3(a) that the 10.5 periodic strategy demonstrates a higher peak mean filter temperature than that generated when adopting the constant injection strategy. As a result, the 10.5 strategy demonstrates an improved quality of regeneration compared to the constant strategy. However, as demonstrated with the 2.7% mixture tests, the constant strategy adopts the fastest regeneration rate. Therefore, it is apparent that although faster regeneration can be achieved with a constant injection strategy, a 10.5 periodic strategy with a 4.5% mixture concentration can ensure more thorough regeneration with substantially less mixture volume, but at a relatively slower rate.

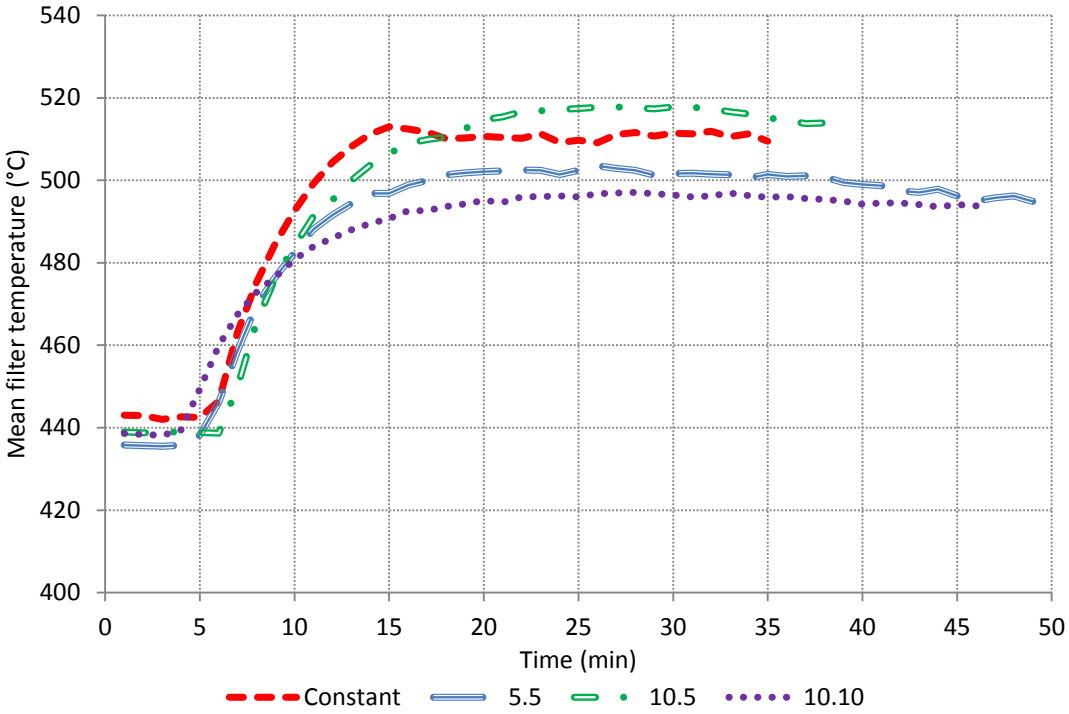

Figure 5-3(a). Effect of 4.5% mixture addition on mean filter temperature using various injection strategies

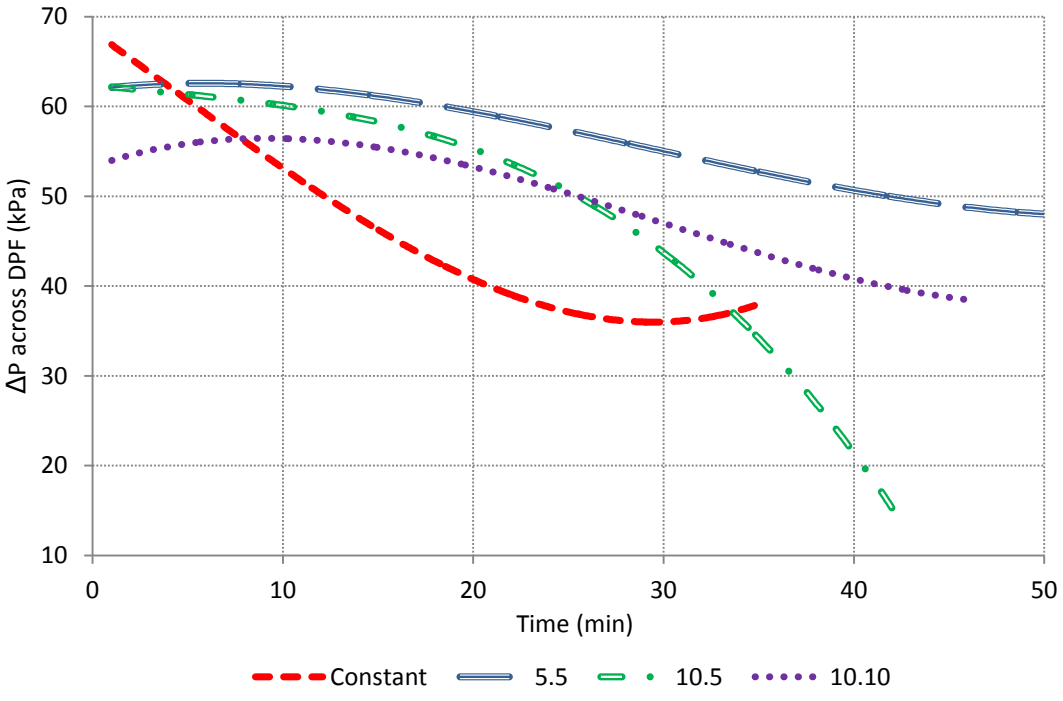

Figure 5-3(b). Effect of 4.5% mixture addition on the regeneration process using various injection strategies

Following the implementation of the constant and 10.5 strategy, a 5.5 strategy was adopted in an attempt to reduce the mixture volume further. Due to the significantly lower volume of mixture (50% less than the constant volume strategy) the peak temperature demonstrated by this strategy was one of the lowest achieved and hence demonstrated the poorest regeneration quality. In a further attempt to achieve the same peak temperature demonstrated by the 10.5 strategy, but with less mixture volume, a 10.10 strategy was then adopted. This was on the assumption that a 10 second initial injection of mixture may be the reason for the initial high mean filter temperature demonstrated by the 10.5 strategy. However, as demonstrated in figure 5-3(a), this assumption was not supported as the lowest peak temperature was achieved. This can be explained by the period between each injection event being too excessive. It must be noted that although the lowest peak mean filter temperature was featured, the 10.10 strategy still managed to achieve the same quality of regeneration as the constant strategy however this took longer to achieve, with the minimum pressure difference being reached 40 minutes after the injection event. When attempting to optimise the volume of mixture required for proficient regeneration, it must be considered that the 10.10 strategy, although slower, matched the regeneration quality of the constant strategy at a significantly lower peak temperature of ~497°C as opposed to ~518°C (as achieved using the 10.5 strategy). Such a factor could significantly enhance the operational lifetime of the DPF.

5.3.4 Effect of space velocity

In addition to investigating the effects of implementing periodic injection strategies, this study also aims to highlight the impact that varying both engine load and space velocity has on the regeneration process. Space velocity was defined in section 2.4.2.1 of the literature review chapter of this study.

In order to identify the effect of SV, the exhaust sampling flow rate was reduced from 70 l/min (SV=82888 h^{-1}) as used in all previous tests, to 40l/min (SV=47364 h^{-1}) and the test described in the previous section repeated. The results are demonstrated in figure 5-4(a) and (b), alongside the data collated in the previous section allowing for comparison.

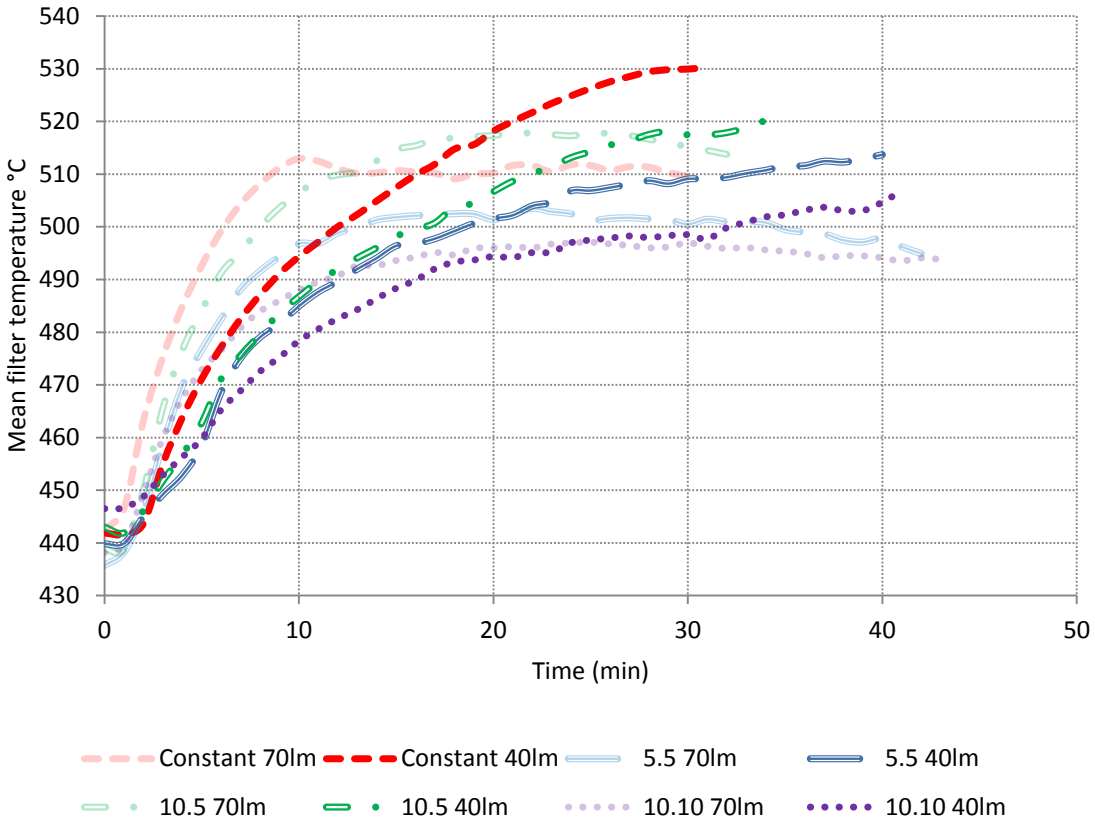

Figure 5-4(a). Effect of space velocity on mean filter temperature using 4.5% (v/v) mixture

When comparing the data between the high and low SV tests, two defined features are apparent regardless of which injection strategy was adopted. Firstly, each strategy performed at the lower SV, demonstrated a higher peak temperature than the equivalent strategy ran at the higher SV. This phenomenon has also been identified in other studies [Kim *et al* (1997)] where an increase in the space velocity induced a reduction in the peak filter temperature. In this particular case it was assumed by the author that this was the result of the increased flow rate encouraging convective heat transfer. As a result, more of the heat generated by the exothermic reaction was removed by the exhaust stream from the filter walls and out of the system [Kim *et al* (1997)].

The second prominent feature from this data is the rate in which heat is generated from the exothermic reaction. For all strategies tested, the data collected at the lower SV always demonstrated a slower rate of mean filter temperature increase when compared to the corresponding high SV data. It is assumed that this slower rate of mean filter temperature

increase was a result of the lower SV introducing the mixture to the DPF at a slower rate, a factor which may have impacted the chemical reaction occurring at the filter.

For each strategy, it is apparent from figure 5-4(a), that the mean filter temperature demonstrated by the data collected at the lower SV overtakes the corresponding data collected at the higher SV when entering a temperature window of ~498-518°C. This indicates that once this temperature window is achieved, the convective heat transfer becomes the dominant influence on the mean filter temperature. It is assumed that this is due to a considerable increase in the convective heat transfer rate as a result of the increased temperature difference between the filter and exhaust gas.

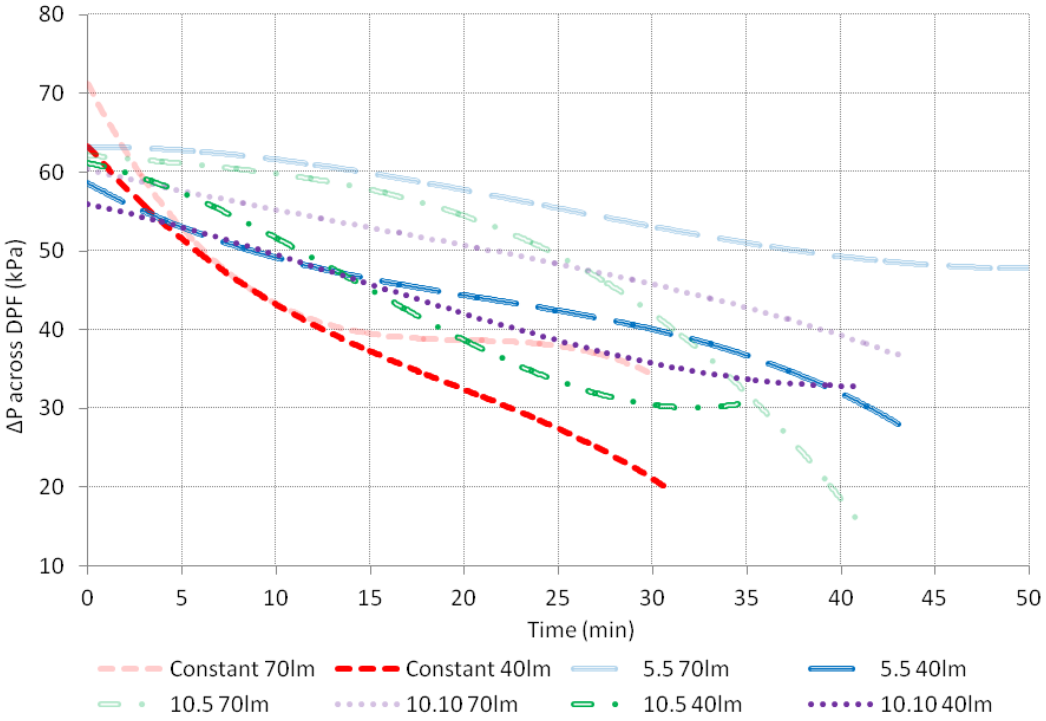

Figure 5-4(b). Effect of space velocity on the regeneration process using 4.5% mixture

Figure 5-4(b) compares the quality of regeneration between the strategies tested at both the high and low SV. It is apparent from this data that the constant, 5.5 and 10.10 strategies tested at the lower SV featured more thorough regeneration than the equivalent strategy tested at the higher SV. For the 10.5 strategy it is apparent that the regeneration is significantly faster but not quite as thorough. These improvements in the quality of regeneration can be explained by the higher peak filter temperatures achieved at the lower SV.

5.3.4.1 Impact of injection strategy on mixture concentration at decreased space velocity

In order to ascertain the extent in which both components of the supporting mixture were involved in each exothermic reaction it was decided to measure the concentration of CO, CO_2 and H_2 both pre and post DPF. Figure 5-5(a) and (b) are evidence that combustion of the CO mixture occurred, regardless of which strategy was adopted. This is not only indicated by a reduction in CO but also by a corresponding increase in CO_2, formed as a result of the CO combusting and reacting with the surrounding oxygen. At the defined test conditions (4.4bar BMEP, 1500rpm) the oxygen content in the exhaust stream pre DPF was 9.74% v/v.

Figure 5-5(c) demonstrates the quantity of H_2 combusted for each strategy. It is apparent that the shape of this curve is quite similar to the one demonstrated in figure 5-5(a). However, while all the adopted periodic strategies combusted the introduced H_2 by 93.5-98.5%, the same strategies only combusted 65-70% of the CO. Therefore it can be stated that, under these conditions, the H_2 was burned more efficiently than CO for all periodic strategies tested. When comparing the data from this section with figure 5-5(a) an expected general trend between volume of mixture combusted and peak filter temperature achieved is apparent.

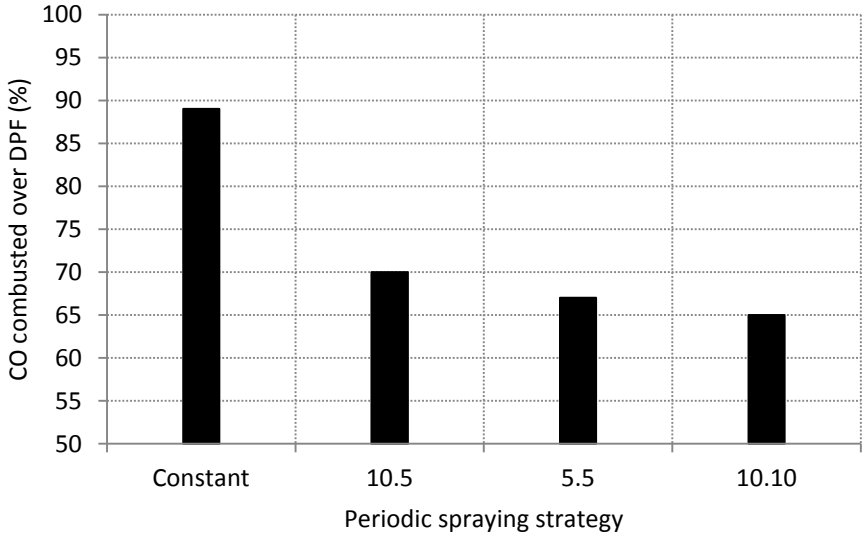

Figure 5-5(a). Effect of various injection strategies on CO concentration using 60% H_2 balanced with CO mixture

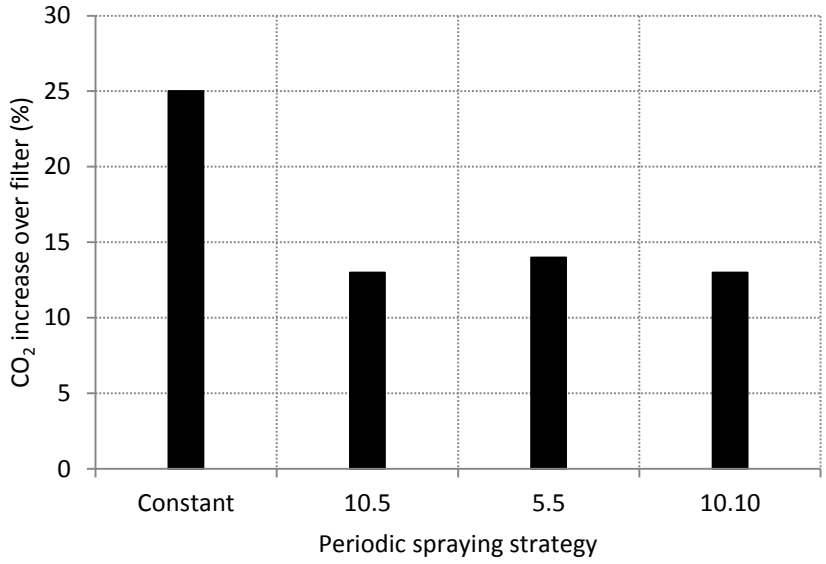

Figure 5-5(b). Effect of various injection strategies on CO_2 concentration using 60% H_2 balanced with CO mixture

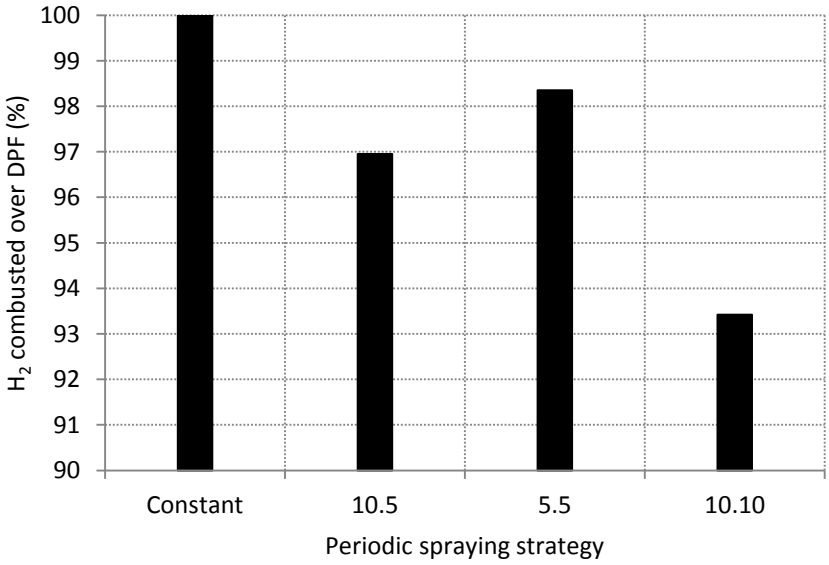

Figure 5-5(c). Effect of various injection strategies on H_2 concentration using 60% H_2 balanced with CO mixture

5.3.5 Effect of engine load

Past research has identified that the production of diesel particulates increases with engine load [Lapuerta *et al* (2003) and EL Shobokshy (1984)]. As a result, this section aims to identify how reducing the engine load, and hence reducing particulate production, impacts

the regeneration process. For this test the engine load condition was reduced from 4.4bar (considered as mid to high engine load) to 2.5bar BMEP (considered as mid-load) and the test previously outlined in section 3.3 repeated. Figure 5-6(a) demonstrates the results, compared with the results displayed previously in section 5.3.3. At this lower engine load the exhaust O_2 content pre filter was 12.96% v/v.

It is apparent from figure 5-6(a) that for all strategies tested, the impact of the lower engine load resulted in substantially lower mean filter temperatures. This is due to the reduction in engine load resulting in lower exhaust gas temperatures (~300°C opposed to ~400°C). Although the filter was kept at the same constant temperature as used in the previous tests (440°C), the reduced exhaust temperature resulted in increased convective heat transfer and hence a reduction in the peak filter temperature.

Figure 5-6(a) demonstrates that under these conditions the heat present at the filter is close to the minimum required for an exothermic reaction to occur using the constant strategy. This is indicated by the minimal increase in filter temperature (10°C).

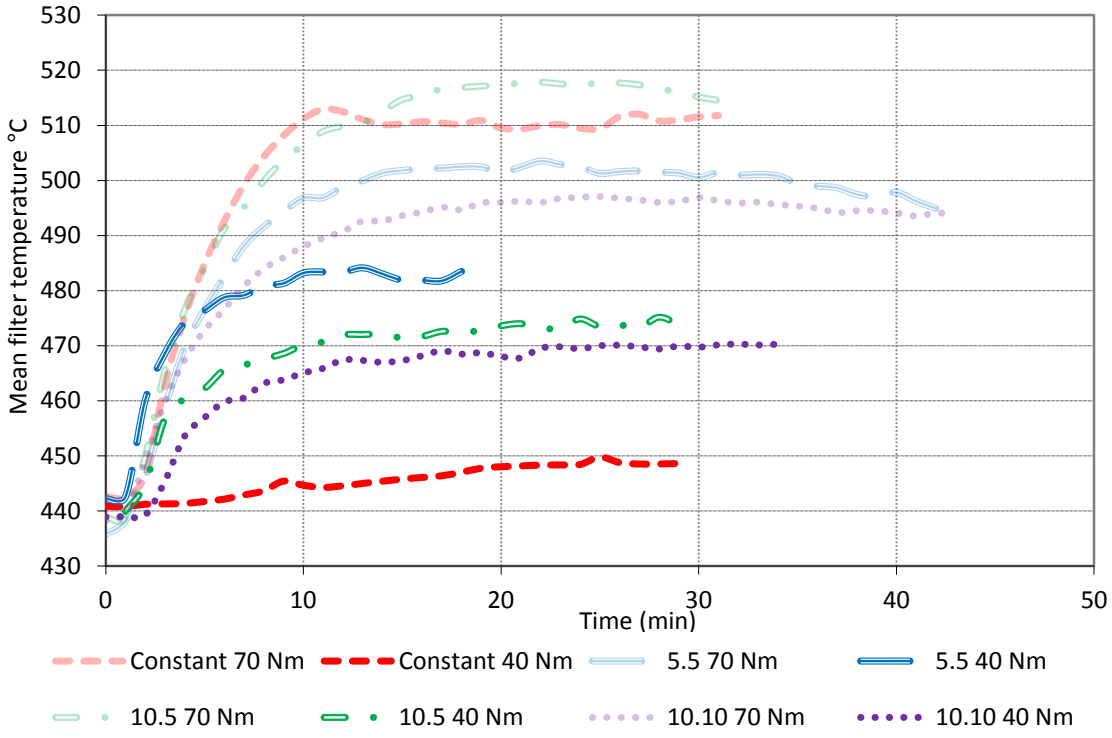

Figure 5-6(a). Effect of engine load on mean filter temperature using 4.5% mixture

Figure 5-6(b) demonstrates the regeneration proficiency for each strategy at the lower engine load. As expected, due to the minimal increase in temperature demonstrated by the

constant strategy, the standard of regeneration is significantly poor, demonstrating a brief period of regeneration before entering loading mode. Regarding the periodic strategies, the regeneration profiles collected at the high and low engine loads demonstrate minimal variance and no defined trend is apparent. This is unexpected due to the significantly lower filter temperatures achieved when adopting the lower engine load.

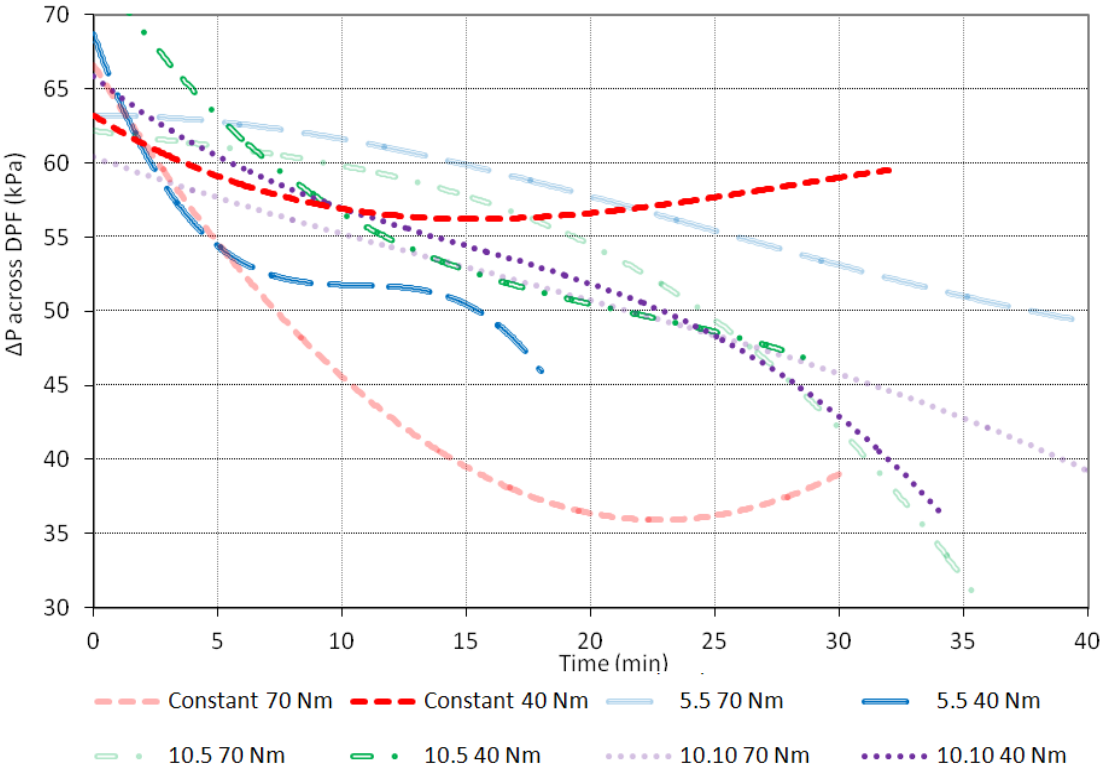

Figure 5-6(b). Effect of engine load on the regeneration process using 4.5% mixture

5.3.5.1 Impact of injection strategy on mixture concentration at low load

When analysing figure 5-7(a), (b) and (c) it is evident that when adopting the constant strategy at the lower load of 2.5 bar BMEP, only 8% H_2 was combusted while no combustion of the CO was evident. Therefore it is unsurprising that a very minimal increase in filter temperature was demonstrated when adopting the constant strategy. This further supports the theory that the amount of heat energy present at the filter was close to the minimum required for an exothermic reaction to be initiated under these conditions for the constant strategy.

When comparing figure 5-7(a) and 5-6(a), there is a strong correlation between quantity of CO combusted and peak filter temperature achieved. However, the same trend is not

apparent between peak filter temperature and quantity of H_2 combusted (see figure 5-7(c)). This indicates that under these conditions, when both hydrogen and CO is adopted in a mixture, the combustion of CO had more of a positive impact on the achievable peak filter temperature than the H_2.

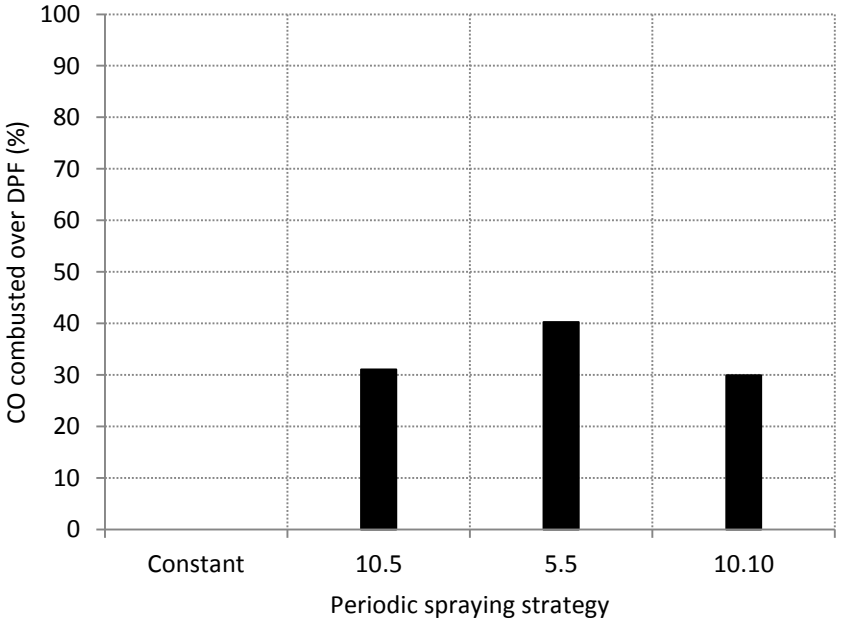

Figure 5-7(a). Effect of various injection strategies on CO concentration

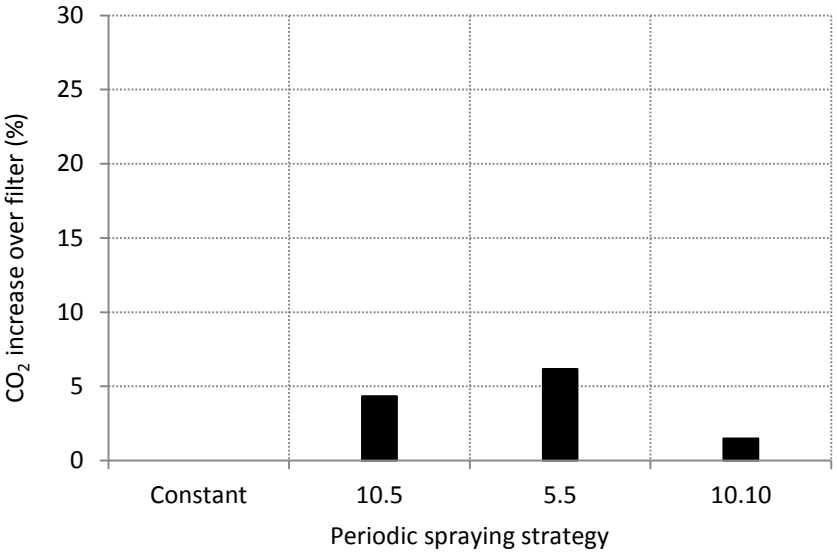

Figure 5-7(b). Effect of various injection strategies on CO_2 concentration

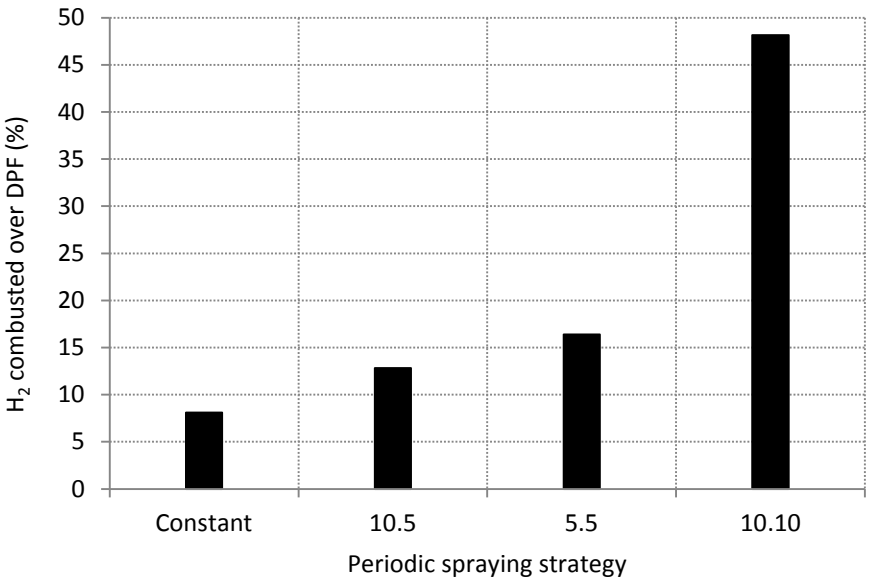

Figure 5-7(c). Effect of various injection strategies on H_2 concentration

5.4 Summary

This chapter has identified the effects of introducing a H_2/CO mixture at a concentration of 2.7% v/v to the passive DPF regeneration process. This was followed by increasing the mixture to 4.5% v/v and introducing it to the DPF regeneration process at a lower mean filter temperature of 440°C. In both cases, the mixture was introduced using both constant and periodic injection strategies. In addition, this chapter also highlighted the effects of varying the space velocity and engine load on the DPF regeneration process. It was concluded from this chapter that when adopting a mixture concentration of 4.5% (v/v) the DPF could be sufficiently regenerated at a filter temperature of 440°C, which is significantly lower than the passive regeneration temperature of 520°C. In addition, the 10.10 periodic injection strategy was found to be the optimised strategy as it demonstrated a quality of regeneration comparable to that of the constant strategy but achieved it with 50% less mixture volume. In addition, this chapter also demonstrated that a reduction in filter space velocity proved beneficial to the regeneration quality whilst varying the engine load demonstrated minimal impact on the regeneration characteristics.

CHAPTER 6

THE EFFECT OF A H2/CO MIXTURE AT VARYING RATIOS ON THE DIESEL PARTICULATE FILTER REGENERATION PROCESS: TOWARDS AN OPTIMISED FUEL REFORMER DESIGN

CHAPTER 6 – THE EFFECT OF A H_2/CO MIXTURE AT VARYING RATIOS ON THE DIESEL PARTICULATE FILTER REGENERATION PROCESS: TOWARDS AN OPTIMISED FUEL REFORMER DESIGN

6.1 Introduction

The primary objective of this study is to identify an optimised H_2/CO mixture ratio to assist with future fuel reformer design. This is to be attempted by varying the mixture ratio incrementally and analysing the resultant impact on filter temperature and both regeneration rate and quality.

The secondary aim of this research is to adopt FTIR emission measurement methodology to identify the impact of introducing various mixture ratios on the chemical composition of the exhaust gas post filter. Due to the FTIR measurement technique having the capability to continually measure the concentration of any gas compound that absorbs infrared, this technique allows for the behaviour of many non legislated exhaust gas components to be easily quantified. As a result of this characteristic and a variety of other continuous improvements, the application of FTIR technology has increased significantly within the automotive industry and is now routinely adopted for measurement of both legislated and non legislated exhaust gas components [Adachi (2000), Shore and deVries (1992), Nabi *et al* (2006), Daham (2005), Yeom *et al* (2004) and Bion *et al* (2003)].

6.2 Experimental apparatus and test procedure

Throughout this test the engine speed and load was set to 1500rpm and 4.4 bar BMEP respectively. The exhaust sampling flow rate was fixed at 70l/m. The filter was regenerated using 6% (v/v) H_2/CO mixture at varying ratios. During regeneration the mean filter temperature was set to approximately 440°C. The ratios investigated during this study are identified below in table 6-1 alongside the calculated flow rates required to generate the correct mixture concentration in the exhaust sampling line.

Test point	H_2 % of supporting mixture by volume	H_2 flow rate for 6% mixture (l/m)	CO % of supporting mixture by volume	CO flow rate for 6% mixture (l/m)
1	100	4.2	0	0
2	80	3.36	20	0.84
3	60	2.52	40	1.68
4	50	2.1	50	2.1
5	40	1.68	60	2.52
6	20	0.84	80	3.36
7	0	0	100	4.2

Table 6-1. Mixture ratios and resultant flow rates

This test again adopted the aftertreatment device test rig outlined in chapter 3. However, in order to introduce the supporting mixture at varying mixture ratios, slight modifications were required. Firstly, a second set of pipework was installed to cater for a second gas to be introduced to the sample line. This included a second flowmeter and needle valve. Secondly, the controller was modified so it could control two solenoids valves simultaneously. These modifications are demonstrated below in figure 6-1:

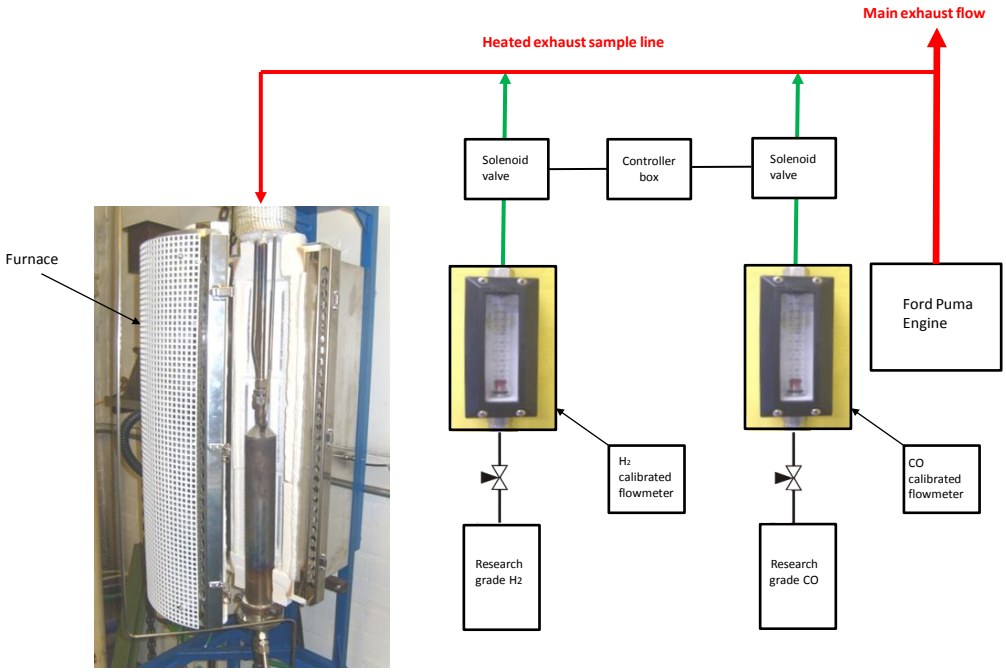

Figure 6-1. Modifications made to aftertreatment test rig

At each test point emission measurements were taken both pre and post filter for a period of 5 minutes each.

6.3 Results and discussion

6.3.1. Effect of mixture ratio on DPF temperature and regeneration process

The effect of the various mixture ratios on the mean filter temperature are demonstrated in figure 6-2. The highest temperature was achieved when a 50/50 mixture ratio was adopted. The 100% CO strategy resulted in no exothermic reaction and hence no noticeable increase in the DPF temperature. In all cases where a mixture of both H_2 and CO was present the peak filter temperature achieved was higher than that attained using 100% H_2. It is evident from this data that the closer the mixture ratio is to 50/50, the higher the filter temperature achieved.

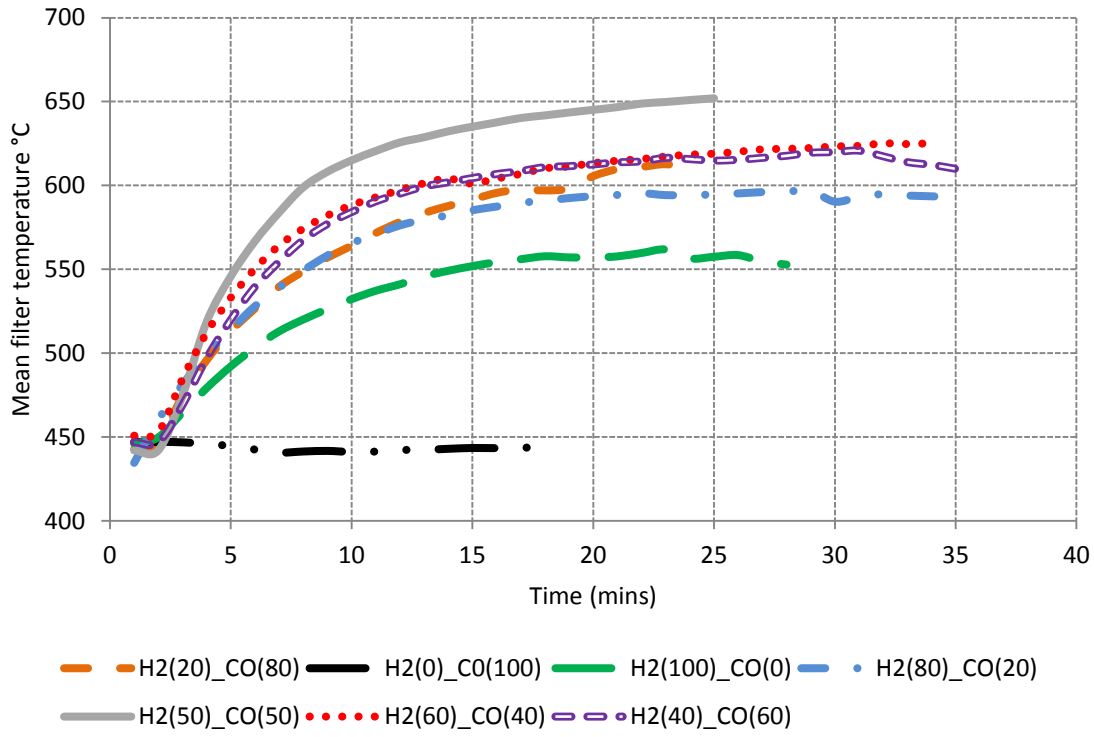

Figure 6-2. Effect of varying mixture ratio on mean filter temperature

Figure 42 demonstrates the resultant change in pressure difference over the DPF as a result of the exothermic reactions highlighted previously in figure 6-2. Due to the lack of an exothermic reaction, the addition of 100% CO resulted in regeneration not initiating. The

mixtures containing both H_2 and CO demonstrated the best quality of regeneration as a result of these mixtures featuring the highest peak filter temperatures. Although the variance between these profiles is minimal, when comparing figures 6-2 and 6-3 a general trend is apparent where the higher the peak filter temperature achieved the better quality of regeneration attained. As a result, the 50/50 mixture ratio demonstrates the most proficient regeneration profile although showing minimal difference when compared to the 60 H_2/40 CO regeneration profile. As a result the addition of a 60 H_2/40 CO mixture ratio is taken to be the optimised ratio as it incurs a quality of regeneration comparable to that of the 50/50 mixture ratio although at a lower temperature (~30°C lower). Regeneration at a lower temperature assists in increasing the robustness and operational lifetime of the DPF aftertreatment system.

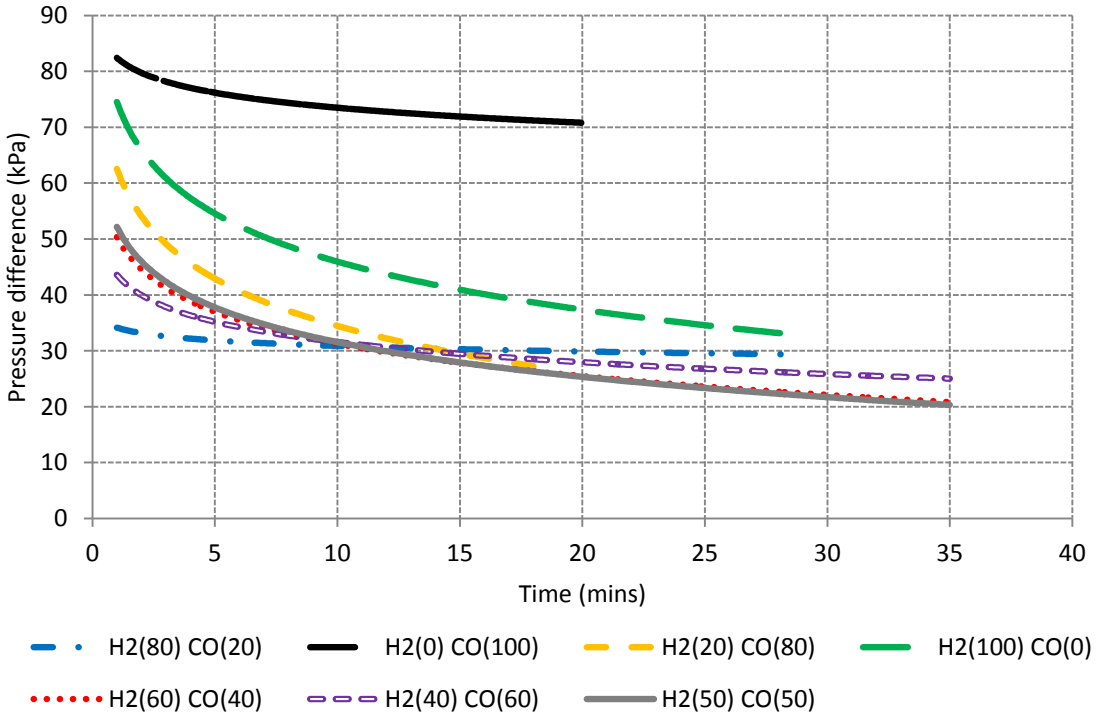

Figure 6-3. Effect of varying mixture ratio on the regeneration process

6.3.2. Effect of mixture ratio on various exhaust species

Figure 6-4 displays the NOx, THC and O_2 percentage difference from pre to post filter for all the mixture ratios investigated. It is apparent from this data that the introduction of H_2 or H_2/CO mixture addition results in an increase in NOx from pre to post filter. This is a result of the exothermic reaction increasing the filter temperature to within the NOx formation

temperature window allowing for the surrounding O_2 and N_2 to react to form NOx. Due to the NOx formation mechanism requiring significant levels of both O_2 and heat, the 100% CO addition does not generate increased NOx post filter as, due to the lack of an exothermic reaction, the peak filter temperature is not within the NOx formation temperature window. Although the introduction of a supporting mixture incurs a NOx penalty for most of the ratios tested, in all cases this was balanced with a beneficial reduction in THC. Without any mixture addition the DPF reduces THC by 15% however, with the addition of a supporting mixture this can be as high as 83% (achieved with the 60 H_2/40 CO mixture ratio) due to the exothermic reaction and resultant increase in temperature allowing for oxidation of the hydrocarbons to occur. This further accounts for the reduction in O_2 demonstrated in figure 6-4.

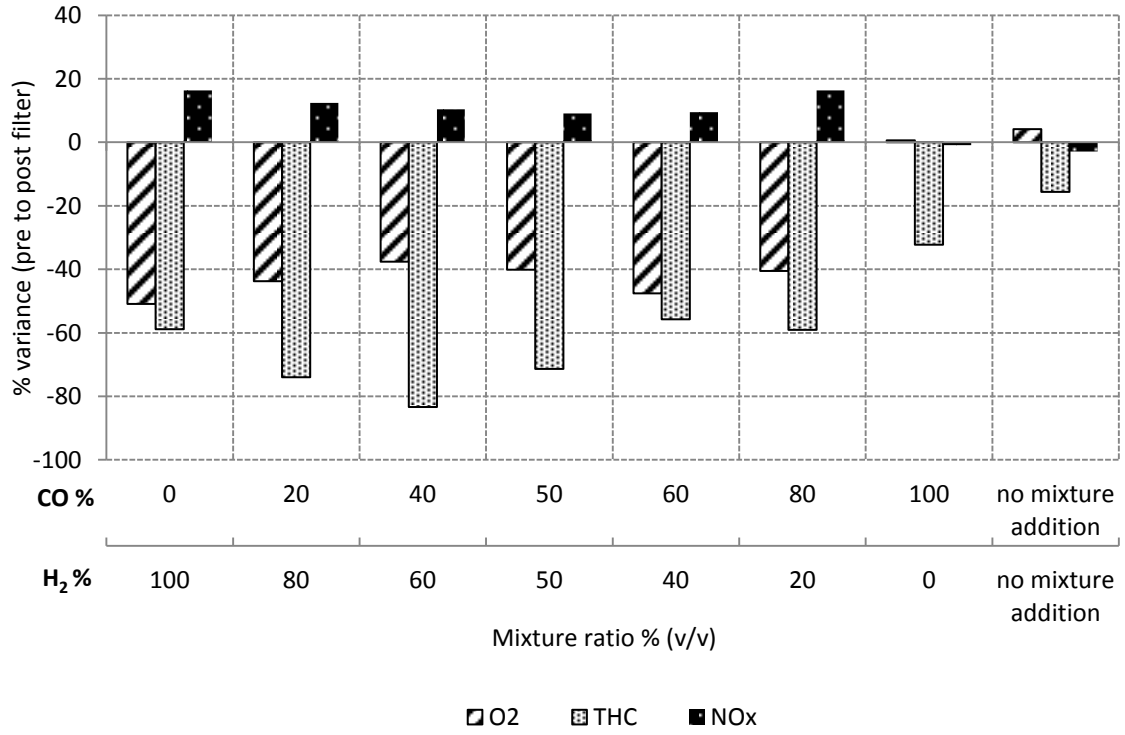

Figure 6-4. Effect of varying mixture ratio on various emission components

Figure 6-5 displays the CO and CO_2 percentage difference from pre to post filter for all the mixture ratios investigated. In all cases where the supporting mixture contained both H_2 and CO, it is evident from figure 6-5 that regardless of mixture ratio, a majority of the CO was oxidised during regeneration. The lowest volume of CO being oxidised was 98% demonstrated by the 80 H_2/20 CO mixture ratio. If the results for the 100% CO mixture addition are ignored, a strong trend is evident where the volume of CO_2 produced post filter increases as the volume of CO contained within the additional mixture is increased. The

100% CO mixture addition does not follow this trend, again due to the lack of an exothermic reaction when using this ratio and hence insufficient heat to convert the CO to CO_2. The data demonstrated in figure 6-5 highlights another reason for the reduction in O_2 post filter demonstrated previously in figure 6-4. As the increasing levels of CO react with the surrounding O_2 as a result of the high filter temperatures, proportional levels of CO_2 are generated post filter and hence the volume of O_2 post filter is reduced.

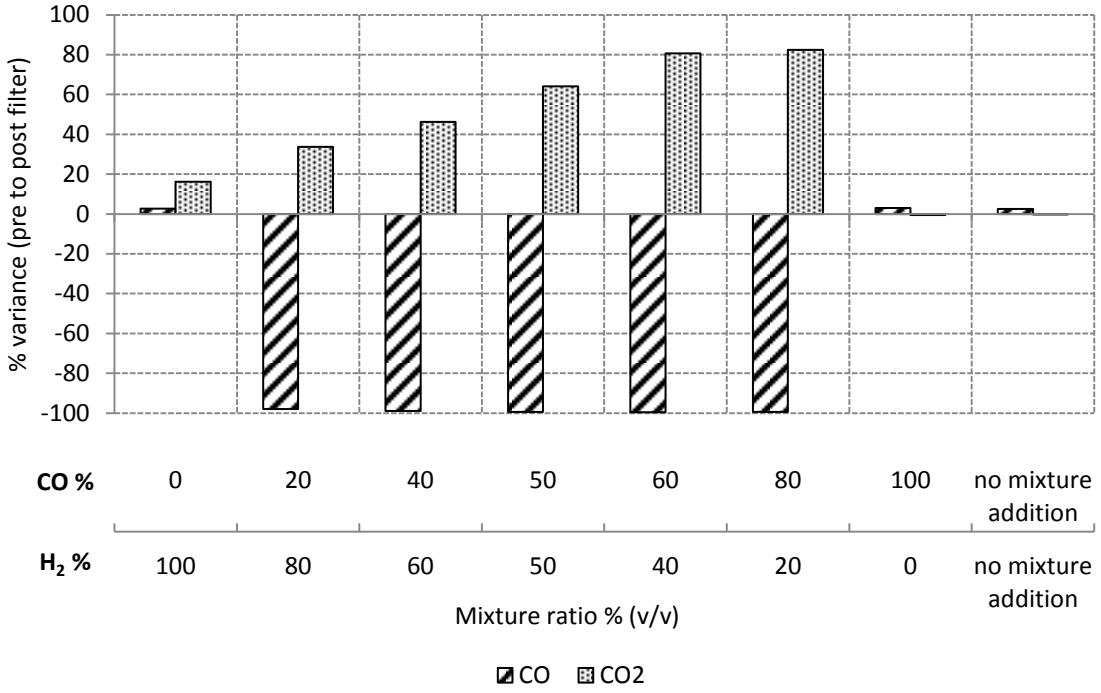

Figure 6-5. Effect of varying mixture ratio on CO and CO_2

As described previously in section 3.5.1 the Multigas 2030 FTIR spectrometer adopted a measurement 'recipe' designed specifically for quantification of diesel engine exhaust species. In addition to the components demonstrated in figures 6-4 and 6-5, this recipe also allowed for measurement of the following species: Ethane, methane, ethylene, propylene, acetylene, urea, formaldehyde and ammonia. For all of these species, a comparison was made pre to post filter for all of the mixture ratios tested, in an attempt to identify the effect that the additional mixture had on these exhaust components.

Figure 6-6 demonstrates the effect of no mixture addition (i.e. the isolated effect of the DPF) on ethylene, propylene, acetylene and methane. It is evident from this data that the DPF alone does not impact the concentration of these species.

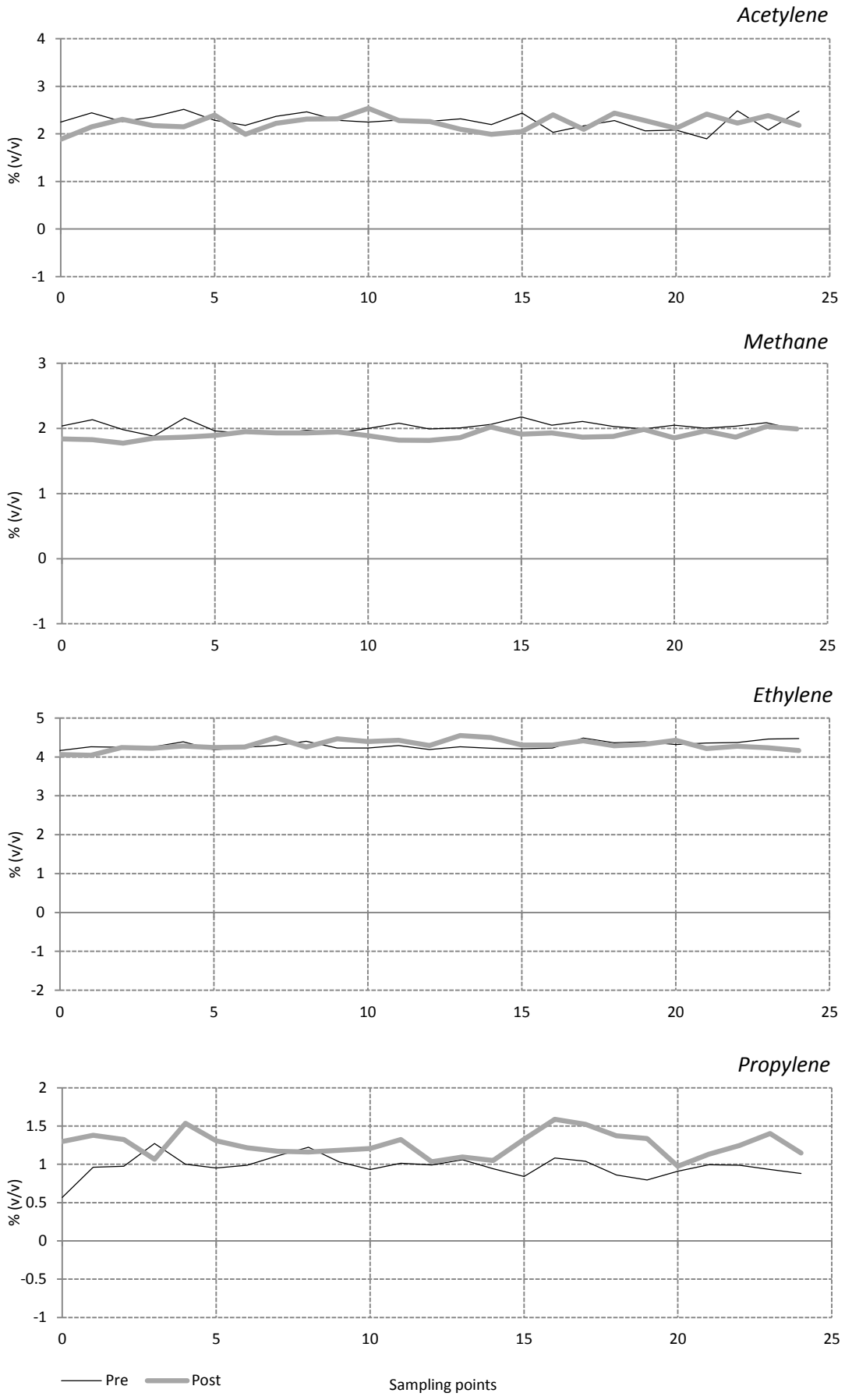

Figure 6-6. Effect of the DPF with no mixture addition

Figure 6-7 demonstrates the effect of the optimised mixture ratio (60% H_2 balanced with CO) on the same four exhaust components. It is evident from this data that in all four cases it appears that the specie was entirely combusted post filter. The reduction of methane is particularly beneficial due to it contributing to the greenhouse effect.

It is evident from this figure that methane, ethylene and propylene demonstrated negative concentrations post filter. It is assumed that the actual readings are zero. As previously described in section 3.5.1, when measuring using the FTIR analyser, a background spectrum was taken using pure N_2 before the commencement of each test run. This provided the FTIR with a zero datum for each component in the recipe. If on completion of the background a residual of the component remains, this can result in slight negative readings when the true reading is actually zero.

The complete combustion of these four hydrocarbons was also apparent when implementing any of the mixture ratios that featured both H_2 and CO. In the case of 100% CO, no reduction in any of these species was evident making it comparable to the data demonstrated previously in figure 6-6. This would indicate therefore that the presence of an exothermic reaction is necessary to oxidise these components. Due to the complete combustion of hydrocarbons resulting in the formation of CO_2, the combustion of these four species may further account for the CO_2 increase demonstrated post filter in figure 6-5. In the case of the remaining species measured by the FTIR spectrometer; ethane, urea, formaldehyde and ammonia, the variance in volume from pre to post filter was between negligible to zero regardless of which mixture ratio was introduced.

As both alkenes and alkynes feature double and triple bonds respectively, other atoms can be readily added across the bonds thus making it easy for addition reactions to occur at low temperature. Due to ethylene and propylene being alkenes and acetylene being an alkyne, it is assumed that these species are subjected to oxidation during the regeneration process. It is interesting to note that while ethane did not feature any change in volume from pre to post filter, methane demonstrated complete combustion. Due to both species being alkanes, this phenomenon requires further investigation.

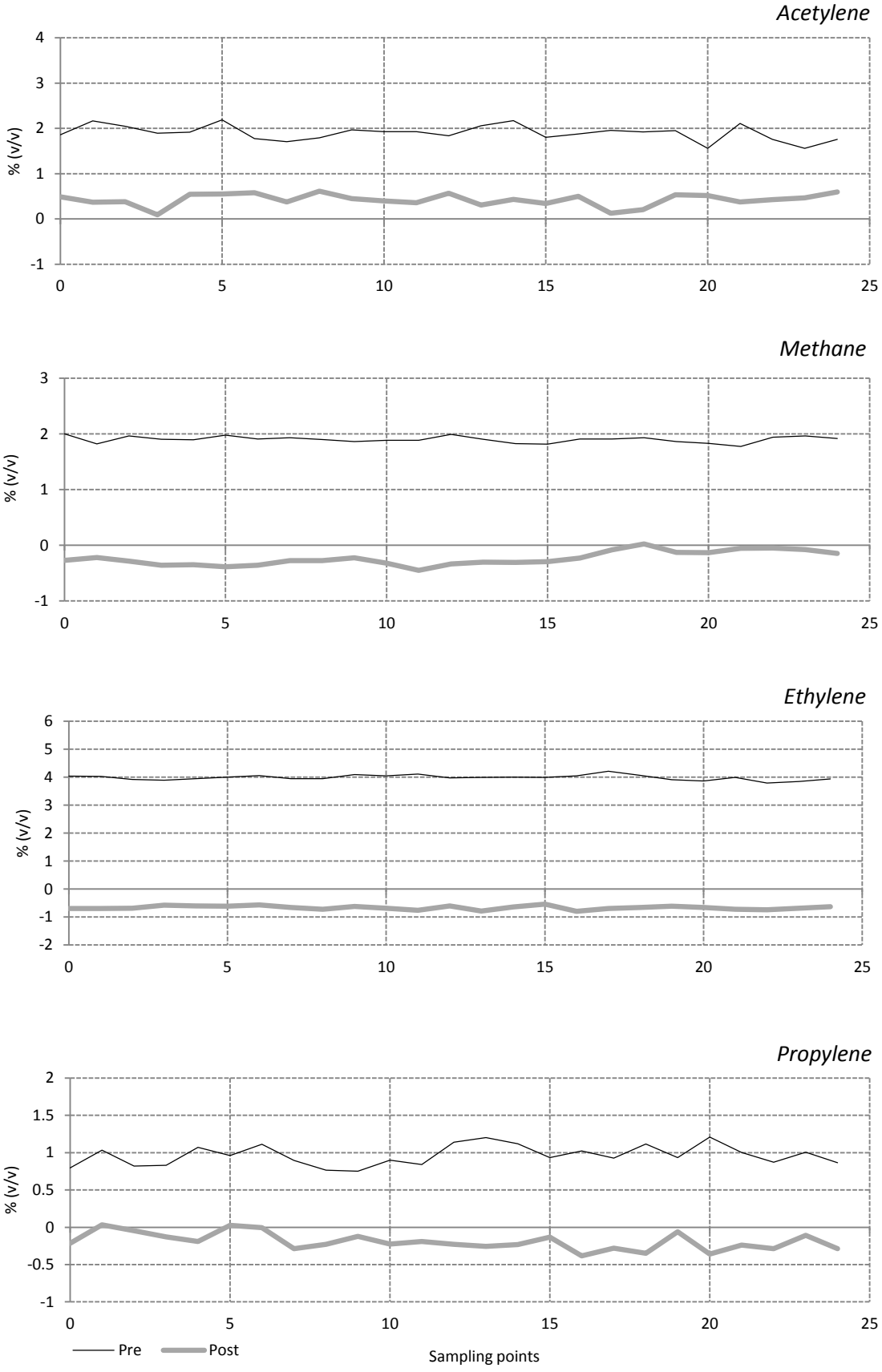

Figure 6-7. Effect of the DPF with 60 H_2/40 CO mixture addition

To enhance the thoroughness of this area of the investigation, the exhaust gas measurements taken pre and post filter for all the various mixture ratios were sent to MKS for analysis. By analysing the various residual spectra it was possible to identify if any foreign species were present outside of the measurement recipe (as previously described in section 2.6). Feedback from this investigation concluded that no foreign species were found.

6.4 Summary

This chapter has identified the effects of introducing a H_2/CO mixture, at varying ratios to the DPF regeneration process. This included the impact on filter temperature, regeneration profile and exhaust composition from pre to post filter. It was concluded from this part of the study that the optimised mixture ratio for DPF active regeneration was 60% H_2 balanced with CO. Furthermore, it has been demonstrated that the introduction of H_2 or H_2 and CO (regardless of mixture ratio) to the DPF regeneration process results in an increase in NOx pre to post filter while THCs reduce. In the case of H_2 and CO mixtures, an increase in CO_2 was apparent from pre to post filter due to high volumes of the additional CO converting to CO_2 during the active regeneration process.

CHAPTER 7

INVESTIGATION INTO THE EFFECTS OF HYDROGEN AND DIESEL DUAL FUELLING ON DPF REGENERATION AND COMBUSTION

CHAPTER 7 – INVESTIGATION INTO THE EFFECTS OF HYDROGEN AND DIESEL DUAL FUELLING ON DPF REGENERATION AND COMBUSTION

7.1 Introduction

The primary aim of this investigation was to establish whether application of hydrogen and diesel dual fuelling resulted in sufficient residual hydrogen being present in the exhaust flow to successfully support the regeneration process. However, as discussed in section 2.4.3 in the literature review of this study, the application of hydrogen and diesel dual fuelling can significantly impact in-cylinder combustion and hence bring improvements to both engine emissions and fuel consumption. As a result, the secondary aim of this study was to identify the effects of hydrogen and diesel dual fuelling on combustion, emissions and fuel consumption in an attempt to further validate previous research.

7.2 Experimental set up and test matrix

Research grade H_2 (purity: 99.9995%) was introduced at a pressure of two bar to the engine inlet immediately downstream of the air box via a flow meter and needle valve. The engine inlet air flow was measured as described in section 3.3.3 of this study. The required H_2 concentration could be achieved by setting the H_2 delivery volumetric flow rate to the required percentage of the air intake volumetric flow rate.

Table 7-1 below demonstrates the various test conditions adopted for this investigation. At each condition, four H_2 inlet concentrations were attempted; 2,4,6 and 8% (v/v). At each data point the following measurements were performed; fuel consumption, exhaust emissions (CO, CO_2, NOx, THC), in-cylinder pressure data and H_2 exhaust content. The techniques adopted for each of these measurements were outlined in chapter 3. The sampling flow rate from the engine to the furnace was set at 70 l/m throughout testing.

✓ = Test point completed

RPM	BMEP (bar)	2%	4%	6%	8%
1500	1.25	✓	✓		
2000	1.25	✓	✓	✓	
2000	2.5	✓	✓	✓	✓
2500	1.25	✓	✓	✓	
2500	2.5	✓	✓	✓	

Table 7-1. Test matrix

7.3 Results and discussion

7.3.1 H_2 exhaust content

Figure 7-1 below displays the resultant H_2 concentration in the exhaust flow as a function of the H_2 inlet concentration at the various test points. A general trend between decreasing engine load and increasing H_2 exhaust content is apparent from this data. In addition to this, this data also demonstrates a general trend between decreasing engine speed and increasing H_2 exhaust content. However, below either a speed of 1500rpm or a load of 1.25bar BMEP, the combustion became considerably unstable (combustion stability was defined previously in section 3.3.7.1) when 2% H_2 inlet concentration was introduced. As a result, 1500rpm and 1.25bar BMEP was considered as the minimum engine running requirements for hydrogen and diesel dual fuelling. However, with appropriate modification to the injection timing it is expected that this could be considerably improved.

It is apparent from table 7-1 and figure 7-1 that a number of data points were not completed. This was the result of the H_2 inlet concentration being too high to support stable combustion at that engine condition. As a result, the data could not be collected. This indicates a maximum upper limit to the extent in which hydrogen can be applied to a dual fuelled engine. However, as previously stated, it may be possible to increase this upper limit with modifications to the injection timing.

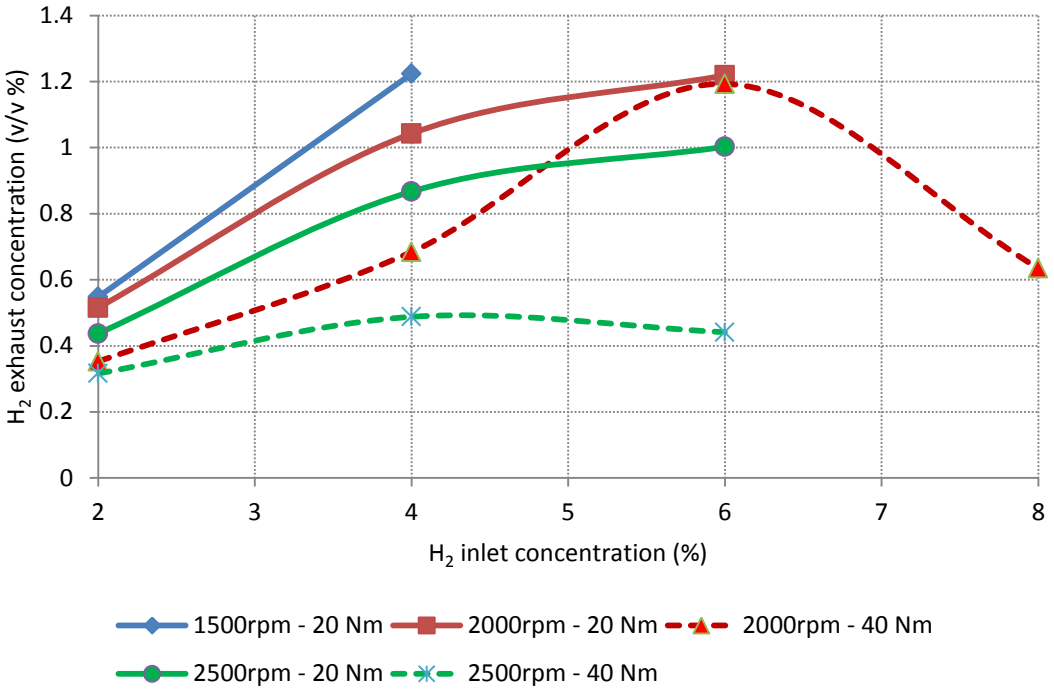

Figure 7-1. H_2 exhaust content as a function of H_2 inlet concentration

The maximum hydrogen concentration achieved in the exhaust flow was 1.22%, attained at 1500 rpm, 1.25bar BMEP and 4% H_2 inlet concentration. To identify if this concentration was substantial enough to support the regeneration process, the filter was first blocked using the standardised blocking procedure (see section 3.4.3) before setting the filter temperature to ~447°C and implementing the above conditions. The results of this investigation are demonstrated in figure 7-2:

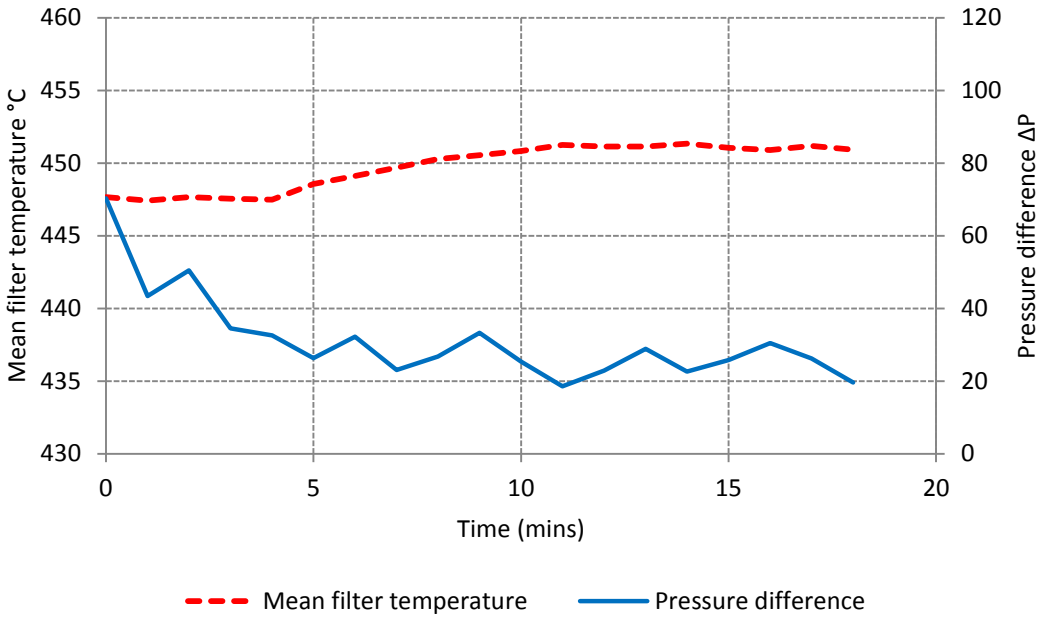

Figure 7-2. Effect of dual fuelling at optimised engine conditions on the regeneration process.

It is apparent from this data that at the aforementioned engine conditions, the hydrogen content within the exhaust is substantial enough to increase the mean filter temperature by ~4°C. Although this is minimal it is evident that this small increase in temperature was enough to both initiate the regeneration process as well as supporting the process until a fully regenerated state was achieved after approximately 10 minutes.

When compared to the data previously outlined in chapter 4 it is apparent that a 4°C temperature rise when introducing H_2 at a concentration of 1.22% is relatively minimal. However, it must be considered that during this investigation the filter temperature was set at 447°C prior to regeneration whilst during the collection of the data demonstrated in chapter 4, the filter temperature was set to a much higher initial temperature of 520°C. In addition to this the cooling effect of the sampling flow must also be considered. At the low load of 1.25 bar BMEP the exhaust temp is approximately 230°C which is considerably lower than the furnace temperature of 447°C. As a result significant convective heat transfer occurs preventing the mixture addition increasing the DPF temperature any further. In comparison the data demonstrated in chapter 4 was at a significantly higher load of 4.4 bar BMEP where the exhaust temp is approximately 360°C and hence significantly less convective heat transfer can take place.

Although the addition of residual hydrogen resulted in a minimal increase in temperature, as previously described this still resulted in thorough regeneration. An explanation for this can again, be the low load of 1.25 bar BMEP. As described in studies by Lapuerta *et al* (2003) and EL Shobokshy (1984), at lower loads particulate matter formation is reduced. Therefore less particulate matter is being introduced during the regeneration process allowing for more thorough regeneration to take place.

Although the data displayed in this section supports the theory of adopting diesel/H_2 dual fuelling for DPF regeneration support as a feasible technique, it must be noted that in practice such a method would prove extremely difficult to implement. As identified in figure 7-1, the quantity of H_2 present in the exhaust when running on dual fuel, is heavily dependent on the engine conditions. Due to typical DPF regeneration taking in excess of 10 minutes to complete, the engine running conditions would have to be fixed, for such a period of time, at conditions that demonstrate the required volume of H_2 in the exhaust to incur thorough regeneration. During a typical drive cycle such a necessity would prove extremely challenging.

7.3.2 Ignition delay

Figure 7-3 below demonstrates the effect of increasing the H_2 inlet concentration on ignition delay. The process adopted to calculate the ignition delay was outlined in section 3.3.7.1 of this study. It is evident from this data that the introduction of increased H_2 either increases the ignition delay or in some cases, has no visible effect. It is assumed that in the event of an increased ignition delay, more thorough mixing between the fuel and air can occur. Such a factor would result in more complete combustion.

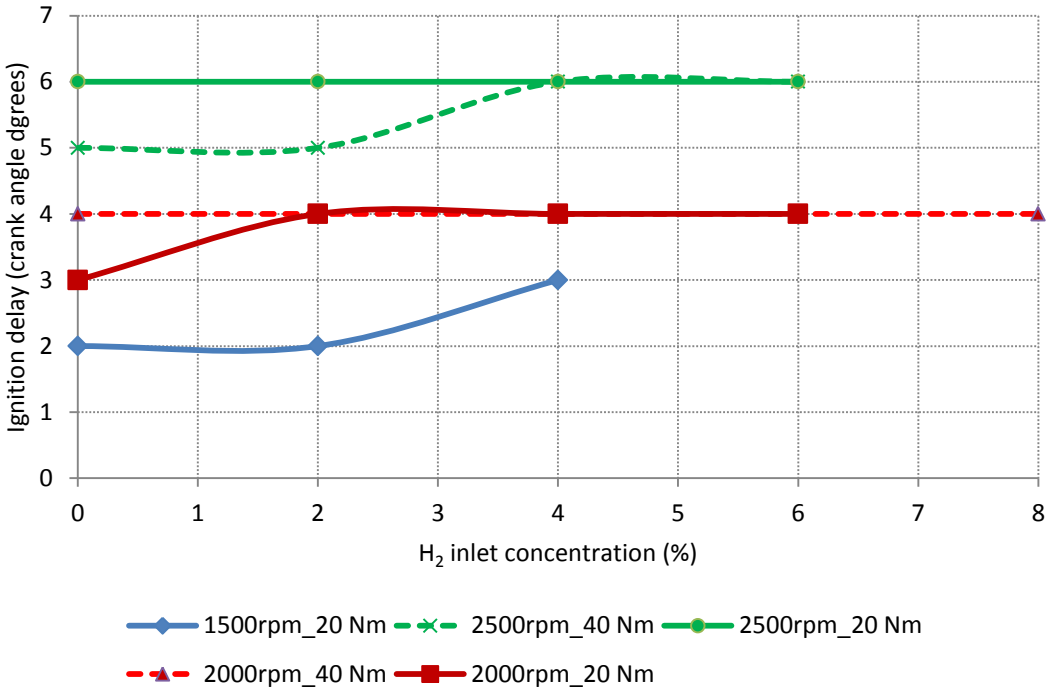

Figure 7-3. Ignition delay as a function of H_2 inlet concentration

7.3.3 Fuel consumption

Figure 7-4 below demonstrates the effect of increasing H_2 inlet concentration on diesel fuel consumption. As expected, there is a very strong correlation present where increasing the H_2 inlet concentration decreased the fuel consumption for all engine conditions tested.

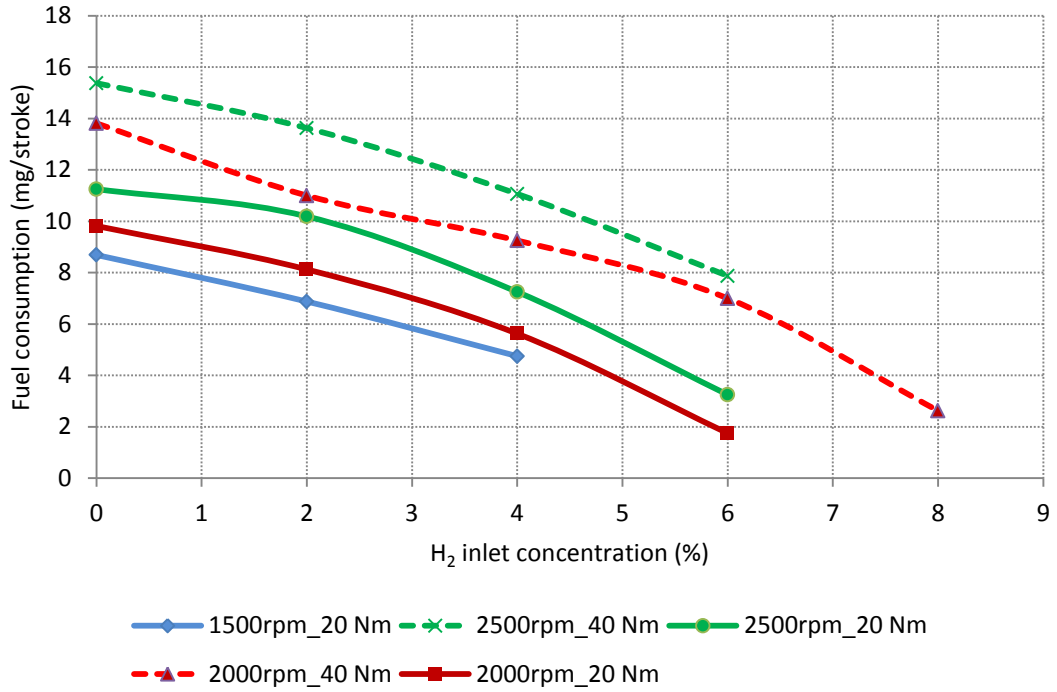

Figure 7-4. diesel fuel consumption as a function of H_2 inlet concentration

This correlation is simply due to the introduced H_2 displacing the diesel. Therefore, it is more beneficial to identify how effectively both fuels are being transferred as a dual fuel into usable energy. This was achieved by calculating the fuel conversion efficiency using equation 7-1 below.

$$\eta = \frac{BP}{(\dot{m}_{f\,diesel} \times CV_{diesel}) + (\dot{m}_{f\,H_2} \times CV_{H_2})}$$

BP = Engine power (kW)
mf_{diesel} = Mass flow rate of diesel fuel (g/s)
CV_{diesel} = Diesel fuel calorific value (45kJ/g)
mf_{H2} = Mass flow rate of diesel fuel (g/s)
CV_{H2} = H_2 fuel calorific value (120kJ/g)

Equation 7-1. Fuel conversion efficiency

This equation identifies the ratio between the amount of energy available in the combined fuel and the resultant power output of the engine. The data from this calculation is demonstrated in figure 7-5 below:

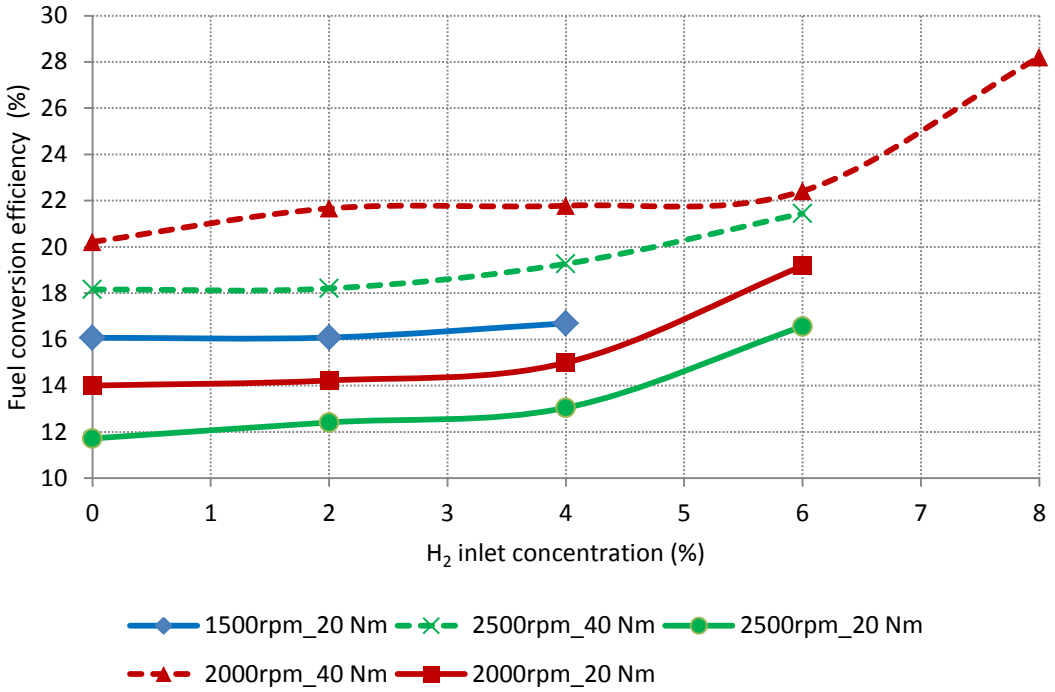

Figure 7-5. Fuel conversion efficiency as a function of H_2 inlet concentration

It is demonstrated in figure 7-5 that the implementation of a H_2 diesel dual fuel is significantly beneficial to the fuel conversion efficiency. It is evident from this data that at lower engine load, the dual fuel is converted into useful energy less efficiently than at higher load. This was expected as the H_2 exhaust content at the lower load was higher (section 6.3.1) when compared to the higher load, indicating that the fuel was being burned more efficiently at higher loads. This data therefore, further supports the argument that low engine loads are required to increase H_2 exhaust content in an attempt to support the regeneration process.

7.3.4 Engine emissions

Figures 7-6 and 7-7 below demonstrate the effect of increasing H_2 addition on CO and CO_2 emissions. It is apparent from this data that CO and CO_2 emissions are decreased as H_2 addition is increased. The reduction in these emissions can be explained by the additional H_2 displacing a portion of diesel fuel. Therefore the combined H_2 and diesel fuel mixture features lower carbon content when compared to just diesel. As a result of less hydrocarbons being present during combustion, the same load output can be produced with lower CO and CO_2 emissions being produced.

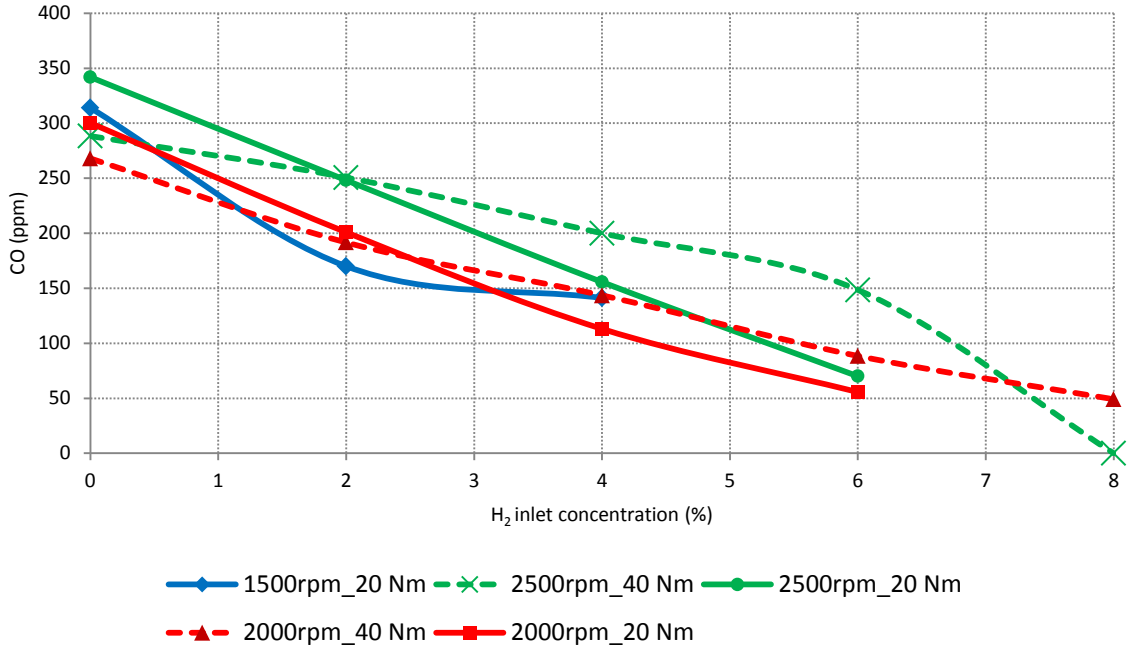

Figure 7-6. CO emission as a function of H_2 inlet concentration

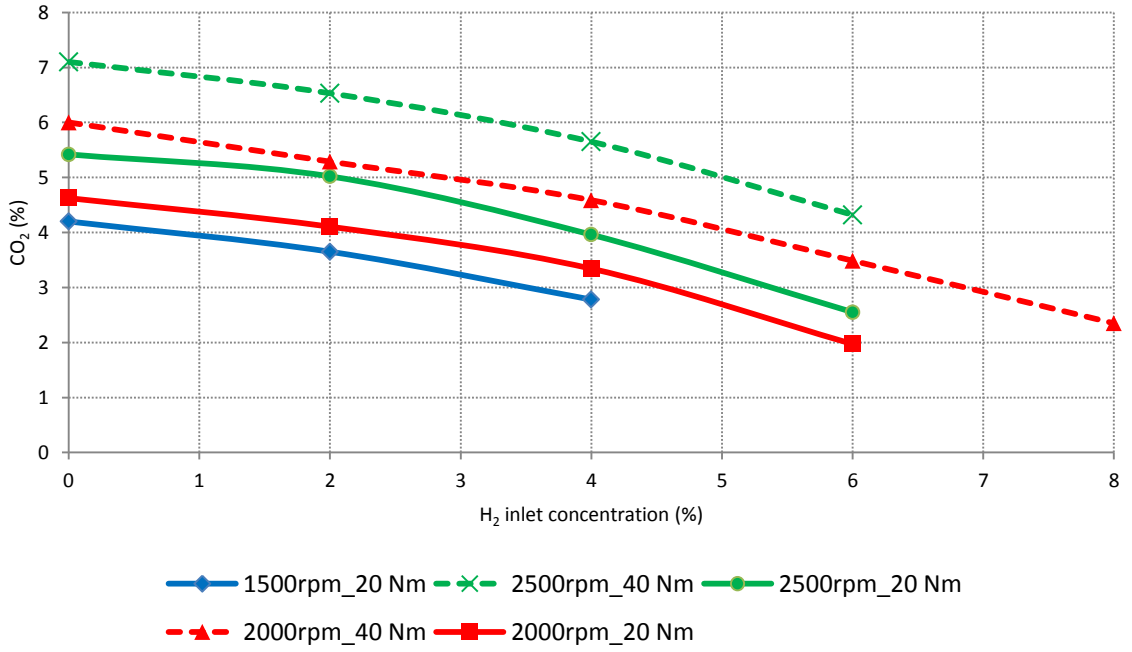

Figure 7-7. CO_2 emission as a function of H_2 inlet concentration

When analysing figure 7-8 below, a general trend is evident where an increase in the H_2 inlet concentration results in a corresponding increase in the formation of NOx. This was expected due to hydrogen addition typically increasing the combustion temperature, a characteristic that greatly enhances NOx formation. It has also been identified in the works of McWilliam (2008) that hydrogen addition can increase the air/fuel ratio resulting in a leaner mixture, a factor that reduces the flame speed and hence increases the time available for NOx formation. Interestingly, at 1500rpm and 20Nm load, a H_2 inlet concentration beyond 2% resulted in a decrease in the NOx formation. This is also evident above 4% H_2 inlet concentration at 2000rpm and 20Nm load. It is assumed that at these conditions the limit of hydrogen use is being approached resulting in unstable combustion. However, as previously stated, it may be possible to significantly improve this with changes to the injection timing.

Figure 7-9 displays the effect of increasing the H_2 inlet concentration on THC emission. A general trend is apparent where an increase in the H_2 inlet concentration results in a decrease in THC emission. This again can be explained by the carbon content of the dual fuel being less than diesel.

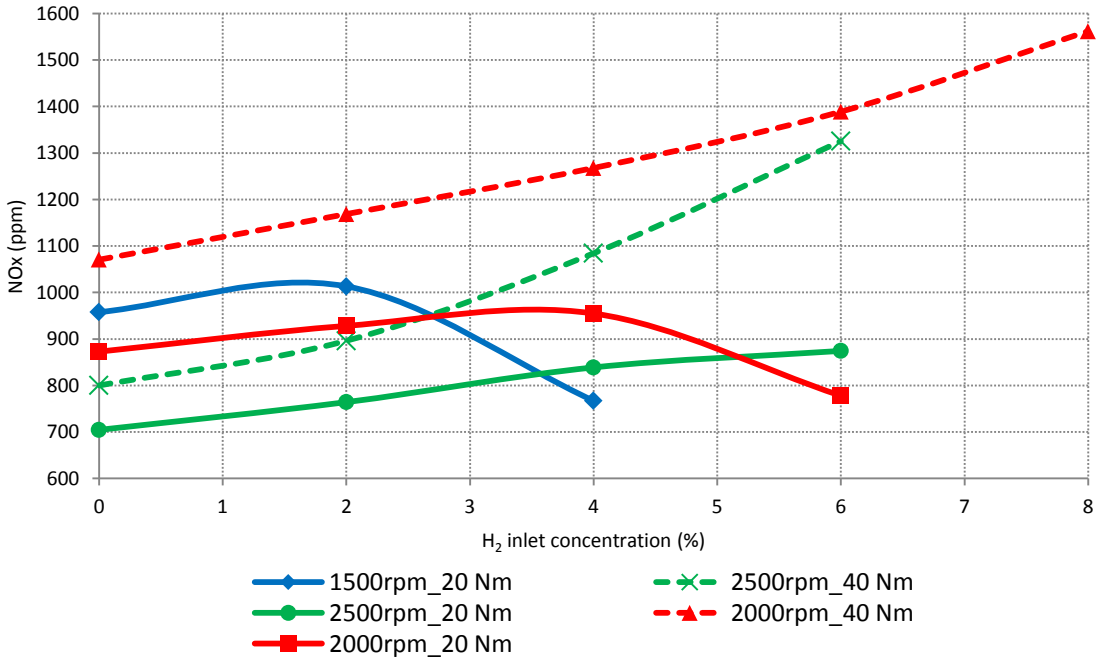

Figure 7-8. NOx emission as a function of H_2 inlet concentration

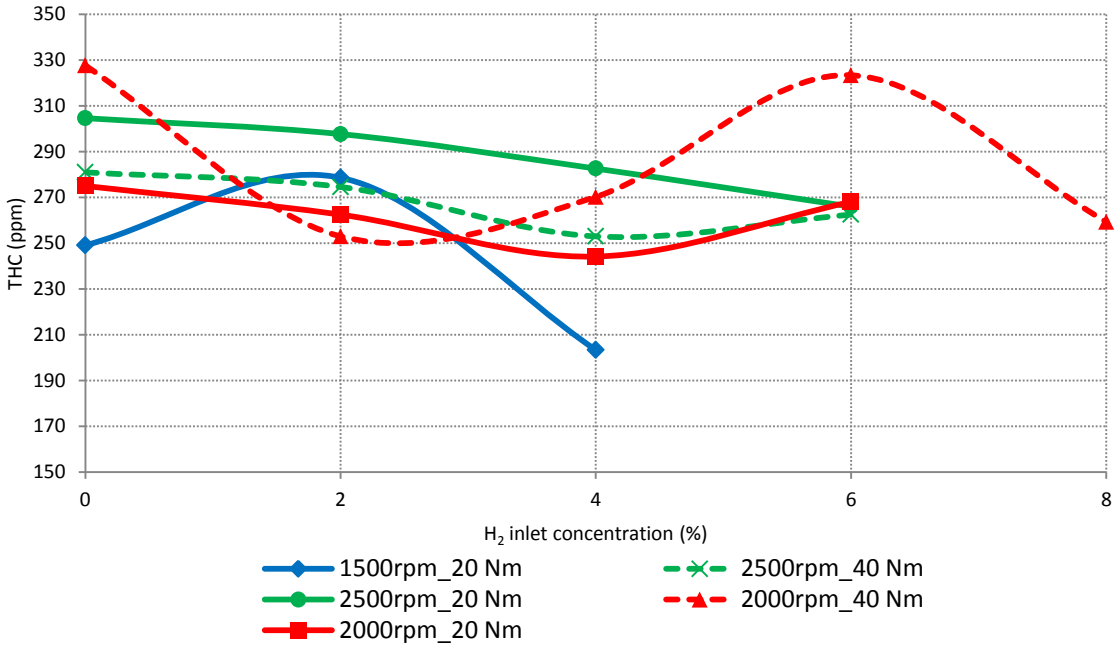

Figure 7-9. THC emission as a function of H_2 inlet concentration

7.4 Summary

This chapter has investigated the effects of H_2/diesel dual fuelling on the DPF regeneration process. In addition to this, the impact of dual fuelling on engine emissions, fuel consumption and ignition delay has also been identified. It has been concluded from this chapter that the maximum achievable hydrogen concentration in the exhaust whilst using H_2 and diesel as a dual fuel was 1.22% (v/v) obtained at 1500rpm, 1.25bar BMEP and 4% H_2 inlet concentration. Although the concentration achieved was relatively minimal it was enough to support the regeneration process and regenerate the filter fully after approximately 10 minutes.

CHAPTER 8

CONCLUSIONS AND FURTHER WORK

CHAPTER 8 – CONCLUSIONS AND FURTHER WORK

8.1 The addition of H_2 to the regeneration process

The primary aim of this part of the project was to investigate the effects of introducing hydrogen to the DPF passive regeneration process. This was to replicate the effects of introducing hydrogen reformate to the DPF that had been generated using an onboard exhaust gas fuel reformer. In addition to this, various injection strategies were investigated in an attempt to optimise the volume of reformate required for proficient regeneration.

The results from this study identified that equilibrium mode was established at a filter temperature of 480°C, indicated by a cyclic process between regeneration and loading mode. At 520°C it was clear that passive regeneration was fully initiated with regeneration occurring with no particulate accumulation for a period of approximately 40 minutes.

It can also be concluded from this study that when introducing H_2 to the regeneration process at a concentration in excess of 1% v/v, an exothermic reaction occurs which increases the filter temperature significantly. This characteristic enhances both the speed and quality of the regeneration process. It was identified during this study that the regeneration profiles generated when implementing H_2 at 2, 3 and 4% were relatively similar. Therefore it was assumed that at the high temperature that passive regeneration occurs only minimal support is required by the additional hydrogen to ensure full DPF regeneration.

Increasing the volume of H_2 introduced to the passive regeneration process resulted in a corresponding decrease in CO formation post filter. However, a general trend of increasing NOx and CO_2 formation was also apparent as the H_2 volume was increased. THC levels were also seen to reduce with a general relationship between increasing H_2 and decreasing THC.

A 5.5 periodic strategy at 4% concentration demonstrated comparable temperature and regeneration characteristics than that demonstrated when adopting a constant 4% injection strategy. However, the 5.5 periodic injection cycle adopts 50% less H_2 volume rendering it a far more efficient strategy than constant H_2 delivery. It was assumed that the high efficiency demonstrated by the 5.5 periodic strategy was the result of a ‘triggering effect’ where the

cyclic introduction of H_2 induced a faster rate of temperature increase and thus similar regeneration characteristics than that generated using a constant injection strategy.

8.2 The effects of a H_2/CO mixture addition on DPF regeneration

This part of the study aimed to support the DPF passive regeneration process by utilising a H_2/CO mixture. A gaseous mixture containing 60% H_2 balanced with CO was tested using both constant and periodic injection strategies. As with the previous test concluded in section 8.1, these gases were representative of reformates that could be generated using an on board exhaust gas fuel reformer. In addition to this, the study also aimed to identify the effect of varying the DPF space velocity and engine load on the regeneration process.

At a mean filter temperature of ~520°C (the passive regeneration temperature) the addition of a H_2/CO mixture at a concentration of 2.7%, resulted in the initiation of an exothermic reaction and hence a resultant increase in the filter temperature for all of the tested strategies. This allowed for the regeneration process to be supported at a lower temperature range outside of the passive regeneration temperature window. At a mean filter temperature of ~440°C and an increase mixture concentration of 4.5%, all strategies again featured evidence of an exothermic reaction. Initiation of the regeneration process was also demonstrated for each of the strategies even though two of the periodic strategies (5.5, 10.10) demonstrated peak temperatures outside of the passive regeneration temperature. This indicated that the mixture is oxidising soot through the presence of a chemical reaction and not just purely by the increase of temperature as a result of an exothermic reaction. Regeneration at a lower temperature would greatly enhance the life cycle and durability of the DPF during application in vehicle.

The constant strategy for both the 2.7% and 4.5% mixture concentrations, did not demonstrate the highest peak temperature in either case, however, in both situations, the fastest regeneration rate was demonstrated. This indicates that a break in the mixture flow rate (as provided by a periodic strategy) is detrimental to the regeneration rate.

An optimised strategy would feature an 4.5% mixture concentration as this allows the filter to regenerate sufficiently at a substantially lower temperature (440°C opposed to 520°C). This is greatly beneficial to the life cycle of the DPF. The 10.10 strategy proved to be the

optimised strategy as this demonstrated a thoroughness of regeneration equal to that of the constant strategy, achieved with 50% less mixture volume and a slightly lower peak filter temperature. However, it must be noted that with this strategy, full regeneration took slightly longer to occur when compared with the constant strategy.

Reducing the space velocity increased the peak filter temperature but reduced the rate in which the temperature increased. The reduction in space velocity had a positive effect on the regeneration quality for all strategies tested. A reduction in engine load resulted in a reduction in the mean filter temperature. However, this had minimal impact on the regeneration quality.

8.3 Effects of introducing a H_2/CO mixture at varying ratios to the DPF regeneration process

The primary aim of this study was to establish an optimised H_2/CO mixture ratio. In addition, this study also aimed to identify the effects that introducing the mixture at varying ratios had on the chemical composition of the exhaust gas post filter.

The highest mean filter temperature and hence most proficient regeneration was achieved using the 50/50 mixture ratio. However, a very similar quality of regeneration was achieved at a lower temperature (~30°C lower) when adopting a 60 H_2/40 CO mixture ratio. Therefore the 60 H_2/40 CO was taken to be the optimum mixture ratio.

Other concluding remarks from this study include:

- The addition of a mixture containing 100% CO resulted in no exothermic reaction and hence provided no support to the regeneration process.

- The addition of H_2 or H_2 and CO to the regeneration process resulted in an increase in NOx post filter while THCs were reduced.

- The addition of a H_2/ CO mixture addition resulted in an increase in CO_2 post filter, the levels of which were proportional to the volume of CO contained within the introduced mixture.

- The addition of a H_2/ CO mixture resulted in the complete combustion of methane, ethylene, propylene and acetylene post filter. As this characteristic was not featured when using 100% CO mixture, it is assumed that for complete combustion of these species an exothermic reaction is required.

8.4 The effects of H_2/diesel dual fuelling on DPF regeneration

The aim of this study was to identify whether during the application of diesel/H_2 dual fuelling, sufficient residual hydrogen existed in the exhaust stream to assist in the DPF regeneration process. In addition to increasing the H_2 concentration, the effect of engine load and speed was also investigated in an attempt to generate sufficient hydrogen exhaust content. The effect of diesel/H_2 dual fuelling on combustion and hence emissions and fuel consumption was also recorded.

The maximum hydrogen concentration achieved in the exhaust flow was 1.22%, attained at 1500 rpm, 1.25bar BMEP and 4% H_2 inlet concentration. When regenerating under these conditions the DPF temperature was increased by ~4°C. Although minimal this small increase in temperature was enough to fully regenerate the DPF following a period of 10-11 minutes.

Other key points from this investigation are as follows:

- A reduction in the engine speed and load increased the concentration of H_2 in the exhaust flow. However this relationship was eventually limited by unstable combustion below 1500rpm and 1.25bar BMEP. Modifications to the injection timing may improve this.

- It was identified that the introduction of H_2 to the engine inlet either increased the ignition delay or had no visible effect.

- As a result of a portion of diesel being displaced by hydrogen, the diesel fuel consumption reduced as the concentration of hydrogen increased.

- Increasing the concentration of hydrogen in the engine inlet increased the fuel conversion efficiency of the dual fuel.

- As the hydrogen concentration was increased CO and CO2 was reduced for all engine conditions tested. This was primarily due to the additional hydrogen displacing the carbon based fuel.

- As the hydrogen concentration was increased, the formation of NOx was generally increased. It was assumed that this was due to hydrogen not only increasing the combustion temperature but also increasing the air/fuel ratio. Two factors that are critical to NOx formation.

- As the hydrogen concentration was increased the THC emission generally decreased. Again this was due to the hydrogen/diesel dual fuel featuring a lower carbon content than diesel alone.

8.5 Recommendations for future work

It was established in this study that with the support of simulated reformates the regeneration process can be initiated and sustained at a filter temperature lower than the passive regeneration temperature. In order to obtain a better understanding of how this occurs, this study would benefit from further research into the chemical kinetics occurring during active regeneration.

As described in section 6.3.2, the introduction of a 60% H_2 / 40% CO mixture at a concentration of 6% significantly impacted the chemical composition of the exhaust gas post DPF. While a number of hydrocarbons were seen to completely combust others remained unchanged. An example of this was the high conversion rates of methane pre to post filter while the volumes of ethane demonstrated negligible to zero variance. Again, this study would benefit from further research being performed into the chemical kinetics of active regeneration to obtain a better understanding of the response demonstrated by the various exhaust gas components post filter.

This study investigated the feasibility of adopting H_2/diesel dual fuelling to assist the DPF regeneration process. It was demonstrated that for most of the tested engine speed and load points, the residual H_2 remaining in the exhaust was not substantial enough to support

the regeneration process. Due to the occurrence of unstable combustion, a variety of engine speed and load conditions could not be tested. However, with modifications to the injection timing it may have been possible to test at an increased number of engine speed and load conditions, increasing the thoroughness of the investigation.

Although this study has demonstrated the benefits of a hydrogen and hydrogen / CO supported active regeneration system, further investigation into the control, storage and implementation of such a system is required. As previously discussed in this study, the necessary reformates can be produced on-board via an exhaust gas fuel reformer, however a method of storage would be required to store the reformates during the intermediate period between reformate production and introduction to the regeneration process when required. Furthermore, the development of a suitable control system is required so the reformates are only introduced to the DPF when predefined conditions are met i.e. minimum filter temperature and optimised level of particulate accumulation at the filter. In addition, issues with packaging during application would also have to be overcome.

As described previously in this study, a current popular method of DPF active regeneration is to adopt diesel fuel as a DPF regenerating agent, introducing it upstream of the DPF. In the interest of both commercialisation and furthering research, it would prove beneficial to produce a like for like comparison between such an active regeneration system and one that has been outlined in this study. Such a comparison should not only be made between the performance characteristics of the two systems but also the cost, weight and packaging implications.

8.6 Overview

It has been demonstrated in this study that the difficulties faced with onboard regeneration of diesel particulate filters is a relevant and predominant problem in the current diesel automotive industry. Due to ever increasing restrictions on particulate matter emissions, the improvement of DPF systems has gained significant focus in recent years.

This study has demonstrated that by using various chemical components and a periodic injection strategy, it is possible to not only enhance the regeneration process but also allow it to initiate at lower temperatures and with reduced volumes of reformate. Due to the

volumes of supporting components being representative of what can be generated on board using an exhaust gas fuel reformer, the application of this active regeneration system is feasible. However, before implementation, the cost and weight penalties must be considered against the apparent benefits in regeneration quality.

REFERENCES

REFERENCES

Abd-Alla, G.H., 2002. *Using Exhaust Gas Recirculation in Internal Combustion Engines: A review*. Jounal of Energy Conversion and Management. Vol 43. Issue 8. pp 1027-1042.

Abu-Jrai, A., Tsolakis, A., Megaritis, A. 2007. *The influence of H_2 and CO on diesel engine combustion characteristics, exhaust gas emissions, and aftertreatment selective catalytic NOx reduction.* Int J Hydrogen Energy. Vol. 32.pp 3565-3571.

Abu-Jrai, A., Tsolakis, A., Theinnoi, K., Megaritis, A., Golunski, S.E., 2008. *Diesel exhaust-gas reforming for H_2 addition to an aftertreatment unit.* Chemical Engineering Journal. 141. pp 290-297.

Adachi, M., 2000. *Emission measurement techniques for advanced powertrains.* Meas. Sci. Technol. Vol 11, R113-R29.

Aldajah, S., Ajayi, O., Fenske, G., Goldblatt, I., 2007. *Effect of exhaust gas recirculation (EGR) contamination of diesel engine oil on wear.* Jounal of Wear. Vol 263. Issue 1-6. pp 93-98.

Ballinger, T., Cox, J., Konduru, M., De, D., Manning, W., Andersen, P., 2009. *Evaluation of SCR Catalyst Technology on Diesel Particulate Filters.* Int. J. Fuels Lubr. Vol 2. Issue 1. pp 369-374.

Bari, S and Esmaeil, M.M., 2010. *Effect of H2/O2 addition in increasing the thermal efficiency of a diesel engine.* Fuel. Vol 89. Issue 2. pp 378-383.

Bensaid, S., Marchisio, D.L., Fino, D. 2010. *Numerical simulation of soot filtration and combustion within diesel particulate filters.* Chem. Eng. Sci. Vol. 65.pp 357-363.

Bensaid, S., Marchisio, D.L., Russo, N., Fino, D., 2009. *Experimental investigation of soot deposition in diesel particulate filters.* Catalysis Today. 147S. S295–S300

Bion, N., Saussey, M., Haneda, M., Daturi, M., 2003. *Study by in situ FTIR spectroscopy of the SCR of Nox by ethanol on Ag/AL203 – Evidence of the role of isocyanate species.* J. Catal. Vol. 217. pp 47.

Borras, E., Tortajada-Genaro, L.A., Vazquez, M., Zielinska, B., 2009. *Polycyclic aromatic hydrocarbon exhaust emissions from different reformulated diesel fuels and engine operating conditions.* Journal of Atmospheric Environment. Vol 43. Issue 37. pp 5944-5952.

Brady, R.N., 1996. *Modern Diesel Technology*. Prentice Hall: New Jersey, USA

Bromberg, L., Cohn, D.R., Hadidi, K., Heywood, J.B., Rabinovich, A., 2004. *Plasmatron fuel reformer development and internal combustion engine vehicle applications.* Massachusetts Institute of Technology. Paper presented at the Diesel Engine Emission Reduction (DEER) workshop: August 29th-September 2nd 2004. No: PSFC-JA-05-22.

Bromberg, L., Cohn, D.R., Rabinovich, A., Heywood, J., 2001. *Emissions reductions using hydrogen from plasmatron fuel converters.* Int. J Hydrogen Energy. Vol 26. Issue 10. pp 1115-1121.

Bromberg, L., Cohn, D.R., Wong, V., 2005. *Regeneration of diesel particulate filters with hydrogen rich gas.* MIT Plasma Science and Fusion Centre report, PSFC/RR-05-2.

Chae, J., 2003. *Non-thermal Plasma for Diesel Exhaust Treatment.* Journal of Electrostatics. Vol 57. No 53. pp 251-262.

Challen, B. & Baranescu, R. eds., 1999. *Diesel Engine Reference Book.* Second Edition, Butterworth-Heinemann: Oxford, UK.

Chen, L. and Jha, B., 2004, *New FeCrAl Alloys for Diesel Engine Catalytic Converters*, SAE paper 2004-01-1491.

Daham, B., Andrews, G., Li, H., Ballesteros, R., *et al*., 2005. *Application of a portable FTIR for measuring on-road emissions.* SAE Paper 2005-01-0676.

De Blas, LJM., 1998. Pollutant formation and interaction in the combustion of heavy liquid fuels. PhD Thesis, University of London.

Eastwood, P. 2010. Exhaust gas aftertreatment for light-duty diesel engines. In: Zhao, H. ed. *Advanced direct injection combustion engine technologies and development.* Cambridge: Woodhead Publishing Ltd, pp. 562-594.

El Shobokshy, M.S. 1984. *The effect of diesel engine load on particulate carbon emissions.* Atmos. Environ. Vol. 18. Issue 11.pp 2305-2311.

Guanglong, Z., Lunhui, L., Jiahua, C., Xiuren, Z., 1994. *Development and Application Experience of Diesel Catalytic Converters,* SAE paper 941773.

Guiochon, G. and Guillemin, C.L., 1988. *Quantitative Chromatography for Laboratory Analysis and Online Process Control – Journal of Chromatography library Volume 42.* Elsevier Science Publishers Company Ltd: New York, USA.

Guyon, M., Blanche, C., Bert, C., Philippe, L., 2000. *NOx-Trap System Development and Characterization for Diesel Engines Emission Control.* SAE paper 2000-01-2910.

Haddad, S.D. & Watson, N. eds., 1984. *Design and Applications in Diesel Engineering.* Ellis Horwood Ltd: Chichester, UK.

Hanamura, K., Karin, P., Cui, L., Rubio, P., Tsuruta, T., Tanaka, T., Suzuki, T., 2009. *Micro- and macroscopic visualisation of particulate matter trapping and regeneration processes in wall-flow diesel particulate filters.* IMechE: Int.J.Engine Res. Vol. 10. pp 305-321.

Heisler, H., 1999. *Vehicle and Engine Technology.* Second Edition, Butterworth-Heinemann: Oxford, UK.

Heywood, J.B., 1988. *Internal Combustion Engine Fundamentals.* McGraw-Hill Book Company.

Hillier, V.A.W. and Coombes, P., 2004. *Hillier's Fundamentals of Motor Vehicle Technology.* Fifth Edition, Nelson Thornes: Cheltenham, UK.

Hirata, K., Masaki, N., Yano, M., Akagawa, H., Takada, K., Kusaka, J., Mori, T., 2009. *Development of an improved urea-selective catalytic reduction-diesel particulate filter system for heavy-duty commercial vehicles.* Int. J. Engine Res., Vol. 10, No.5, pp. 337-348.

Horiba 7170 DEGR Users Manual. 2003.

Husselbee, W.L., 1984. *Automotive Emission Control.* Prentice Hall: USA.

Jamal, Y., Wyszynski, M.L., 1994. *On-board generation of hydrogen-rich gaseous fuels – a review.* Int. J. Hydrogen Energy. Vol. 19, No. 7, pp. 557-572.

Janiszewski, A., Nagorski, Z., Teodorczyk, A., 2001. *Trap 1.0 – A zero-dimensional computer code for the preliminary analysis of soot regeneration process in diesel particulate filter.* Journal of Kones. Combustion Engines., Vol 8, No.1-2, pp. 184-194.

Japanese Emission Standards for Diesel Passenger cars, http://www.dieselnet.com/standards/jp/onroad.php [Accessed 06/03/2010]

Jarrod, A., Mundschau, B., Mundschau, M.V., 2006. *Reformer for conversion of diesel fuel into CO and Hydrogen.* DOE Hydrogen Program, FY 2006 Annual Report, III.B.4.

Johannes, E., Li, X., Towgood, P., 2007. *Performance of a non-catalytic syngas generator for LNT and DPF regeneration.* SAE paper 2007-01-1238.

Johnson, T., 2008. *Diesel Engine Emissions and Their Control.* Platinum Metals Review., Vol 52, Issue 1, pp. 23-37.

Kandylas, I.P., Koltsakis, G.C. 2002. *NO_2 assisted regeneration of diesel particulate filters: A modelling study.* Ind.Eng.Chem.Res. Vol. 41, Issue.9, pp. 2115-2123.

Kim, J.U., Hyeon, B.Y., Park, D.S., Kim, E.S., 1997. *Regeneration characteristics of a burner type diesel particulate trap system in a steady-state engine operation.* Combustion science and technology., Vol. 130, Issue.16, pp. 115-130.

Kittelson, D.B., Arnold, M., Winthrop, F.W $_{Jnr}$., 1999. *Review of Diesel Particulate Matter Sampling Methods Final Report.* University of Minnesota. Department of Mechanical Engineering. Center for Diesel Research. Minneapolis, USA.

Klein, H., Lopp, S., Lox, E., Kawanami, M., Horiuchi, M., 1999. *Hydrocarbon DeNOx Catalysis – System Development for Diesel Passenger Cars and Trucks.* SAE paper 1999-01-0109.

Kong, Y., Crane, S., Patel, P., Taylor, B., 2004. *NOx Trap Regeneration with an On-Board Hydrogen Generation Device.* SAE paper 2004-01-0582.

Labecki, L., 2010. *Combustion and emission characteristics of biofuels in diesel engines.* Brunel University; School of Engineering and Design, PhD Theses.

Ladommatos, N., Abdelhalim, S., Zhao, H., 1999. *The effects of exhaust gas recirculation on diesel combustion and emissions.* Int J Engine Research. Vol 1, no. 1, pp 107-126.

Lapuerta, M., Hernandez, J.J., Ballesteros, R., Duran, A. 2003. *Composition and size of diesel particulate emissions from a commercial European engine tested with present and future fuels.* SAE J. Automot.Eng. Vol. 217. Issue 10.pp 907-919.

Lee, K., 2010. *Development of advanced diesel particulate filtration DPF systems.* [online] Illinois, USA: Argonne national laboratory. Available at: <http://www1.eere.energy.gov/vehiclesandfuels/pdfs/merit_review_2010/emissions_control/ace024_lee_2010_o.pdf>[Accessed 31 December 2012].

Lepperhoff, G., Stommel, P., Luers, B., Searles., 2000.*Vehicle Study on the Impact of Diesel Fuel Sulfur Content on the Performance of DeNOx Catalysts and the Influence of DeNOx Catalysts on Particle Size and Number.* SAE paper 2000-01-1877.

Li, C.G., Mao, F., Swartzmiller, S.B., Wallin, S.A., Ziebarth, R.R. 2004. *Properties and performance of diesel particulate filters of an advanced ceramic material.* SAE paper 2004-01-0955.

Liu, Z., Shah, A.N., Ge, Y., Ding, Y., Tan, J., Jiang, L., et al., 2011 *Effects of continuously regenerating diesel particulate filters on regulated emissions and number size distribution of particles emitted from a diesel engine.* J.Environ. Sci. Vol. 23, Issue 5, pp. 798-807.

Macleod, N., Lambert, R.M. 2002. *Lean NOx reduction with CO+H_2 mixtures over a Pt/AL203 and Pd/AL203 catalysts.* Appl. Catal. B35.pp 269.

Majewski, W.A. and Khair, M.K., 2006. *Diesel Emissions and their Control.* SAE International: USA.

Mandal, N.G., 2008. *Measurement of gas concentrations: Oxygen, carbon dioxide, nitrogen, nitrous oxide and volatile anaesthetic agents.* Anaesthesia and Intensive Care Medicine. Vol. 9, Issue 12, pp. 559-563.

Marshik, B., 2011. FTIR user group meeting. *Theory and Application of FTIR.* June 15. Crewe: Ramada Encore Hotel.

Mayer, A., Czerwinski, J., Petermann, J., Wyser, M., Legerer, F., 2004. *Reliability of DPF-systems: Experience with 6000 applications of the Swiss retrofit fleet.* SAE paper 2004-01-0076.

McWilliam, L., 2008. *Combined hydrogen diesel combustion: An experimental investigation into the effects of hydrogen addition on the exhaust gas emissions, particulate matter size distribution and chemical composition.* Brunel University; School of Engineering and Design, PhD Theses.

MECA – Manufacturers of Emission Controls Association, 2000. *Catalyst-Based Diesel Particulate Filters and NOx Absorbers: A summary of the Technologies and the Effects of Fuel Sulfur.* Washington DC, USA.

Megaritis, A., Tsolakis, A., 2004. *Exhaust Gas Fuel Reforming for Diesel Engines - A Way to Reduce Smoke and Nox Emissions Simultaneously*. SAE paper, 2004-01-1844.

Megaritis, A., Tsolakis, A., 2005. *Partially premixed charge compression ignition engine with on-board hydrogen production by exhaust gas fuel reforming of diesel and bio diesel*. International journal of Hydrogen Energy. Vol 30, pp 731.

MG2000 Software Manual. 2006. MKS Instruments Inc. Printed in the USA.

MKS application note. 2010. *MKS FTIR Analysis for the Reforming of Hydrocarbons. http://www.mksinst.com/docs/r/FTIR-ReformingHydrocarbons-appnote.pdf* [Accessed 07.01.2011].

Nabi, Md.N., Akhter, Md.S., Shahadat, Md.Z., 2006. *Improvement of engine emissions with conventional diesel fuel and diesel-biodiesel blends*. Bioresource Technol. Vol 97, pp 372-378.

Official Journal of the European Union, 20th June 2007, *Type approval of motor vehicles with respect to emissions from light passenger and commercial vehicles (Euro 5 and Euro 6).* Regulation (EC) No 715/2007 of the European Parliament and of the Council.

Ozturk, S., McKinnon, D.L., Puliafito, J.L., Irigo, C. and Sans, J., 2004. *International Experience Using Diesel Catalytic Converters for Urban Buses,* SAE paper 940238

Park, K., Song, S., Chun, K., 2010. *Low temperature active regeneration of soot using hydrogen in a multi-channel catalyzed DPF.* SAE paper 2010-01-0562.

Parks, J., Huff, S., Pihl, J., Choi, J., West, B., 2005. *Nitrogen Selectivity in Lean NOx Trap Catalysis with Diesel Engine In-Cylinder Regeneration.* SAE paper 2005-01-3876.
Plint, M., Martyr, A., 1999. *Engine Testing: Theory and Practice.* Second Edition, Butterworth-Heinemann: Oxford, UK.

PSA Peugeot Citroen Press Kit., 2001. *Non-Thermal Plasma (NTP) exhaust aftertreatment.* http://www.psa-peugeot-citroen.com/document/presse_dossier/psa-delphi_2001_11_281017849837.rtf [Accessed 06.04.2010].

Pyzik, A., Ziebarth, R., Han, C., Yang, K., 2011. *High Porosity Acicular Mullite Ceramics for Multifunctional Diesel Particulate Filters.* International Journal of Applied Ceramics Technology. Vol. 8. Issue 5.pp 1059-1066.

Rizi, E., 2011. *Is your diesel filter out of kilter?* British Broadcasting Corporation: Watchdog. http://www.bbc.co.uk/blogs/watchdog/2011/10/diesel_particulate_filters.html [Accessed 02.04.2012].

Satokawa, S., Shibata, J,. Shimizu, K., Satsuma, A., Hattori, T., 2003. *Promotion effect of H2 on the low temperature activity of the selective reduction of NO by light hydrocarbons over Ag/Al2O3.* Applied Catalysis B: Environmental. Vol. 42. Issue 2. pp 179-186.

Schaefer, M., Hofmann, L., Girot, P., Rohe, R., 2009. *Investigation of NOx- and PM- reduction by a Combination of SCR catalyst and Diesel Particulate Filter for Heavy-duty Diesel Engine*. SAE paper 2009-01-0912.

Schaefer Sindlinger, A., Lappas, I., Vogt, C.D., Ito, T., Kurachi, H., Makino, M., et al., 2007. *Efficient material design for particulate filters.* Top. Catal. Vol. 42-43. Issue 1-4.pp 307-317.

Schenck, C., 1984. *Instruction manual: Eddy Current Dynamometer.* Type: W130

Scott, R.P.W., Perry, J.A., 1998. *Introduction to Analytical Gas Chromatography.* Second Edition, Marcel Dekker Inc: New York, USA.

Shore, P., deVries, R., 1992. *On-line hysrocarbon speciation using FTIR and CI-MS.* SAE paper: 922246.

Stone, R., 1999, *Introduction to Internal Combustion Engines,* Third Edition, MacMillan Press Ltd: Basingstoke, Hampshire.

Summers, J., Van Houtte, S., Psaras, D., 1996. *Simultaneous control of particulate and NOx emissions from diesel engines.* Applied Catalysis B: Environmental. Vol. 10. Issues 1-3. pp 139-156.

Tadrous, T.N., Brown, K., Towgood, P., McConnell, C., 2010. *Development of passive/active DPF system utilizing syngas regeneration strategy- retrofit, real life optimization and performance experience.* SAE paper 2010-01-0560.

The Automobile Association Ltd., 2011. *Diesel Particulate Filters*. http://www.theaa.com/motoring_advice/fuels-and-environment/diesel-particulate-filters.html [Accessed 02.04.2012].

Theinnoi, K., Gill, S.S., Tsolakis, A., Wyszynski, M.L., Megaritis, A., Yang, C., et al. 2010. *Fuel efficient continuously regenerating diesel particulate filter with on board hydrogen production: Towards a fuel reformer – diesel engine aftertreatment system.* FISITA, Paper No. F2010-A-125.

Thermo Nicolet Corporation., 2001. *Introduction to Fourier Transform Infrared Spectrometry*. http://mmrc.caltech.edu/FTIR/FTIRintro.pdf [Accessed 15.06.2010].

Tonkyn, R., Barlow, S., Hoard, J., 2003. *Reduction of NOx in synthetic diesel exhaust via two-step plasma-catalyst treatment.* Applied Catalysis B: Environmental. Vol. 40. Issue 3. pp 207-217.

Tsolakis A., Hernandez, J.J., Megaritis A., Crampton M., 2005 *Dual fuel diesel engine operation using hydrogen effect on particulate emissions*. Energy and Fuels, vol 19, p 418.

Tsolakis, A., Megaritis, A., 2004. *Catalytic exhaust gas fuel reforming for diesel engines – effects of water addition on hydrogen production and fuel conversion efficiency.* International Journal of Hydrogen Energy. Vol. 29. pp 1409-1419.

US Environmental Protection Agency (EPA), Office of Transportation and Air Quality, February 2000, *Federal Certification Exhaust Emission Standards for Light Duty Vehicles (Passenger Cars) and Light Light-Duty Trucks: Federal Test Procedure (FTP), Cold CO, and Highway and Idle Test*. Ref:EPA420-B-00-001

Wellington, B and Asmus, A., 1995. *Diesel Engines and Fuel Systems.* Fourth Edition. Longman Australia Pty Ltd: Melbourne, Australia.

Wen, B., 2002. *NO reduction with H_2 in the presence of excess O_2 over Pd MFI catalyst*. Fuel. Vol. 81. pp 1841.

West, B., Huff, S., Parks,J., Lewis,S., Choi,J., Partridge, W., Storey, J., 2004. *Assessing reductant chemistry during in-cylinder regeneration of diesel lean NOx traps.* SAE paper 2004-01-3023.

Wichterlová, B., Sazama, P., Breen, J.P., Burch, R., Hill, C.J., Capek, L., Sobalíka, Z., 2005. *An in situ UV–vis and FTIR spectroscopy study of the effect of H2 and CO during the selective catalytic reduction of nitrogen oxides over a silver alumina catalyst.* Journal of Catalysts. Vol. 235. Issue 1. pp. 195-200.

Won, H.W., 2010. *Investigation of Cluster-Nozzle Concepts for Direct Injection Diesel Engines.* Journal of Atomization and Sprays., Vol.19. Issue 10, pp. 986-996.

Wyman, V., 2012. *Breathing Spaces.* Professional Engineering. Vol.25. Issue 2, pp. 47-50.

Yamamoto, K., Oohori, S., Yamashita, H., 2009. Daido, S. *Simulation on soot deposition and combustion in diesel particulate filter.* P. Combust. Inst. Vol. 32. Issue 2. pp 1965-72.

Yao, S., 2009. *Plasma Reactors for Diesel Particulate Matter Removal.* Recent Patents on Chemical Engineering. Vol. 2. pp 67-75.

Yap, D., Peucheret, S.M., Megaritis, A., Wyszynski, M.L., Xu, H., 2006. *Natural gas HCCI engine operation with exhaust gas fuel reforming.* Int J Hydrogen Energy. Vol. 31.pp 587-595.

Yeom, Y.H., Wem, B., Sachtler, W.M.H., Weitz, E., 2004. *NOx Reduction from diesel emissions over a nontransition metal zeolite catalyst: A mechanistic study using FTIR spectroscopy.* J. Phys. Chem. B. Vol . 108. pp 5386-5404.

York, A.P.E., Ahmadinejad, M., Watling, T.C., Walker, A.P., Cox, J.P., Gast, J., et al. 2007. *Modelling of the catalysed continuously regenerating diesel particulate filter (CCR-DPF) system: model development and passive regeneration studies.* SAE paper 2007-01-0043.

Zabetta, E.C and Hupa, H.M., 2005. *Gas-born carbon particles generated by combustion: a review on the formation and relevance.* Combustion and Materials chemistry. Biskopsgatan8, FIN-20500 Åbo, Finland.

Zheng, M and Banerjee, S., 2009. *Diesel oxidation catalyst and particulate filter modelling in active – flow configurations.* Applied Thermal Engineering. Vol. 29. Issues 14-15, pp 3021-3035.

APPENDIX A

REACTOR DESIGN DRAWINGS

Appendix A

Reactor design drawings

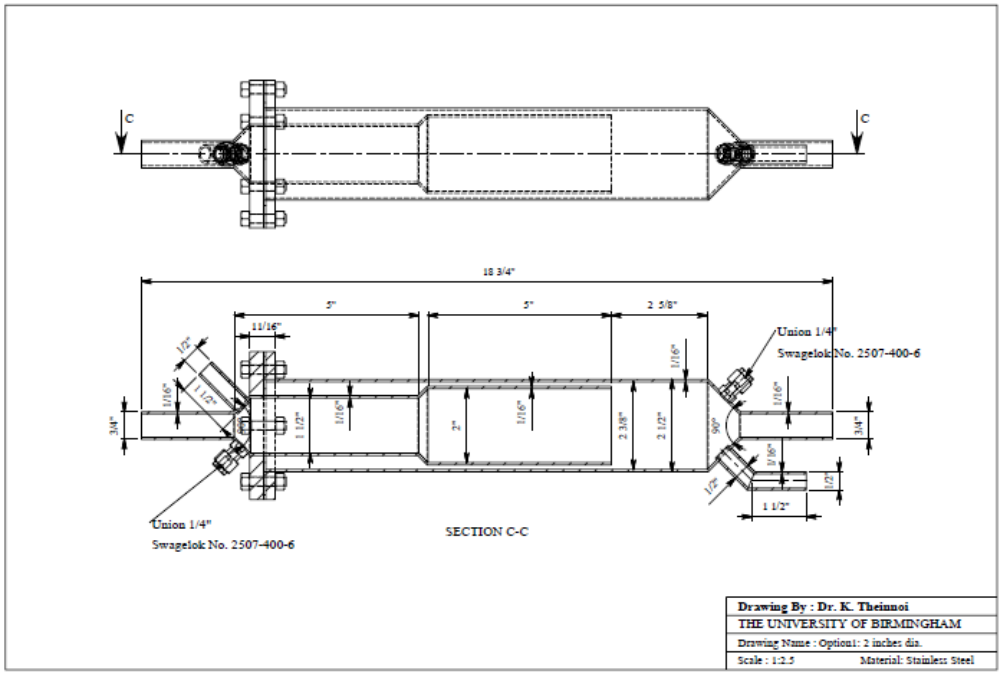

Design suitable for 2” diameter DPF (Designed by Dr.K.Theinnoi – University of Birmingham)

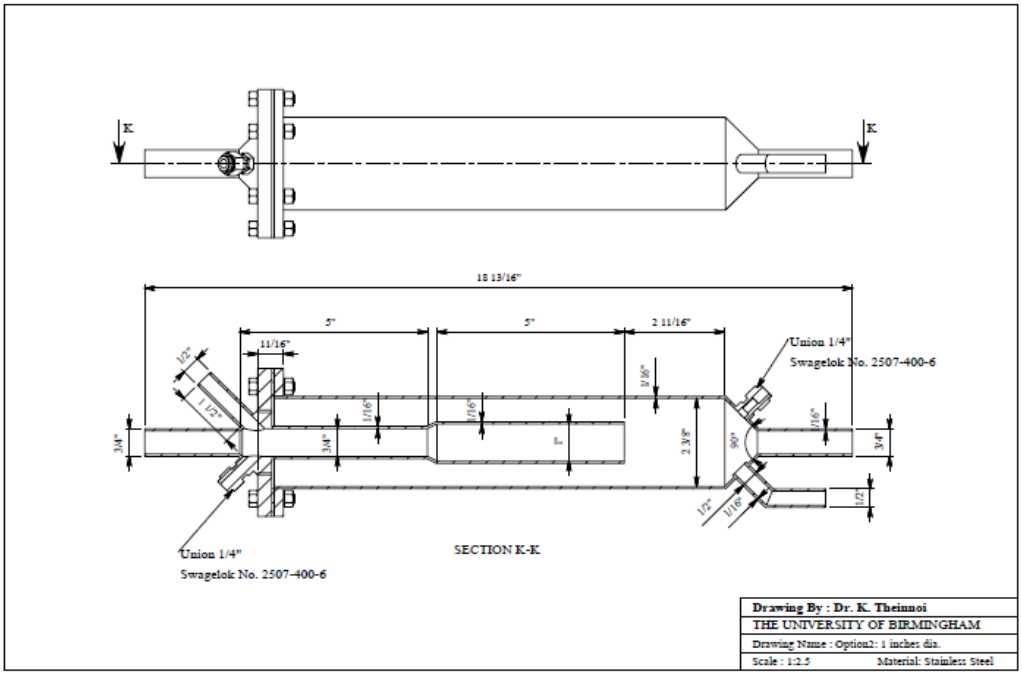

Design suitable for 1” diameter DPF (Designed by Dr.K.Theinnoi – University of Birmingham)

APPENDIX B

PUBLICATIONS BY THE AUTHOR

Appendix B

Publications by the author

Hemmings, S., Megaritis, A., 2012, *Periodically regenerating diesel particulate filter with a hydrogen/carbon monoxide mixture addition*. Int J Hydrogen Energy. 32 (4) pp 3573-84.

Hemmings, S., Megaritis, A., 2012, *The effect of a H_2/CO mixture at varying ratios on the diesel particulate filter regeneration process: towards an optimised fuel reformer design – diesel engine aftertreatment system.* Int J Hydrogen Energy. DOI: 10.1016/j.ijhydene.2012.06.035.

Hemmings, S., Megaritis, A., Zhao, H., 2011, Periodically regenerating diesel particulate filter with a H2/CO mixture addition: towards a fuel reformer –diesel engine aftertreatment system. In: IMechE (Institution of Mechanical Engineers), *Internal Combustion Engines: Improving Performance, Fuel Economy and Emissions.* London, England 29-30 November 2011. Woodhead Publishing.

Yang, C., Theinnoi, K., Hemmings, S., Megaritis, A., Tsolakis, A., Zhao, H., 2010. *Periodically Regenerating Diesel Particulate Filter with Hydrogen Addition: Towards a Fuel Reformer – Diesel Engine Aftertreatment System.* FISITA paper no. F2010-A-116.